

Synthesis, Characterization and Catalytic Applications of Mesoporous Materials

THESIS

Submitted in partial fulfillment
of the requirements for the degree of
DOCTOR OF PHILOSOPHY

by

Divya Khetarpal

Under the supervision of

Dr. Amit Dubey



**BIRLA INSTITUTE OF TECHNOLOGY AND SCIENCE
PILANI (RAJASTHAN) INDIA**

2010

**BIRLA INSTITUTE OF TECHNOLOGY AND SCIENCE
PILANI (RAJASTHAN)**

CERTIFICATE

This is to certify that the thesis entitled “**Synthesis, Characterization and Catalytic Applications of Mesoporous Materials**” submitted by **Divya Khetarpal** ID No **2006PHXF011** for award of Ph. D. Degree of the Institute embodies original work done by her under my supervision.

Signature in full of the Supervisor:

Name in capital block letters: **Dr. AMIT DUBEY**

Designation: Assistant Professor

Date:

Dedicated to

My Family

And

My Teachers

ACKNOWLEDGEMENTS

Words are inadequate to acknowledge my research guide, Dr. Amit Dubey. It is my great pleasure to express my sincere appreciation towards my supervisor who is generous, optimistic, enthusiastic and have shown constant support and motivation throughout this research work. I am grateful to him for giving me liberty in the work undertaken and for continuous encouragement. My deepest personal regards are due for him forever.

I owe my indebted thanks to the Institutes like IISC Bangalore, IIT-Kanpur, SAIF-Chandigarh, AIF facility at JNU, for their timely analysis of the samples and without their assistance, this work would have been incomplete.

I am thankful to Prof. L. K. Maheshwari, Vice-Chancellor BITS, Pilani, for allowing me to pursue my research work successfully. My sincere thanks to Director Prof. G. Raghurama, Director, Prof. R. N. Saha, Deputy Director (Research & Education Development), Prof. N.V.M Rao, Dean (Engineering and Hardware Division) for providing the necessary infrastructure and other facilities.

I also express my sincere regards to Dean, Research and Consultancy Division, BITS, Pilani Prof. A.K. Das for his motivation, constant support and encouragement.

It gives me great pleasure to thank Prof. V. S. Rao, Director, BITS- Hyderabad, and Prof. G. Sundar, Dean (Practice School Division) BITS, Pilani, Prof. S.C. Sivasubramanian, Unit Chief, CAHU and Dr. Dalip Kumar (Group Leader, Chemistry) for their motivation, guidance, constant help, technical support, valuable suggestions and making all the facilities available during various stages of this dissertation.

Sincere gratitude is also expressed to the members of my Doctoral Advisory Committee, Dr. Paritosh Shukla and Dr. Bharti Khungar, Chemistry Group, BITS, Pilani for their time and valuable suggestions and comments on my research work.

I thank Dr. Hemant Jadhav, Mr. Dinesh Kumar, Ms. Monica Sharma, Mr. Sharad Shrivastava, Mr. Gunjan Soni and Mr. Amit Kumar, nucleus members of RCD, BITS, Pilani, for their cooperation and guidance during each of the past few semesters.

I am thankful to all the respectable faculty members of Chemistry Group, BITS, Pilani for their generous help and fruitful discussions during the different stages of my doctoral study.

It gives me great pleasure to thank my friends Dr. Swapna Sundree, Mallari A. Naik, , Dr Buchi Reddy, Dr Priyanka Bagaria, Prakash, Gautam Patel and Maruthi Kumar from whom I have received unfailing support and encouragement during the years of research work that they have shown to me in their own special way.

The assistance of my colleagues, Bhupendra Mishra, Amit Tiwari, Sibi, Dr. Thirumurthy, K. P. Chandrashekhhar, Soumen Saha, Manoj, Kameshwar Rao, Sowmya, Kiran Soni and Sudershan Rao during the entire work is highly acknowledged. My heartfelt thanks to the lab oriented project students Aditya Kapoor and Manish for their help in investigating various studies.

A special thank to my teachers Dr. Sunita Dhingra and late Dr. Anita Tandon (Miranda House) from whom I got interest in Organic Chemistry and without their timely help I would not have joined BITS-Pilani.

Thanks are also due to all the office staff of Chemistry Group, BITS, Pilani, Sita-Ramji, Goukulji, Omprakashji and Pushpaji for their help during my work. I also convey my thanks to Mathuramji for his kind behavior in issuing me the chemicals for my research work. My sincere thanks to Dr. M. Ishwara Bhat, Unit Chief, Librarian, BITS, Pilani and other staff of library for their co-operation and help rendered while utilizing the library services.

My thanks are duly acknowledged to CSIR, New Delhi for their valuable support in the form of Senior Research Fellowship (SRF) during my research tenure.

I am falling short of words to thank my in-laws (Mummyji, Daddyji and Nivedita Di) and other members of my in laws family who blessed me , encouraged me and endorsed me in completing this thesis work. The thesis could not have been completed without the endless love and blessing from my mother and father who were the path makers to this dream. I must thank them for showing patience and believing in me. Due adoration to my

sisters Jyotsana and Vrinda; regards to my nani, nana, mami, mama and Lubhavani and Lakshmi for their unwavering love and support.

No words of appreciation can be adequate to express my feelings for my dear husband Subodh and my son Namish for their sacrifices. Without their constant love, patience, encouragement and co-operation I would not have been able to fulfill this dream. Last but not the least I thank God for giving me all this.

Divya Khetarpal

Abstract

In the current scenario there is regular demand to eliminate waste and avoid the use of toxic hazardous reagents, solvents in the manufacture and application of commercial products. Hence our attention was drawn to the problem of waste in the fine chemical industry (approx E factor-5 {kg of waste per kg of product}) that is less favorably viewed compared to the petroleum, gas, electricity and paper industries. The range of fine chemical products is enormous and these products make an invaluable contribution to the quality of our lives with manufacturing plants having capacities ranging from a few tonnes per year compared to 500,000 tonnes per year in the petrochemicals area. Hence a new approach is required which sets out to reduce the materials and energy intensity of chemical processes and products by maximizing the use of renewable resources and extending the durability, recyclability in a way which increases industrial competitiveness.

Solid catalyst in this regard provides numerous opportunities for recovering and recycling catalysts from reaction environment with improved processing steps, better process economics and environmental friendly ways. So to achieve desired activity and selectivity, efforts were devoted to develop new heterogeneous systems. Nanoporous materials offer such possibilities in this regard, exhibiting wide range of properties with desired functionalities and properties. These materials are of immense importance scientifically and industrially because of their advantages such as large surface area, small particle size and well-defined pore sizes; therefore at present there is focus for the development of nanocatalyst wherein the funding is raised from \$116 million to \$9 billion and still projected to increase further by 2014.

The thesis is composed of two separate projects. The first project deals with hydrotalcites (layered double hydroxides, LDH) wherein the flexibility in the composition led to increased interest in these materials. LDH represent an inexpensive, versatile and recyclable source of catalyst support or actual catalyst. Particularly, mixed metal oxides obtained by controlled thermal decomposition of LDHs have large specific surface areas (100–300m²/g), basic properties and a homogeneous thermally stable dispersion of the metal ion components. The interest emerged in studying the acid-base behavior of these materials

in carrying out fine chemical synthesis and replacing traditional homogeneous catalyst KOH, NaOH, Na₂CO₃ such as synthesis of phenytoin. Furthermore, transition metal based LDH's are employed for selective oxidation reactions of benzoin and vanillin for the first time. Various kinds of transition metal cations can readily be incorporated into the hydrotalcite framework for liquid phase oxidation reactions via isomorphic substitution for Mg²⁺ or Al³⁺ so as to reduce the formation of large volume of toxic and corrosive wastes.

The second part of the thesis aims at the synthesis of mesoporous material with high surface area (~1000 m²/g), narrow pore size distribution with tunable and accessible pore diameters (8-10 nm). The mesoporosity and very high surface area of these materials can be exploited for the immobilization of different catalytically reactive species via surface modification methods. Therefore, there is ample opportunity to explore new methods of surface modification which will be advantageous than the state-of-the-art methods. The principal aim of the second part of work is to design and create new organic-inorganic hybrid catalyst via immobilization of acidic, basic ligands on ordered mesoporous silica material that allows sufficient diffusion of the bulky reactant and product molecules and shows importance in fine chemicals and pharmaceutical industry. In-depth characterizations of these immobilized catalysts are highlighted to understand the mode of interaction of the ligands with the silicate network, to evaluate the stability of the composite system, and to explore the origin of catalytic activity.

List of Tables

Table 1.1	Ordered Mesoporous Silicas	10
Table 1.2	Catalytic Applications of Hydrotalcites	14
Table 1.3	Organic Moieties functionalized–Organic Inorganic Hybrid Material	25
Table 2.1	Structural parameters of Mg/Al-HTs calcined at 873K	49
Table 2.2	Base strength of Mg/Al HTs calcined at 873K.	50
Table 2.3	Effect of different fresh hydrotalcites M(II)Al-3 on the conversion of phenytoin.	52
Table 2.4	Variation of total conversion, product selectivity and product yield over different catalysts (Hydrotalcites used are calcined at 873K)	52
Table 2.5	Effect of different calcined hydrotalcites on conversion of phenytoin	53
Table 2.6	Effect of different ratio of M(II)/Al-HTs calcined at 873K on the yield of phenytoin.	54
Table 2.7	Variation of the yield of phenytoin over different Mg/Al compositions	54
Table 2.8	Variation of calcination temperature on the conversion of the phenytoin over calcined Mg/Al-3 HT	55
Table 2.9	Effect of the molar ratio (benzil:urea) on the conversion of phenytoin over Mg/Al-3 HT	57
Table 3.1	Structural parameters of CuMgAl-HTs.	66
Table 3.2	Variation of conversion and yield of vanillin over different CuM(II)Al-HTs	68
Table 3.3	Effect of subs:oxidant ratio on the conversion of vanillin over CuMgAl-5 HT	70
Table 3.4	Effect of C ₂ H ₅ OH:H ₂ O (molar ratio) on conversion of vanillin over CuMgAl-5	71
Table 3.5	Effect of different binary M(II)/Al=3 HTs on the conversion of benzoin.	74

Table 3.6	Variation of the product yield with different solvents on CuMgAl HTs	74
Table 3.7	Variation of different CuM(II)Al-3 HTs on the yield of benzil	75
Table 3.8	Variation of different Cu/Mg composition on the conversion of benzil	75
Table 3.9	Effect of the weight of the catalyst on the product yield over CuMgAl-3 HTs	76
Table 3.10	Effect of the reaction temperature on the product yield over CuMgAl-3 HTs	76
Table 3.11	Effect of different oxidants on the product yield over CuMgAl-3 HTs	78
Table 3.12	Variation of different Cu/Mg composition on the product yield	78
Table 3.13	Effect of molar ratio of methanol: ethanol at different pH	80
Table 4.1	Structural Parameters of Al/SBA-15 samples	88
Table 4.2	Vibrational Frequencies of SBA/Al samples	91
Table 4.3	Variation of different amount of catalyst loading on the yield of DHPM's	92
Table 4.4	Variation of solvent on the yield of DHPM's over SBA/(15)Al catalyst	92
Table 4.5	Variation of temperature on the yield of DHPM's over SBA/15Al catalyst	93
Table 4.6	Effect of substituted aldehydes on the yield of DHPM's over SBA/(15)Al catalyst	95
Table 5.1	Structural parameters of SBA/PPA catalysts	106
Table 5.2	FT-IR peaks of the samples	109
Table 5.3	Effect of different catalyst on the conversion and selectivity of acylation of naphthalene	112
Table 5.4	Variation of conversion of naphthalene with different solvents	113
Table 5.5	Effect of different amount of acetic anhydride on the conversion and selectivity of acylation of naphthalene	115
Table 6.1	Structural parameters of SBA/CA catalyst	124

Table 6.2	Variation of conversion of products over different catalysts.	128
Table 6.3	Effect of catalyst weight on the conversion of product (A) over SBA/CA	129
Table 6.4	Knoevenagel condensation of aromatic aldehydes with ethyl cyanoacetate	133
Table 7.1	Structural parameters of the SBA/PP catalysts.	141
Table 7.2	Effect of different catalyst on the conversion of nitroalcohol	147
Table 7.3	Effect of different solvents on the conversion and selectivity of the selectivity of nitroalcohol	148

List of Figures

Figure 1.1	Layered crystal structure of hydrotalcite-like compounds	4
Figure 1.2	Applications of Hydrotalcites	5
Figure 1.3	Co-Precipitation method for synthesis of Hydrotalcites	6
Figure 1.4	M41S type of ordered mesoporous silica materials	8
Figure 1.5	Surfactant Silica organization in aqueous solution	9
Figure 1.6	Synthetic strategy for synthesizing ordered mesoporous silica	9
Figure 1.7	Grafting (postsynthetic functionalization) of mesoporous pure silica with (R'O)3SiR. R=organic functional group	12
Figure 1.8	Co-condensation method (direct synthesis) of mesoporous pure silica R=organic functional group	12
Figure 1.9	Polymerization Mechanism (a) Selective adsorption of vinyl monomers on the silica mesopore walls and (b) subsequent thermal polymerization	13
Figure 1.10	Structure of phenytoin	16
Figure 1.11	Phenytoin	16
Figure 1.12	Benzil derivatives	23
Figure 2.1	PXRD patterns of (A) Mg/Al-3 calcined at different temperatures and (B) with different Mg/Al ratio calcined at 873K.	47
Figure 2.2	FT-IR of fresh (a) Mg/Al-5, (b) Mg/Al-3, (c) Mg/Al-2, (d) Mg/Al-1 (e) Mg/Al-0.2 HTs	48
Figure 2.3	FT-IR of (a) Mg/Al -5, (b) Mg/Al-3, (c) Mg/Al-2, (d)Mg/Al-1, (e) Mg/Al-0.2 HTs calcined at 873K.	48
Figure 2.4	FT-IR and 1H-NMR of the desired product (phenytoin)	53
Figure 2.5	Influence of catalyst weight on the conversion of phenytoin over Mg/Al-3 HT	56
Figure 2.6	Variation of total conversion (A) and product selectivity of phenytoin (B) with the reaction time over KOH and Mg/Al calcined hydrotalcites	57

Figure 2.7	Variation of conversion of phenytoin with temp over Mg/Al-3 HT	58
Figure 2.8	Effect of different solvents over Mg/Al HT.	59
Figure 3.1	PXRD pattern of fresh CuMgAl-HTs, top (a) , bottom (e).	65
Figure 3.2	FT-IR of (a) CuMgAl-5 (b) CuMgAl-3 (c)CuMgAl-1 (d) CuMgAl-0.5 (e) CuMgAl-0.2 HTs.	65
Figure 3.3	Effect of catalyst weight on the conversion of vanillin over CuMgAl-5 HT.	69
Figure 3.4	Effect of the reaction time on the conversion of vanillin over CuMgAl-5 HT	70
Figure 3.5	Effect of different solvent on conversion of benzil over CuMgAl-3 catalyst.	77
Figure 3.6	Variation of the product yield with time over CuMgAl-3 catalyst	79
Figure 3.7	Variation of the product yield with pH of the reaction over CuMgAl-3 catalyst	79
Figure 4.1	PXRD patterns of SBA-15 and 15 wt.%Al/SBA-15	87
Figure 4.2	N ₂ -adsorption –desorption isotherm of SBA/(15)Al. (Inset: Pore size distribution (BJH, desorption branch of isotherm).	88
Figure 4.3	N ₂ -adsorption –desorption isotherm of SBA/(5)Al. (Inset: Pore size distribution (BJH, desorption branch of isotherm).	89
Figure 4.4	Temperature Programmed Desorption (TPD) of SBA/Al	90
Figure 4.5	FT-IR spectra of (a) SBA-15, (b) SBA(15)Al and (c) SBA(5)Al samples.	90
Figure 4.6	Effect of the reaction time on conversion of product over SBA/(15)Al catalyst	93
Figure 4.7	FT-IR of DHPM	95
Figure 5.1	PXRD pattern of (a) SBA/15(d) and (b) SBA/15(I) catalysts	105
Figure 5.2	Nitrogen adsorption-desorption isotherms of (a) SBA/15(d) and (b) SBA/15(I) catalysts	106
Figure 5.3	³¹ P spectra of (A) SBA/PPA (I) and (B) SBA/PPA (d)	107
Figure 5.4	Distinct nature of phosphorus in PPA.	107
Figure 5.5	EDXRF spectrum of P in SBA/PPA (I) “orange” and SBA/PPA (d)	108

	“green”	
Figure 5.6	SEM images of SBA/PPA (I)	108
Figure 5.7	FT-IR spectra of (a) Neat PPA (b) SBA/10(d) (c) SBA/15(d) samples.	109
Figure 5.8	Temperature programmed desorption (TPD) of a) SBA/15(I) (b) SBA/15(d) (c) SBA/10(d) samples	110
Figure 5.9	Differential Scanning Calorimetry of SBA/PPA(d)	111
Figure 5.10	Effect of weight of the SBA/15(d) catalyst on the conversion of naphthalene	113
Figure 5.11	Effect of time on the conversion and product selectivity of 2-acetyl naphthalene over SBA/PPA (d) and SBA/PPA (I) catalysts	114
Figure 5.12	FT-IR spectra of (a) PPA (b) after first run and (c) after second run of SBA/15(d) catalysts	115
Figure 6.1	PXRD pattern of a) SBA-15 and b) SBA/CA catalysts.	123
Figure 6.2	N ₂ -adsorption –desorption isotherm and pore size distribution of SBA/CA	123
Figure 6.3	¹³ C CPMAS NMR spectra of SBA/CA catalyst.	125
Figure 6.4	EDXRF spectrum of chlorine in SBA/CA.	125
Figure 6.5	FT-IR spectra of a) chloroacetic acid and b)SBA/CA.	126
Figure 6.6	Temperature Programmed Desorption (TPD) of SBA/CA.	127
Figure 6.7	Effect of different solvents on the conversion of product (A).	129
Figure 6.8	Variation of reaction temperature on the conversion of product (A) over SBA/CA catalyst.	130
Figure 6.9	FT-IR of product (A) (4E)-2-cyano-3-hydroxy-5-phenylpent-4-enoate	132
Figure 6.10	¹ H-NMR of product (4E)-2-cyano-3-hydroxy-5-phenylpent-4-enoate	133
Figure 7.1	Direct functionalization of SBA-15 with piperazine (SBA/PP)	139
Figure7.2	SBA-15 Polymer nanocomposites (SBA-PS) functionalized with piperazine.	140
Figure7.3	PXRD pattern of (a) SBA-(10)PS/PP and (b) SBA/PP catalysts	141

Figure 7.4	N ₂ -adsorption –desorption isotherm of (a) SBA-(10)PS/PP and (b) SBA/PP catalysts	142
Figure 7.5	¹³ C CPMAS NMR spectra of (a) SBA/PS and (b) SBA-(10)PS/PP catalysts.	143
Figure 7.6	¹³ C CPMAS NMR spectra of A) SBA/CPTS and B) SBA/PP catalysts.	143
Figure 7.7	SEM image of SBA-(10)PS/PP.	144
Figure 7.8	FT-IR spectra of piperazine a) PPA (neat), b) SBA/PP and c) SBA-(10)PS/PP catalysts.	145
Figure 7.9	Basicity of SBA-Piperazine catalysts	146
Figure 7.10	Effect of the catalyst weight on the conversion of β –nitroalcohols	149
Figure 7.11	Variation of conversion and selectivity of β- nitroalcohol with temperature	149
Figure 7.12	Variation of conversion and selectivity of β- nitroalcohol with time	150
Figure 7.13	FT-IR of β –nitroalcohol	153

List Of Abbreviations/Symbols

Abbreviation/Symbol	Description
α	Alpha
Å	Angstrom
APTS	3-Aminopropyltrimethoxy silane
BET	Brunauer-Emmett-Teller
2θ	Bragg Angle
BJH	Barrett-Joyner-Halenda
^{13}C	Carbon-13
CMC	Critical Micelle Concentration
CP MAS	Cross Polarization Magic Angle Spinning
CPTS	3-Chloropropyltrimethoxy silane
CTAB	cetyltrimethyl ammonium bromide
δ	delta
d	diameter
DSC	Differential Scanning Calorimetry
DTA	Differential Thermal Analysis
EDXRF	Energy Dispersive X-Ray Fluorescence
FT-IR	Fourier Transform Infrared
GC	Gas Chromatography
h	hour
HTlc	Hydrotalcites like materials
Hz	Hertz
IR	Infrared
IUPAC	International Union Pure and Applied Chemistry
LDH	Layered Double Hydroxides
LLC	Lyotropic Liquid Crystalline
M.p	melting point
MCM	Mobil Composition of Matter
μM	micromolar
MeOH	methanol
NMR	Nuclear Magnetic Resonance
OMS	Ordered Mesoporous Silica
P123	Pluronic 123 surfactant
PPA	Polyphosphoric acid
PXRD	Powder X-Ray Diffraction
SAXS	Small Angle X-ray Scattering
SBA	Santa Barbara Amorphous
SDA's	Structure Directing Agent
SEM	Scanning Electron Microscopy
SS-NMR	Solid State Nuclear Magnetic Resonance
TEOS	Tetraethyl orthosilicate
TOF	Turnover Frequency

TPD
WAXS

Temperature Programmed Desorption
Wide Angle X-ray Scattering

TABLE OF CONTENTS

Certificate	i
Acknowledgements	ii
Abstract	v
List of tables	vi
List of figures	ix
List of Abbreviations and Symbols	xii
Chapter 1 Introduction	1
1.1 Introduction	2
1.2 Mesoporous Materials	2
1.3 Layered Double Hydroxides (Anionic Clays or Hydrotalcite like materials).....	3
1.3.1 Cationic Clays.....	3
1.3.2 Anionic Clays	3
1.4 Hydrotalcites	3
1.4.1 Historical Background	3
1.4.2 Structural Features	4
1.4.3 General Molecular Formula.....	5
1.4.4 Synthesis of Hydrotalcites	5
1.5 Mesoporous Siliceous Materials	6
1.5.1 Historical Background.....	7
1.5.2 Synthesis of Ordered Mesoporous Silica Materials (OMS)	8
1.5.3 Synthesis mechanism of Ordered Mesoporous Silica Materials	9
1.5.4 Mesoporous Materials of M41S family.....	10
1.5.5 Ordered Mesoporous SBA-n family (n=1,2....11, 15, 16 etc.)	10
1.6 Catalytic Applications of Mesoporous Materials.....	13
1.7 Catalytic Application of Hydrotalcites.....	14

1.7.1 Base Catalysis.....	15
1.7.2 Redox Catalysis	18
1.8 Catalytic Applications of Ordered Mesoporous Silica Materials.....	25
1.8.1 Acylation of Naphthalene.....	26
1.8.2 Nitroaldol Condensation.....	27
1.9 Physiochemical Characterization	30
1.9.1 Powder X-ray Diffraction (PXRD).....	30
1.9.2 Fourier Transform Infra-red spectroscopy (FT-IR).....	30
1.9.3 Solid State Nuclear Magnetic Resonance Spectroscopy (SS-NMR).....	31
1.9.4 Microscopy	31
1.9.5 N ₂ Adsorption-Desorption Isotherms	31
1.9.6 Temperature Programmed Desorption studies (TPD)	32
1.9.7 Thermal Analysis.....	32
1.9.8 Energy-dispersive X-ray fluorescence (EDXRF).....	32
1.10 Organization/Outline of thesis	32
1.11 References	36
Chapter 2 Synthesis, Characterization and Catalytic Applications of Calcined M(II)Al-Hydrotalcites, where M(II)=Mg, Ni, Zn, Co, Cu	44
2.1 Introduction	45
2.2 Liquid phase synthesis of phenytoin over Mg/Al-HTs	45
2.3 Synthesis of M(II)Al Calcined Hydrotalcites.....	46
2.4 Physiochemical Characterizations.....	46
2.4.1 PXRD.....	46
2.4.2 FT-IR	47
2.4.3 Surface area Measurements	49
2.4.4 Basicity Measurements.....	49
2.5 Catalytic Studies.....	50
2.5.1 Synthesis of phenytoin.....	50
2.5.2 Effect of different bivalent metals in binary M(II)/Al.....	51
2.5.3 Effect of calcined ternary hydrotalcites	53
2.5.4 Effect of M(II)/Al catalyst ratio on M(II)/Al-HTs	54
2.5.5 Effect of calcinations temperature on Mg/Al-3	55

2.5.6 Effect of the catalyst weight	55
2.5.7 Time-on-stream studies (TOS)	56
2.5.8 Effect of substrate: urea molar ratio	57
2.5.9 Effect of the reaction temperature	58
2.5.10 Effect of the different Solvent	58
2.5.11 Plausible Mechanism of the reaction.....	59
2.5.12 Reusability of the catalysts	60
2.6 Conclusions	61
2.7 References	62
Chapter 3 Synthesis, Characterization and Catalytic Applications of CuM(II)Al-Ternary Hydrotalcites	63
3.1 Introduction	64
3.2 Synthesis of M(II) Al and CuM (II)Al Hydrotalcites.	64
3.3 Physiochemical Characterizations.....	64
3.3.1 PXRD.....	64
3.3.2 FT-IR	65
3.3.3 Surface Area Measurements.....	66
(A) Liquid phase oxidation of Vanillin over CuM(II)Al-HTlc.....	66
3.4 Catalytic Studies.....	67
3.4.1 Effect of different co-bivalent metal in CuM(II)Al-HTs.....	67
3.4.2 Effect of the substrate:catalyst ratio	68
3.4.3 Effect of the reaction time	69
3.4.4 Effect of the substrate:oxidant ratio.....	70
3.4.5 Effect of pH on the reaction	70
3.4.6 Effect of ethanol addition	71
3.4.7 Effect of the calcination temperature.....	71
3.4.8 Reusability of the catalysts	72
(B)Liquid Phase Aerial Oxidation of benzoin over CuM(II)Al-HTlc	72
3.5 Catalytic Studies.....	73
3.5.1 Effect of the different metal ion concentration.....	73
3.5.2 Effect of the weight of the catalyst.....	75
3.5.3 Effect of the reaction temperature	76

3.5.4 Effect of the solvent.....	76
3.5.5 Effect of different oxidants with oxidant: substrate molar ratio.....	77
3.5.6 Time on stream studies (TOS).....	78
3.5.7 Effect of the pH on the reaction and plausible mechanism	79
3.5.8 Effect of calcinations temperature	81
3.5.9 Reusability of the catalysts	82
3.6 Conclusions	82
3.7 References	83
Chapter 4 Liquid Phase One Pot Multicomponent Synthesis of Dihydropyrimidinones (DHPM's) over Aluminated Mesoporous SBA-15	85
4.1 Introduction	86
4.2 Liquid phase synthesis of 3,4-dihydropyrimidin-2(1H)-ones	86
4.3 Synthesis of SBA-15	86
4.4 Synthesis of Al/SBA-15 catalyst.....	87
4.5 Physiochemical Characterizations.....	87
4.5.1 PXRD.....	87
4.5.2 N ₂ Adsorption-Desorption Studies	88
4.5.3 TPD of Al/SBA-15	89
4.5.4 FT-IR	90
4.6 Catalytic Studies.....	91
4.6.1 Synthesis of 3,4-dihydropyrimidine-2(1H)-ones.....	91
4.6.2 Effect of the different catalysts.....	92
4.6.3 Effect of the solvents	92
4.6.4 Effect of the temperature	93
4.6.5 Time on Stream Studies.....	93
4.6.6 Plausible Mechanism	94
4.6.7 Reusability	98
4.7 Conclusions	98
4.8 References	100
Chapter 5 Synthesis, Characterization and Catalytic Application of Ordered Mesoporous Silica Functionalized with Polyphosphoric acid (SBA-15/PPA).....	102
5.1 Introduction	103

5.2 Liquid phase acylation of naphthalene over SBA/PPA.	103
5.3 Synthesis of SBA-15	103
5.4 Direct synthesis of SBA/PPA(d) catalysts	104
5.5 Post-impregnated synthesis of SBA/PPA(I) catalysts.....	104
5.6 Physiochemical Characterization	105
5.6.1 PXRD.....	105
5.6.2 N ₂ Adsorption-Desorption Studies	105
5.6.3 SS-NMR	106
5.6.4 Energy Dispersive X-ray Fluorescence Spectrometry (EDXRF).....	107
5.6.5 Scanning Electron Microscopy (SEM).....	108
5.6.6 FT-IR	108
5.6.7 TPD of SBA/PPA	109
5.6.8 Differential Scanning Calorimetry (DSC).....	110
5.7 Catalytic Studies.....	111
5.7.1 Effect of the different Catalysts.....	112
5.7.2 Effect of the different Solvents.....	112
5.7.3 Effect of the weight of catalyst.....	113
5.7.4 Time on Stream studies	114
5.7.5 Effect of the amount of acetic anhydride.....	114
5.7.6 Reusability	115
5.7.7 Plausible Mechanism.....	116
5.8 Conclusions	117
5.9 References	118
Chapter 6 Synthesis, Characterization and Catalytic Applications of Chloroacetic acid	
Grafted on Ordered Mesoporous Silica (OMS)	120
6.1 Introduction	121
6.2 Knoevenagel Condensation of cinnamaldehyde with ethylcyanoacetate	121
6.3 Synthesis of chloroacetic functionalized SBA-15 (SBA/CA).....	121
6.4 Physiochemical Characterizations.....	122
6.4.1 PXRD.....	122
6.4.2 N ₂ Adsorption-Desorption studies	123
6.4.3 SS-NMR	124

6.4.4 Energy Dispersive X-ray Fluorescence Spectrometry (EDXRF).....	125
6.4.5 FT-IR	126
6.4.6 Temperature Programmed Desorption (TPD) of SBA/CA	126
6.5 Catalytic Studies.....	127
6.5.1 Effect of the different catalysts.....	128
6.5.2 Effect of the solvent.....	128
6.5.3 Effect of the catalyst weight	129
6.5.4 Effect of reaction temperature	130
6.5.5 Time on stream studies (TOS).....	131
6.5.6 Plausible Mechanism.....	131
6.5.7 Reusability	131
6.5.8 Effect of the different aldehydes	133
6.6 Conclusions	134
6.7 References	135
Chapter 7 Synthesis, Characterization and Catalytic Applications of Silica-Polymer Nanocomposites Functionalized with Piperazine.....	136
7.1 Introduction	137
7.2 Synthesis of β –nitro alcohols over Silica-Polymer nanocomposites functionalized with piperazine	137
7.3 Synthesis of SBA-15	138
7.4 Synthesis of direct functionalized SBA-Piperazine catalyst (SBA/PP).....	138
7.5 Synthesis of SBA-Polymer nanocomposites (SBA-PS) functionalized with piperazine (SBA/PS/PP).	139
7.6 Physiochemical Characterizations.....	140
7.6.1 PXRD.....	140
7.6.2 N ₂ Adsorption-Desorption studies.....	141
7.6.3 SS -NMR	142
7.6.4 Scanning Electron Microscopy (SEM).....	144
7.6.5 FT-IR	144
7.6.6 Basicity Measurements.....	145
7.7 Catalytic Studies.....	146
7.7.1 Effect of the different catalysts.....	147

7.7.2 Effect of the solvent.....	148
7.7.3 Effect of the catalyst weight	148
7.7.4 Effect of the reaction temperature	149
7.7.5 Time-on-stream studies	150
7.7.6 Plausible Mechanism.....	151
7.7.7 Reusability	151
7.8 Conclusions	153
7.9 References	154
Chapter 8 Summary and Conclusions	156
8.1 Summary and Conclusions.....	157
8.2 Future Scope of the research work.....	159
 Appendices	
List of Publications	A-1
List of papers presented in conference	A-2
Brief Biography of the Candidate	A-3
Brief Biography of the Supervisor	A-4

Chapter 1
Introduction

1.1 Introduction

Nanoporous materials are receiving tremendous attention because of their unique structural properties compared to bulk materials such as high surface area, tunable pore size, pore diameter, flexibility to incorporate different organic moieties and better dispersion of active centers. Porosity, volume ratio of pore space to the total volume of the material, is the major characteristic required for a solid to be used in various applications such as catalysis, storage and molecular separation etc. Generally nanoporous materials are a subset of porous materials having pore diameters between 1-100 nm and porosity < 0.4 ¹. According to IUPAC classification, nanoporous materials can further be subdivided into the following categories based on their pore diameters: ^{2,3}

1. Micropores- $d < 2\text{nm}$
2. Mesopores- $2\text{nm} < d < 50\text{nm}$.
3. Macropores- $d > 50\text{nm}$.

1.2 Mesoporous Materials

Microporous materials are of immense importance in various commercial applications but the small pore diameter, inability to incorporate larger organic functionalities and limited functional group densities limit their practical utilization for advanced applications⁴. Therefore mesoporous materials exhibit significant advantages over microporous materials because of the variable pore size, pore diameters and flexibility to incorporate larger organic moieties. The porosity in the materials can be generated during the growth of the nanoparticles via particle–interaction, almost most of the materials exhibit non uniform pore diameter. Anionic clays such as Layered Double Hydroxides (LDH) or otherwise referred as Hydrotalcites (HTs) belong to this category and provide significant catalytic properties⁵. The mesoporosity can also be generated by liquid crystal templating techniques wherein the materials possess uniform pore sizes, pore diameters characteristics of surfactant properties⁶. Ordered mesoporous silicas (OMS), mesoporous carbons and their functionalized nanocomposites cover the wide range of this class of materials.

In the present research work, emphases are devoted to synthesize and characterize both kinds of mesoporous materials namely, LDH and OMS materials, for their unique structural activity relationships for catalytic organic applications.

The brief historical background of these materials is discussed one by one⁷⁻⁹.

1.3 Layered Double Hydroxides (Anionic Clays or Hydrotalcite like materials)

Clays, one of the most common minerals present in the earth's crust, forms a subset of large discipline of catalysis in particular as heterogeneous catalysts. In addition to their use as catalysts they find their potential applications in ceramics, building materials, adsorbents, ion exchangers and decolorizing agents¹⁰⁻¹².

Clays can be broadly classified into two categories

1.3.1 Cationic Clays

Cationic or smectite type clays having layered lattice structure in which two dimensional oxyanions are separated by layers of hydrated cations or most commonly formed by negatively charged alumino-silicate layers with cations as counterions in the interlayer region. Cationic clays are abundant in nature.

1.3.2 Anionic Clays

Anionic Clays (Layered Double Hydroxides) in which the charge on the layer and the gallery anion is reversed are complementary to smectite-type clays. Anionic clays are relatively rare in nature. They are formed by metal hydroxide layers with compensating anions and water molecules in the interlayer region^{10, 11}.

1.4 Hydrotalcites

1.4.1 Historical Background

Hydrotalcite (HT), the name transcended for these compounds was a mineral, first discovered in Sweden around 1842, a hydroxy carbonate of magnesium and aluminum occurs in foliated and contorted plates. The exact molecular formula of hydrotalcite and other isomorphous materials was presented by Manesse¹²⁻¹⁴, who recognized that carbonate ions were essential for this type of structure. Aminoff and Broome first recognized the existence of two polytypes of hydrotalcites with rhombohedral and hexagonal symmetry from X-ray investigation¹⁵. The structural features of these hydrotalcites in 1960 were later determined by Taylor and Allman based on X-ray crystallography. They concluded that both the cations (M^{2+} and M^{3+}) are confined in the same layer and only carbonate and water molecules are present in the interlayer. Miyata and coworkers¹⁶ have done the extensive

studies on the synthesis and physiochemical properties of these materials, especially on their anion exchange properties.

1.4.2 Structural Features

The structure of these HT-like materials (HTlc) is best visualized from the structure of brucite (Figure 1.1)¹⁵. In brucite structure, Mg^{2+} is surrounded by six hydroxyl groups in an octahedral co-ordination and these octahedra are connected through edge sharing to form infinite sheets. These infinite sheets are stacked upon one another to give layered network held through hydrogen bonding. If one of the Mg^{2+} ions is substituted by a trivalent cation having a similar radius like Al^{3+} (in hydrotalcite) the positive charge density of the layer increases. To maintain the electric neutrality, the anions occupy the interlayer positions where water of crystallization also finds a place. These sheets containing both bivalent and trivalent cations occupy randomly in the octahedral holes of the close packed configuration of hydroxyl ions and the interlayer constituents namely the anion and water are randomly located in this region and possess a high degree of mobility^{13, 14} (Figure 1.1).

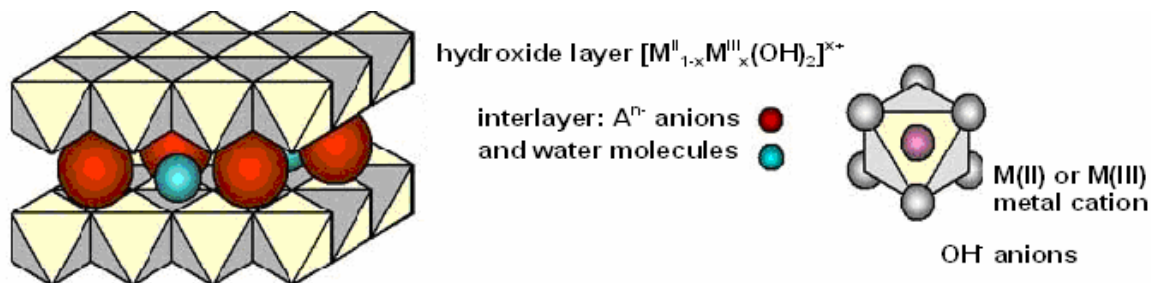


Figure 1.1 Layered crystal structure of hydrotalcite-like compounds¹²

It is this net positive charge that makes HTlc extremely efficient with anionic uptake and has effective applications in various fields (Figure 1.2). Large variety of synthetic hydrotalcites can be prepared with different compositions of M^{II} (divalent metal ion) as Mg^{2+} , Ca^{2+} , Zn^{2+} , etc, and M^{III} (trivalent metal ion) as Al^{3+} , Cr^{3+} , Fe^{3+} , Co^{3+} , etc and A^{n-} (anion) as Cl^- , CO_3^{2-} , NO_3^- , etc. The anions occupy the interlayer region of these layered crystalline materials. The pure phase of hydrotalcite is usually obtained for a limited range as $0.2 \leq x \leq 0.33$ ¹⁵ where $x = M^{II}/(M^{II} + M^{III})$.

1.4.3 General Molecular Formula

These materials are characterized by the general formula $[M^{(II)}_{1-x}M^{(III)}_x(OH)_2]^{x+} [A^{n-}]_{x/n} \cdot yH_2O$ where M(II) and M(III) are various divalent and trivalent metal ions, A is the interlayer anion, x can have the values between 0.20 to 0.35 and y can generally have the value four^{15, 17}. Due to high versatility, easily tailored properties and low cost, hydrotalcite like materials can be designed to fulfill specific requirements. HTs can be effectively utilized as such or after calcinations (thermal decomposition) (Figure 1.2) for various applications in catalysis, ion-exchange, adsorption, pharmaceuticals, photochemistry and flame retardants etc.

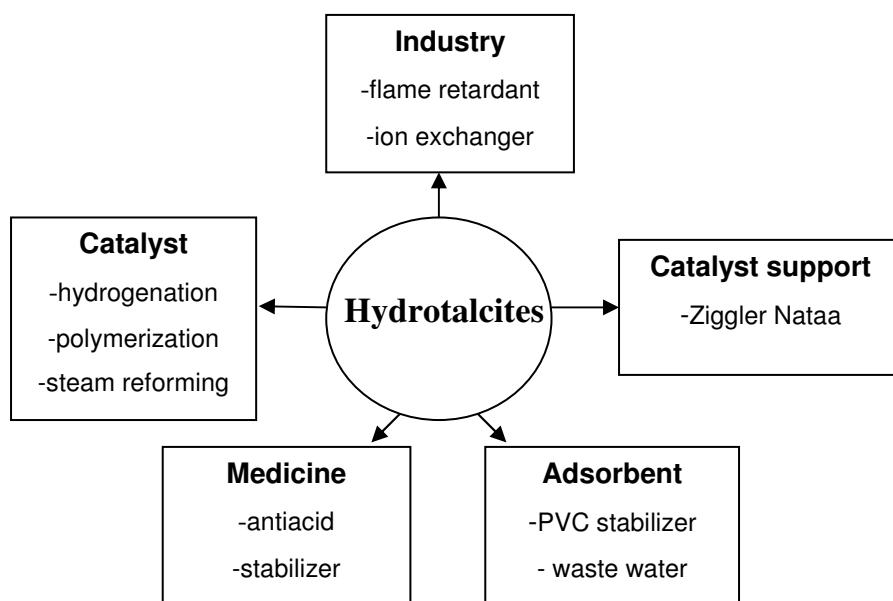


Figure 1.2 Applications of Hydrotalcites

1.4.4 Synthesis of Hydrotalcites

Hydrotalcite-like materials can be synthesized by various techniques, namely, precipitation at constant pH, precipitation at variable pH, deposition or precipitation reactions, hydrothermal synthesis, anion exchange, sol-gel, structure reconstruction, microwave and ultraso-nification¹⁸. Most commonly used technique is co-precipitation method under low super saturation. Co-precipitation under low super saturation conditions usually give rise to precipitates which are more crystalline with respect to those obtained at the high super saturation conditions, because at low super saturation the rate of nucleation is higher than the rate of crystal growth and large number of particles is obtained which, however, are

usually small in size and have better catalytic activity^{5,16,20}. Brief overview of this methodology (Figure 1.3) involves a large number of unit operations such as precipitation, aging, filtration, washing, drying, grinding and shaping. HTlc materials synthesized from this methodology showed rhombohedral polytype with 3R lattice geometry, wherein 3R indicates, 3R indicates 3 layers per unit cell¹⁴.

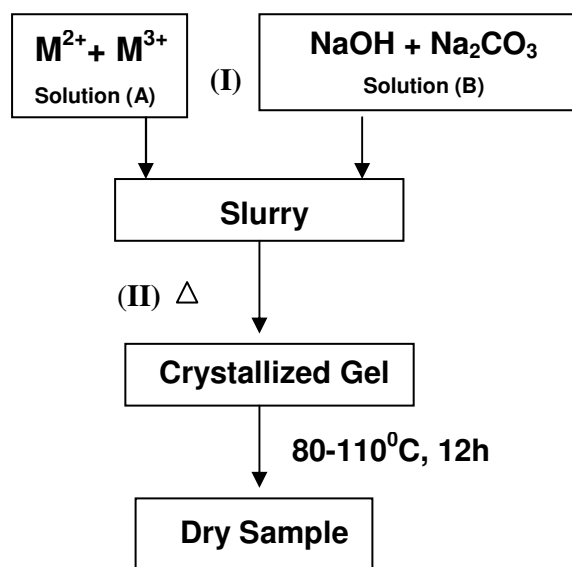


Figure 1.3 Co-Precipitation method for synthesis of Hydrotalcites¹⁸

1.5 Mesoporous Siliceous Materials

Fumed silica, silica gels, layered silicates, zeolites and mesoporous silicas are currently the most common classes of silica materials. Silica materials are further divided into amorphous and crystalline substances. The amorphous silica materials include the polymeric silicic acids such as silica gel, aerosols, xerogels, fumed silicas, and porous glasses. The crystalline substances include zeolites, crystalline silicic acids¹⁹, and dense silicas²⁰ (quartz, cristobalite, and tridymite). Crystalline materials such as zeolites contribute to microporous materials with narrow uniform pore sizes limited to 1-1.2 nm. Mesoporous silicas having a meso-scale ordering are not truly crystalline materials but are frequently used as adsorbents and catalyst supports because of their high surface areas, large pore volumes and uniform pore size distribution²¹. Silica gels are widely used as catalyst supports and are macroporous

in nature with only textural porosity and non-uniform pore size distributions. Mesoporous silicas represent a good compromise between the high structural uniformity of zeolites and easily modified macroporous silica gel and thus hold the potential for a much larger range of effective chemical functions than micro- or macro- porous materials.

1.5.1 Historical Background

Ordered mesoporous silica (OMS) is a category of siliceous materials containing periodically arranged mesopores²¹⁻²³. The first types of OMS were developed by the Mobil Corporation in the early 1990's and are commonly referred to as M41S. Researchers of Mobil Oil Company combined sol-gel chemistry with surfactant liquid crystal micelles to form OMS materials. These materials possess extremely high surface areas ($>700\text{m}^2/\text{g}$) and easily accessible, well defined tunable mesopores, by which pores size constraint of microporous zeolites can be overcome⁴.

The most well-known representatives of this class included MCM-41 (with a hexagonal arrangement of the mesopores, space group $p6mm$), MCM-48 (with a cubic arrangement of the mesopores, space group $Ia3d$), and MCM-50 (with a laminar structure, space group $p2$) (Figure 1.4)^{6, 23}. In the initial report of the synthesis of mesoporous M41S, long-chain quaternary ammonium surfactants such as cetyltrimethyl ammonium bromide (CTAB) were used as the structure-directing agents (SDA) under basic conditions, where the electrostatic charge matching between cationic surfactant (S^+) and anionic inorganic precursors (I^-) generate organic/inorganic hybrid mesostructures. Later, the synthesis approaches were extended to S^-I^+ (anionic surfactants such as sulfonates and cationic inorganic precursors), $S^-M^+I^-$ (M^+ = metal ion) and $S^+X^-I^+$ (X^- = counter anion) to synthesize mesoporous materials with various compositions²⁴, Pinnavaia and coworkers first demonstrated that neutral amine surfactants (S^0) and neutral inorganic precursors (I^0) could be used to prepare mesoporous metal oxides by a S^0I^0 pathway²⁵. However, these ionic surfactants and neutral amine surfactants were relatively expensive and toxic, limiting the future applications of mesoporous materials in industries. A careful search in the surfactant categories by the same group shortly led to the nonionic polyethylene oxide (PEO) surfactants, which were relatively of low-cost, nontoxic and biodegradable^{26, 27} and could also be used as templates to synthesize disordered mesoporous materials MSU-X in a near neutral condition. Stucky and coworkers employed commercial PEO block copolymers under acidic aqueous

solutions and successfully synthesized a family of mesoporous materials (SBA-n) with various ordered structures and large pore sizes (up to 30 nm)^{21, 28}. Since then, much attention has been paid to the synthesis, characterization and application of mesoporous materials by using PEO amphiphilic block copolymers as the templates.

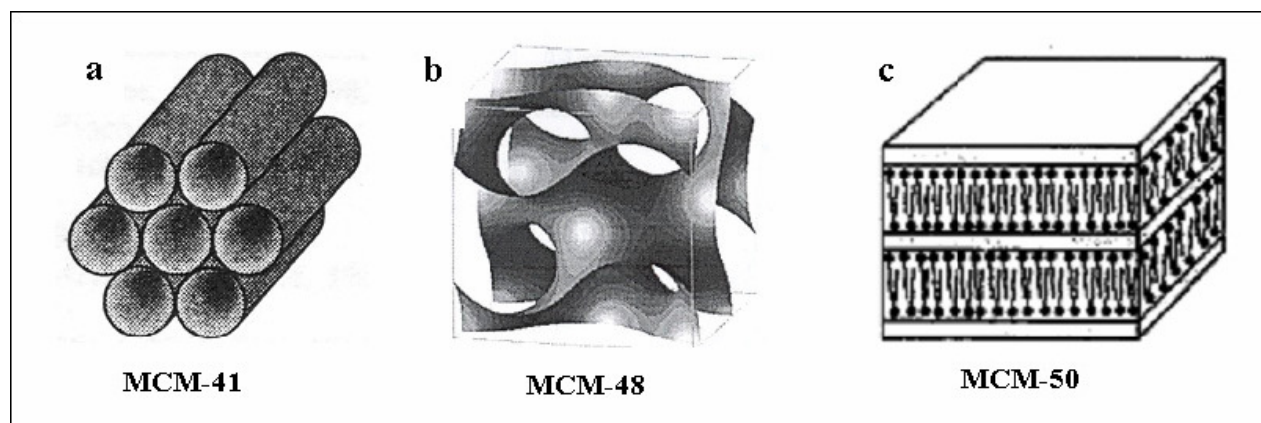


Figure 1.4 M41S type of ordered mesoporous silica materials

1.5.2 Synthesis of Ordered Mesoporous Silica Materials (OMS)

The synthetic strategy of these novel OMS material involves structure directing agents or template as supramolecular aggregates of long chain surfactants. These structure directing agents SDA's are amphiphilic molecules (surfactants) that self organizes into aggregate structures in water by separating the hydrophilic and hydrophobic part of the molecule²⁹. As a result, the aggregates can form structures such as micelles, vesicles or highly ordered assemblies with nanometer scale-geometries known as lyotropic liquid crystalline (LLC) phase. The LLC phase geometries are highly dependent on composition, temperature, pH, pressure and result in mesoporous structures³⁰. Based on the composition and temperature Figure 1.5 gives the surfactant/silica organization in aqueous solution and L, V₁ and H₁ correspond to lamellar, cubical and hexagonal respectively.

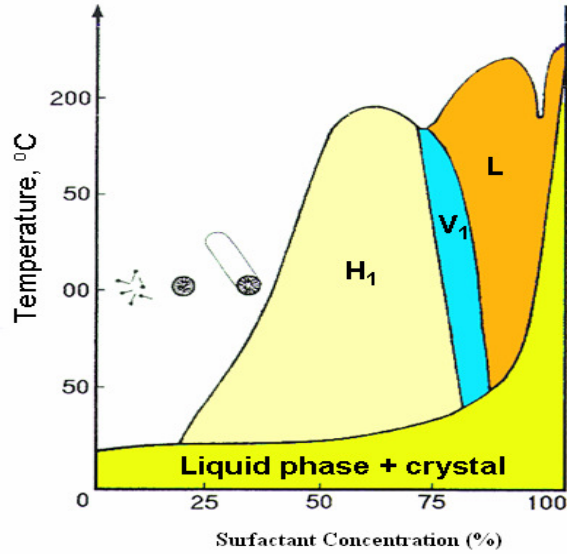


Figure 1.5 Surfactant Silica organization in aqueous solution²⁹

1.5.3 Synthesis mechanism of Ordered Mesoporous Silica Materials

The mechanism to synthesize OMS involves formation of a stable emulsion in which the inorganic precursor (silica source) surrounds a 3-dimensional template (surfactant) of organic micelles. The interaction between the inorganic precursor and the surfactant micelles is created *via* electrostatic forces, Van der Waals or hydrogen bonding. These interactions subsequently determine the textural characteristics of the final material. A condensation or cross-linking reaction occurs around the template to produce the ordered structure and the - template is subsequently removed by either refluxing in a suitable solvent

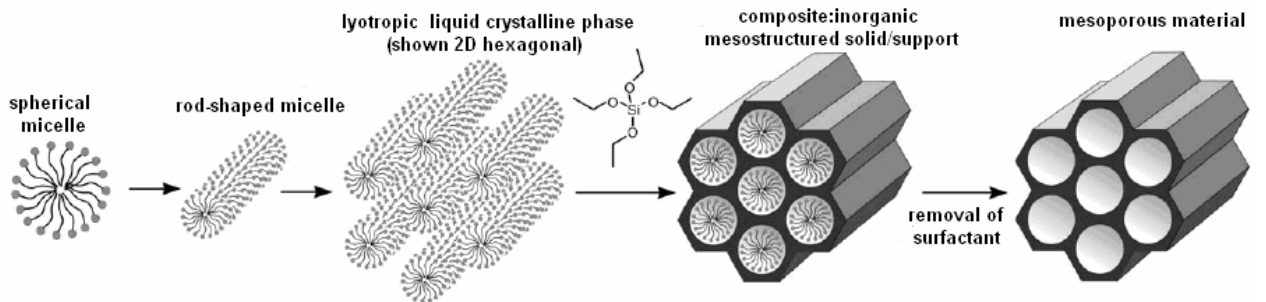


Figure 1.6 Synthetic strategy for synthesizing ordered mesoporous silica³³

or calcining at higher temperatures as shown in Figure 1.6. This kind of synthesis is described as soft-templating approach^{6, 31, 32}. Wide range of materials has been reported with different porous and non-porous forms. Table 1.1 gives a naming system for materials with range of structures and pore sizes.

Table 1.1 Ordered Mesoporous Silicas³⁴

Material acronym	Full name	Typical pore size (nm)
FSM	Folded sheet material	2 – 4
HMS	Hexagonal mesoporous silica	2 – 4
MCM	Mobil composition of matter	2 – 4
MSU	Michigan state university	2 – 4
MTS	Micelle templated silica (generic term)	Up to 10
PMO	Periodic mesoporous organosilica	Potentially up to 10
PMS	Periodic mesoporous silica	Up to 10
SBA	Santa Barbara Amorphous	Up to 30

1.5.4 Mesoporous Materials of M41S family

MCM-41 material has a one-dimensional, hexagonally ordered pore structure while MCM-48 has a three-dimensional bicontinuous cubic (space group Ia3d) ordered pore structure and MCM-50 has an unstable lamellar structure. In their pioneering work on the M41S materials³⁵, Mobil researchers used combinations of sodium silicate, tetraethoxy silicate (TEOS), fumed silica and Ludox as the silica source³⁶. Alkyltrimethyl ammonium halides were used as surfactants under alkaline conditions using sodium hydroxide or tetraethyl ammonium hydroxide to control pH of the solution²³.

1.5.5 Ordered Mesoporous SBA-n family (n=1,2....11, 15, 16 etc.)

In 1998, Stucky and coworkers reported a new synthesis method for the SBA-n class of materials, with variable pore sizes of 3 to 30 nm. SBA-n type of materials are synthesized using nonionic surfactant triblock poly (ethylene oxide)-poly (propylene oxide)-poly

(ethylene oxide) (PEO-PPO-PEO) copolymers, as structure-directing agent^{22,27,28}. Most prominent member of this family is SBA-15 synthesized using Pluronic P123, a triblock copolymer with molecular weight 5800 and units{(EO)₂₀(PO)₇₀(EO)₂₀}, as a structure-directing agent where ethylene oxide (EO) and propylene oxide (PO) are hydrophilic and hydrophobic groups respectively. Block copolymers have the advantage that their ordering properties can be continuously tuned by adjusting solvent composition, molecular weight or copolymer architecture. Moreover, the critical micellar concentration (CMC) can be achieved at lower concentration of these block copolymer surfactants. Mesoporous silicas thus obtained using block copolymers are more stable than the MCM materials, due to the increase in the wall thickness of the silica framework³⁷.

In view of various advantages discussed, we have synthesized SBA-15 mesoporous material in our thesis work to carry out catalytic applications. Ordered Mesoporous Silica OMS materials cannot be used as such because of their inactive nature. To utilize these mesoporous materials for several specific applications including catalysis, adsorption, ion exchange, sensing *etc.*, the introduction of reactive organic functional groups by modifying the inner surfaces of these materials, to form inorganic–organic hybrid materials, is essential.³⁸ The inorganic components of these inorganic–organic hybrid materials can provide mechanical, thermal or structural stability, while the organic components can introduce flexibility into the framework and can more readily be modified for specific applications³⁹. The functionalization process introduces distinct functionality to the material, through changes in the physical and/or chemical properties of the mesoporous material. Organotrialkoxysilanes are frequently used to incorporate organic functional groups, which include alkyl halides, amines, alkenes, or thiols, onto the mesostructure^{40, 41}. Three pathways are generally available for the synthesis of inorganic–organic hybrid materials based on organosilica units:

1. Grafting- Grafting involves the post synthesis modification (i.e. after removal of the surfactant) of a mesoporous material by reacting organic groups with the surface hydroxyl (silanol) groups (Figure 1.7)³⁸.

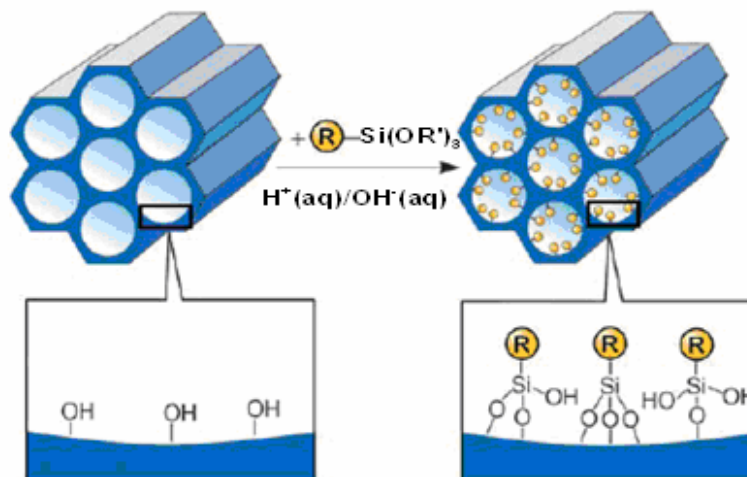


Figure 1.7 Grafting (postsynthetic functionalization) of mesoporous pure silica with $(R'O)3SiR$. R=organic functional group³³

2. Co-condensation- (or one pot synthesis) involves the direct incorporation of the organic functional group during the synthesis of OMS material⁴² as shown in (Figure 1.8) (silica precursor, surfactant, and functional groups precursors are simultaneously introduced).

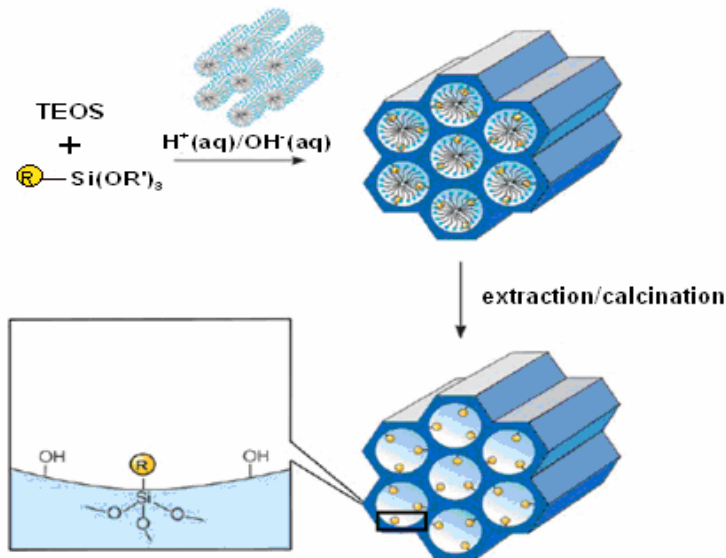


Figure1.8 Co-condensation method (direct synthesis) of mesoporous pure silica R=organic functional group³³.

3. Periodic Mesoporous Organosilicas (PMOs)- Synthesis of PMO's involves the incorporation of organic groups as bridging components directly into the pore walls by the use of bissilylated single-source organosilica precursors⁴³⁻⁴⁵.

4. Surface Modification (Polymerization route) – This polymerization route involves the surface modification by in-situ growth of the vinyl monomers (via free radical method) inside the silica framework (Figure 1.9) while maintaining the well defined mesoporous structure⁴⁶.

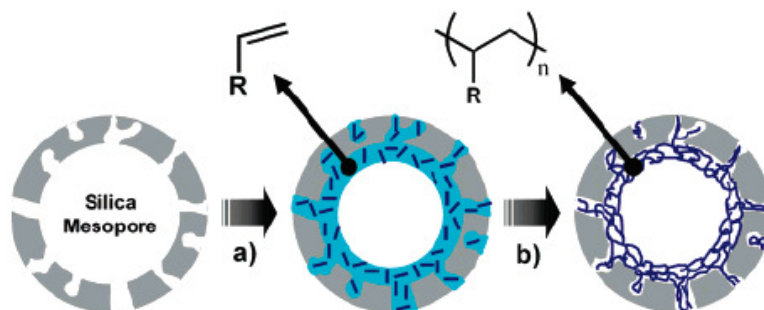


Figure 1.9 Polymerization Mechanism (a) Selective adsorption of vinyl monomers on the silica mesopore walls and (b) subsequent thermal polymerization⁴⁶.

Surface modification via this method provides an advantage of incorporating the organic moieties within the silica framework via the formation of C-C bond rather than hydrolysis susceptible siloxane bond as shown in above methods⁴⁴.

1.6 Catalytic Applications of Mesoporous Materials

The stringent environmental regulations has forced the chemical industry for the development of cleaner methods of chemical production, to eliminate the effluent treatment problems, to avoid the use of toxic and/or hazardous reagents and solvents, recovering and reusing the catalysts and separation of the desired products⁴⁷. In this respect, heterogeneous catalysts can play a major role to overcome the above cited problems.

Microporous materials such as zeolites have shown tremendous potential as solid acid catalyst for many commercial applications. However, the small pore diameter (<2nm) prevents them to incorporate bulky substrates for advanced application. Therefore a strong need is desired to fabricate new nanomaterials/composites with variable pore sizes 2-20 nm to achieve better conversion, yield and selectivity of desired product(s)⁴. Recent development of mesoporous materials with pore diameter (2-50nm) especially OMS and hydrotalcites like materials have shown credibility in many liquid or gas phase catalytic

conversions. Therefore in the present section a brief overview of the catalytic applications is discussed mainly over hydrotalcites like materials and ordered mesoporous silica materials.

1.7 Catalytic Application of Hydrotalcites

Hydrotalcites have been tremendously used in various forms such as fresh (as-synthesized), calcined, rehydrated and functionalized⁴⁸ for various catalytic conversions

Table 1.2 Catalytic Applications of Hydrotalcites

Synthetic Processes/Compounds	Product Importance	Reference
Citronitril	<i>Perfume and Soap Industry,</i>	15, 41, 45
Chalcones and Flavanoids via Aldol, Michael condensation	<i>Pharmaceuticals industry</i>	55, 56
Diacetone Alcohol, α -isophorone, glycol ethers	<i>Fine chemical</i>	46-50
O-Methylation of catechol to guaiacol	<i>Fine chemical</i>	57
Vesidryl (chalcone)	<i>Pharmaceuticals importance in diuretic and choleric</i>	58
Isomerization of Eugenol, Saferole, estragole	<i>Fragrances, oil and pharmaceutical industry</i>	53-55
Synthesis of methylisobutyl ketone (MIBK)	<i>Fine chemical</i>	59
Epoxidation of olefin	<i>Fine chemicals</i>	60
Hydroxylation of phenols	<i>Photographic chemicals, antioxidants, flavoring agents, drugs and pharmaceuticals</i>	61, 62
Oxidation of Isophorone with TBHP	<i>Fine chemical</i>	51, 63
Oxidation of allylic and benzylic alcohols	<i>Fine chemicals</i>	51
Oxidation of diphenylmethane to benzophenones	<i>Pesticides, radical initiator</i>	64

such as steam reforming⁴⁹, methanol and higher alcohol synthesis⁵⁰, base-catalyzed organic transformations^{18,52,53}, selective oxidation^{51,52}, N₂O/NO_x/SO_x decomposition^{53,54}, hydrogenation, alkylation of phenol with alcohols and isomerization of allylic compounds⁵⁷⁻⁵⁹. Important catalytic applications of hydrotalcites for the synthesis of important organic compounds are summarized in Table 1.2.

1.7.1 Base Catalysis

HTlc are used in the catalysis as such and largely after calcination. These materials upon calcination result in non-stoichiometric mixed oxides⁷⁰⁻⁷² with unique properties such as:

1. High surface area (100–300 m²/g).
2. Basic properties.
3. Homogeneous interdispersion of the elements that is thermally stable with formation of small metal crystallites.
4. *Memory effect*, which allows reconstruction under mild conditions of the original structure by contact with solutions containing various anions.⁵

In the present research work, the basic properties of the calcined hydrotalcites were studied for the liquid phase synthesis of phenytoin.

1.7.1.1 Liquid phase synthesis of phenytoin

1. Historical Background

Phenytoin (diphenylhydantoin) was first synthesized by German chemist Heinrich Biltz in 1908⁶⁵. In 1938, H. Houston Merritt and Putnam neurologists discovered phenytoin's usefulness in controlling seizure⁶⁶.

*An epileptic seizure is a transient symptom of excessive or synchronous neuronal activity in the brain. It can manifest as an alteration in mental state, tonic or clonic movements, convulsions, and various other psychic symptoms*⁶⁷.

Phenytoin (5,5 diphenyl hydantoin) (Figure 1.10) is a highly effective and widely prescribed anticonvulsant drug used alone, or in combination with phenobarbital or other anticonvulsants⁶⁸ to treat grand mal epileptic patients with focal and psychomotor seizures⁶⁹⁻⁷¹. Phenytoin has been used in the treatment of Parkinson's syndrome to control involuntary movements⁷², for the treatment of trigeminal neuralgia^{66, 73}, migraine⁷⁴, polyneuritis of pregnancy⁷⁵ and acute alcoholism⁷⁶. Phenytoin has been investigated as a treatment for more than 100 diseases^{70, 77}. Recent studies have shown that 5,5-diphenylhydantoin inhibits binding of human immunodeficiency virus (HIV) to lymphocytes^{78, 79}.

Phenytoin sodium has been marketed as **Phenytek** by Mylan Laboratories, and **Dilantin** by Australia also **Dilantin Kapseals**, **Dilantin Infatabs** in the USA, **Eptoin** by Abbott Group in India and as **Epanutin** in the UK^{80, 81}.

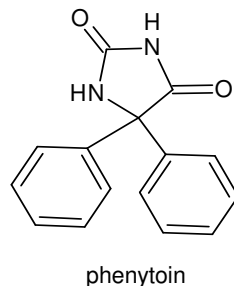


Figure 1.10 Structure of phenytoin

In US phenytoin sales for 1990 and 1995 were 1,093,290 and 984,527 standard dosage units, respectively. Phenytoin is imported as a sodium salt around 25,000 lb in US alone itself⁸².

2. Methodology

Generally, 5,5 diphenyl hydantoin (phenytoin) compound is a N-1 and N-3 unsubstituted form of hydantoin^{83, 84} (Figure 1.11). The synthetic methodology involves the introduction of two carbonyl and two nitrogen unit in the structure. One of the C=O and N-1 nitrogen can be introduced in the phenytoin moiety by a reaction of a carbonyl compound with inorganic cyanide and the other carbonyl unit and second nitrogen (N-3) by the use of ammonium carbonate⁷⁰.

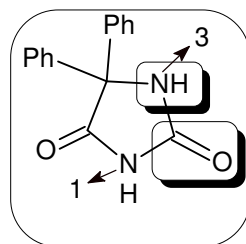
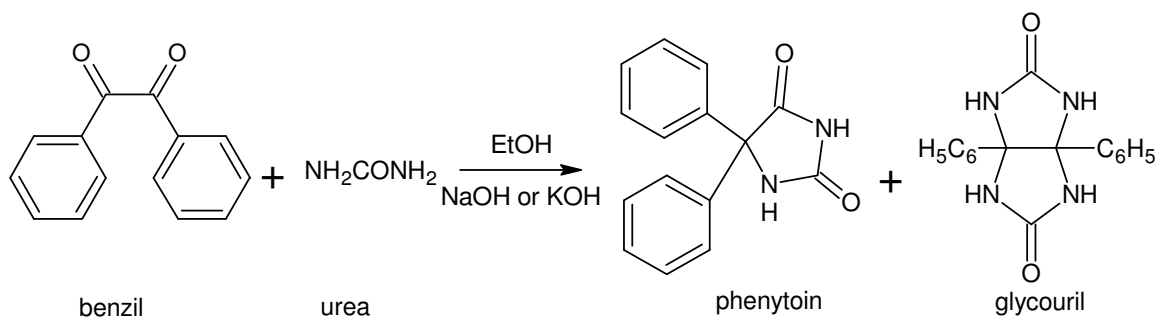


Figure 1.11 Phenytoin

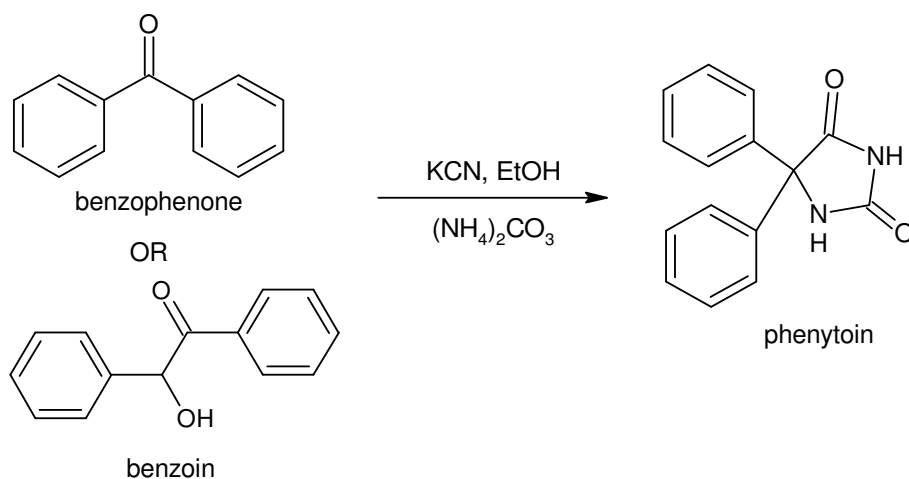
I. Homogeneous methods

1. **Bucherer–Bergs method**- This method involves the condensation of benzil and urea in the presence of ethanolic sodium hydroxide solution which 75% yields of product phenytoin⁸⁵ (Scheme 1.1).



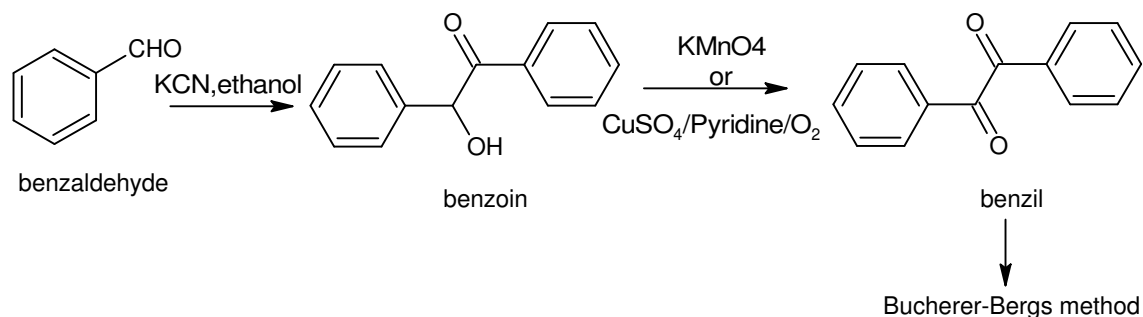
Scheme 1.1 Burcherer-Bergs synthesis of phenytoin

2. Similar to the Burcherer Berg's method phenytoin is also synthesized by treating carbonyl compound with KCN and ammonium carbonate^{86, 87} which undergoes benzilic rearrangement to form product with yield around 80-90% depending on the type of reactant used (Scheme 1.2).



Scheme 1.2 Modified synthesis of phenytoin

3. Phenytoin synthesis can also be performed from benzaldehyde (Scheme 1.3) followed by reaction with KCN and ethanol to form benzoin, this benzoin formed is oxidized further with KMnO_4 , to generate benzil which undergoes Burcherer- Berg's reaction to form the product phenytoin⁸⁸.



Scheme 1.3 Benzaldehyde to phenytoin

4. Another method for synthesis of phenytoin was devised by two phase system wherein KOH/n-BuOH and PEG 600 as phase transfer catalyst was used to reduce the quantity of side product⁸⁹ and improved the separation of product.

Various methodologies provided in the literature are all homogeneous and use toxic reagents such as KCN, NaOH which cannot be reused further⁸⁵. Apart from these materials many other homogeneous methods are also available but most of them are toxic reagents and suffer

from various disadvantages.

II. Heterogeneous Method

Based on the best of the literature knowledge no heterogeneous methods have been reported for the synthesis of this important compound phenytoin. Hence we have investigated for the first time and liquid phase synthesis of phenytoin selectively over calcined MgAl-HTlc heterogeneous catalyst (discussed in Chapter 2).

1.7.2 Redox Catalysis

All redox catalysts prepared from HT-like materials contain transition metal ions. HTs can be synthesized using transition bivalent metal ions for many interesting oxidation transformations in liquid or gas phases. For example, epoxidation of cyclohexene was done over M(II)Al-HTs and M(II)M'(II)Al-HTs where M(II)=Mg²⁺ and M'(II) = Zn²⁺, Ga²⁺ hydrotalcites, in liquid phase with (58-66%) yield and (66-76%) product selectivities^{56, 90}. Baeyer-Villiger oxidation of cyclohexanone over Mg/Al/Sn hydrotalcites to form

cyclohexane ester is an efficient heterogeneous method to replace organic oxidants with more environmentally benign reagents⁹¹.

HTlc especially transition metal containing ions were used for various selective oxidation/hydroxylation of aromatics⁶¹. Having known the above properties, in the present research work, the transition metal containing HTs were used efficiently for the first time for the oxidation of vanillin and benzoin. A brief literature background on the oxidations of vanillin and benzoin is given below (discussed later in detail in chapter).

1.7.2.1 Oxidation of vanillin to vanillic acid

Vanillic acid a kind of polyphenol, is widely studied for its chemical, biological, agricultural and medicinal applications.

Vanillin and vanillic acid are components of natural vanilla extract which has inhibitory activity against a range of microorganisms⁹² including molds, yeast, spoilage bacteria and human pathogens such as *Listeria monocytogenes* and *E. coli* O157:H. Vanillin and its derivatives can be used as flavoring agents and as preservatives⁹³. There are reports for vanillic acid as one of the ten phytotoxins which retard the growth of weeds and act as herbicides⁹⁴. Few herbs such as chicory (*Cichoriumintybus L.*), Coriander (*Coriandrumsativum L.*), Fennel (*Foeniculumvulgare L.*) consist of vanillic acid which has analgesic, anti HIV effect and aids in the inhibition of free radicals and show anticancerous effects⁹⁵.

Apart from the use of vanillic acid in biological applications it can be effectively used in chemical industry for the production of polymers^{96, 97}, as a catalyst for polymerization, as antimicrobial agents in production of building and textile materials^{98, 99}. Very often key flavor chemicals such as vanillin and vanillic acid cannot be obtained from nature via natural routes at reasonable prices^{100, 101}. If the waste product kraft lignin, is employed for vanillin products extraction then only 10% yield is obtained with a market price of below U.S. \$15/kg. Approximately, 12,000 t/yr of vanillin based products are consumed alone in US¹⁰². In comparison, natural vanillin from vanilla beans has a market price 300 times higher than the synthetic one^{103, 104}.

Thus the high market price of vanillin derivatives has led to extensive research in the synthesis of vanillin derivatives.

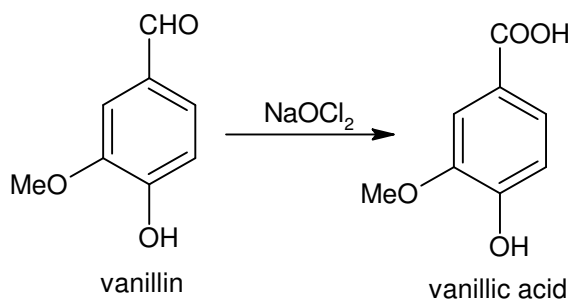
Methodology

Vanillin can be oxidized to vanillic acid both via chemical or biological routes. A brief overview of this interesting synthesis is given below.

I Homogeneous Methods - All the methods given below were carried out under homogeneous medium.

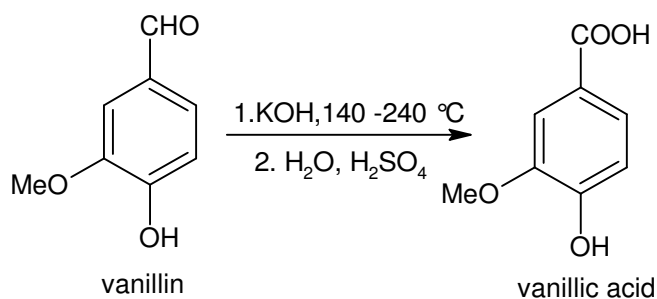
A. Chemical Methods

1. Oxidation of vanillin in presence of **sodium perchlorate** gave vanillic acid with 70-80% yield¹⁰⁵ (Scheme 1.4).



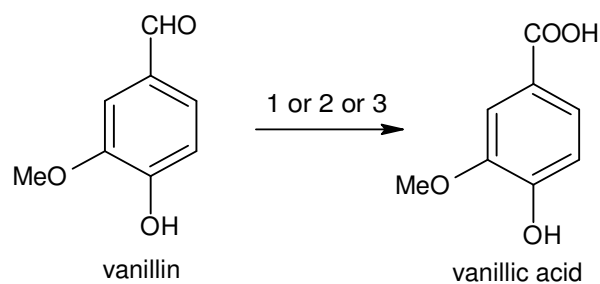
Scheme 1.4 Oxidation of vanillin

2. I.A.Pearl et.al. has reported another improved method wherein vanillin is initially treated with potassium hydroxide (Scheme 1.5) and subsequently with sulfuric acid to yield vanillic acid with 55-65% yield¹⁰⁶.



Scheme 1.5 Synthesis of vanillic acid in presence of alkali

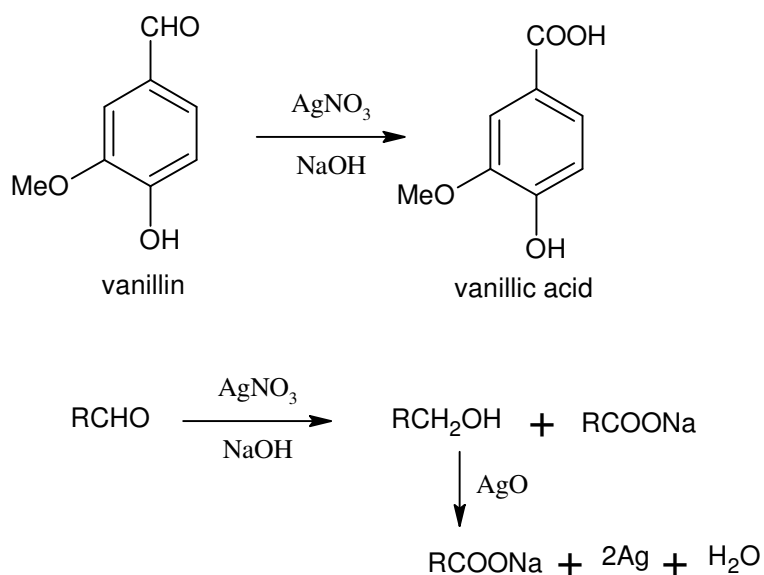
3. Oxidation of vanillin to vanillic acid can also be carried out by using catalysts such as diperiodonickelate¹⁰⁷(IV), Hexacyanoferrate¹⁰⁸(II) and sodium N-chlorop-toluene sulfonamic acid¹⁰⁹ (Scheme 1.6).



1. Dipericadatonickelate(IV)
2. Hexacyanoferrate(III)
3. Sodium N-chloro p-toluenesulfonamide

Scheme 1.6 Synthesis of vanillic acid

4. Simple and efficient homogeneous process (Scheme 1.7) for converting vanillin to vanillic acid in presence of silver oxide and aqueous alkali exhibited 80% yield¹¹⁰.

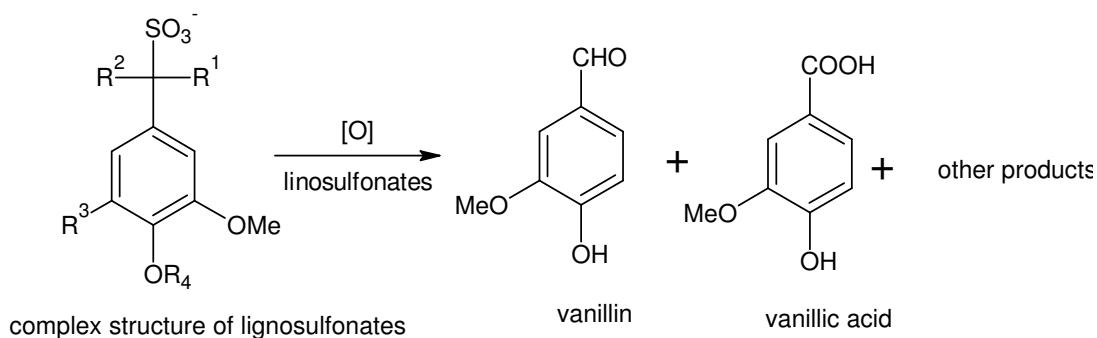


Scheme 1.7 Oxidation of vanillin in presence of AgNO₃

B. Biological Methods

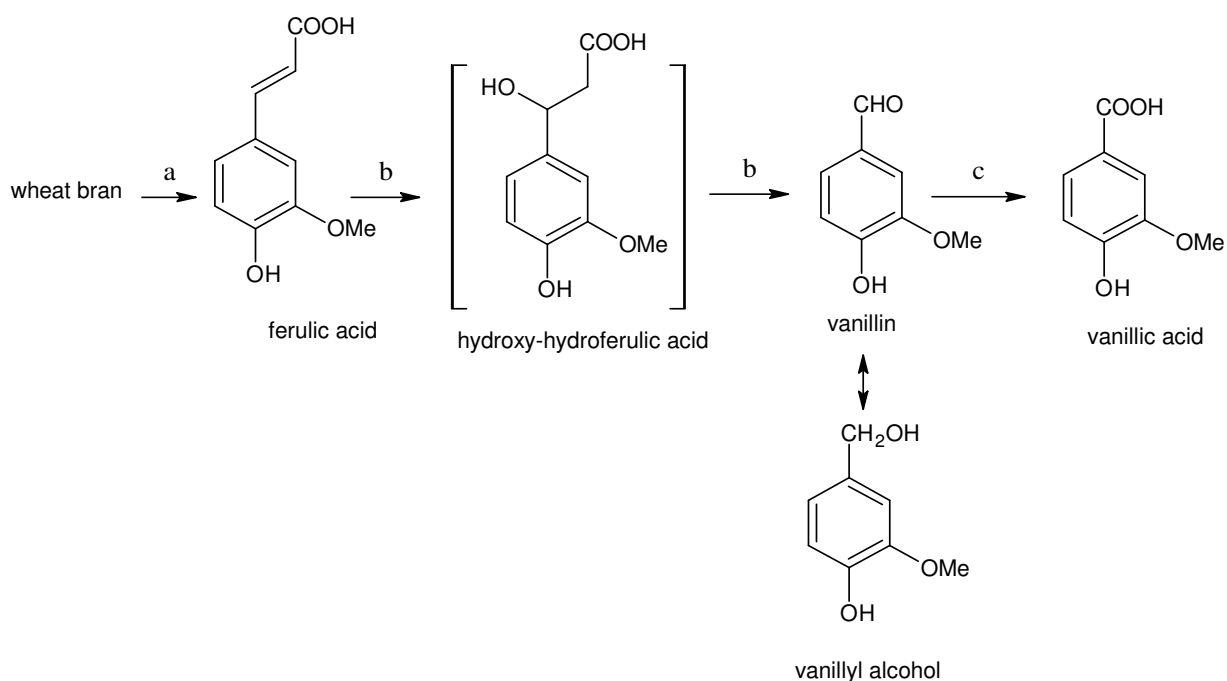
Varied methods are reported in the literature for biological synthesis of vanillic acid.

1. Degradation of the complex materials such as lignosulfonates, (Scheme 1.8) affords a large variety of compounds useful in fine chemical synthesis. Particularly, vanillin and vanillic acid are also produced by oxidation of lignosulfonates^{103, 111}.



Scheme 1.8 Synthesis of vanillic acid from linosulfonates

2. Wheat bran is initially converted to ferulic acid by ferulic acid esterase which is further converted to vanillin and vanillic acid¹¹⁶⁻¹¹⁹(Scheme 1.9).



a – *ferulic acid esterase from Aspergillus. Niger,*

b- Further oxidation by enzymes *from Streptomyces setanii or Pseudomonas putida or Pycnoporus cinnabarinus or Halomonas elongata DSM2581T.*

Scheme 1.9 Synthesis of vanillic acid from ferulic acid

II. Heterogeneous Method

So far no reports for oxidation of vanillin are reported in the literature, we attempted to oxidize vanillin to vanillic acid in presence of CuMgAl-HTlc which will be discussed in detail in further chapters.

1.7.2.2 Oxidation of benzoin to benzil

Benzil, an alpha diketone is one of the important organic intermediate that has received a great deal of attention because of its practical implications in organic and pharmaceutical industry^{112, 113}. Benzil and its analogues are found to be non-toxic selective carboxylesterases inhibitors where carboxylesterase is a protein involved in the metabolism of esterified drugs (including cocaine and heroin) and xenobiotics¹¹⁴.

Benzil is extensively used as substrate in benzylic rearrangements and also act as a starting material for the synthesis of heterocyclic compounds^{115, 116} such as anticonvulsant derivative dilantin¹¹⁷ (Figure 1.12).

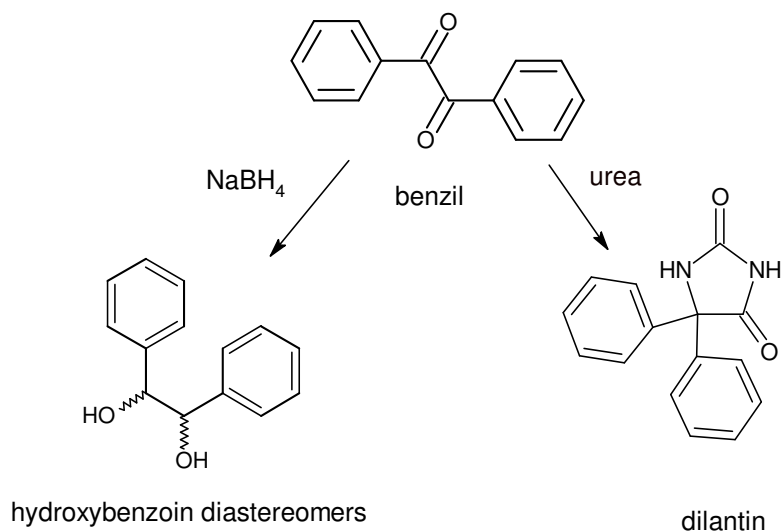


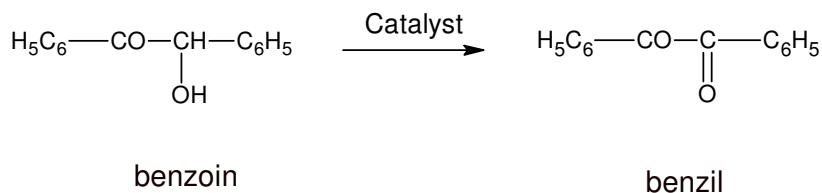
Figure 1.12 Benzil derivatives

Apart from this benzil plays an important role in synthesis of pesticides and act as a photosensitizer in U.V resin^{118, 119}. Essentially benzil possess high absorption in far UV region ($\lambda_{\text{max}} = 300\text{-}400\text{ nm}$, $\epsilon_{\text{max}} \geq 100\text{-}200\text{ l mol}^{-1}\text{ cm}^{-1}$) and exhibit relatively short triplet state and therefore they are widely used as photoinitiators for the radical polymerization of vinyl monomers¹²⁰. In order to seek for the direct and selective conversion of benzoin to benzil, many efforts have been devoted during the last two to three decades some of which are summarized below.

I. Homogeneous Method

1. Oxidation of secondary alcohols to ketones was reported using stoichiometric amounts of RuCl_3 (1.0 mol %) and trichloroisocyanuric acid (TCCA; 1.0 equiv) in the presence of *n*- Bu_4NBr (2.0 mol %) and K_2CO_3 in 1:1 MeCN/ H_2O or 1:1 AcOEt/ H_2O . The product benzil in 77% yield was achieved (Scheme 1.10)¹²¹.

2. Alternative routes were also reported for the oxidation of benzoin which used KMnO_4 adsorbed on the solid support such as alumina or carbon. After the completion of reaction, catalyst was filtered off and found to be coated with MnO_2 . The product benzil was reported with 97% of yield¹²².



Scheme 1.10 Oxidation of benzoin to benzil

Both the methods described above, suffered from limitations such as in the initial method RuCl_3 catalyst is a complex and cannot be reused hence very unlikely to be feasible for commercial process. Similarly in the second method catalyst is no more active once MnO_2 coats the solid support. Therefore HTlc can be effectively employed for carrying out these reactions in an environmentally friendly.

II. Heterogeneous Method

1. Oxidation of benzoin in heterogeneous medium employed vanadyl and molybdenyl complexes anchored on organic polymer and alumina. The catalyst effectively utilized *t*-butylhydroperoxide as oxidant to oxidize benzoin with 85-89% yield of benzil¹²³.

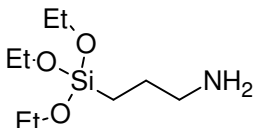
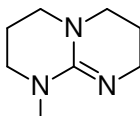
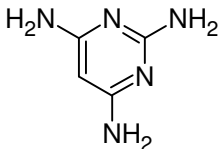
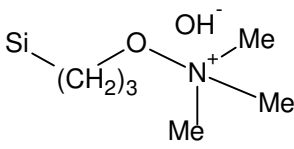
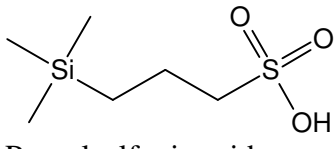
2. Heteropolyacids were reported as a catalyst for the oxidation of benzoin to benzil in presence of dioxygen as oxidant and *t*-butanol as solvent with 96% of yield and 50% of product selectivity¹²⁴.

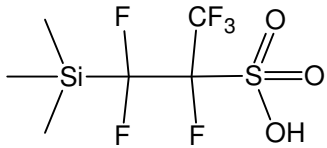
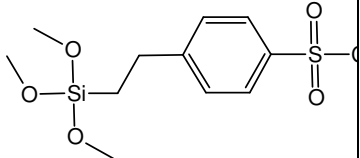
The overall yield of benzil may be high over these heterogeneous catalysts but the control on selectivity of the product benzil, remains a challenge. Therefore we have attempted to use copper containing ternary hydrotalcites for the first time for this conversion (discussed in Chapter 3).

1.8 Catalytic Applications of Ordered Mesoporous Silica Materials.

Ordered Mesoporous Silica materials are versatile supports that can host a variety of catalytically active functional groups. A brief summary of the catalytic applications over these functionalized materials is summarized in Table 1.3

Table 1.3 Organic Moieties functionalized –Organic Inorganic Hybrid Material

Organic Group	Mesoporous Silica/ Method	Catalytic Activity	Importance	References
 <p>Aminopropyl triethoxysilane (APTS)</p>	MCM-41 SBA-15 Grafting, Co- condensation	Knovengal Condensation Michael Addition for Synthesis of flavones	Alkene intermediate s Pharma products	31, 70-75
 <p>1,5,7-triazabicyclo[4.4.0] dec-5ene (TBD)</p>	MCM-41 Grafting	Transesterificati on Michael addition	Pharma products	31, 76, 77
 <p>2,4,6 triaminopyrimidine</p>	MCM-41 Grafting	Glycerides synthesis	Fine chemicals	40
 <p>PropylN,N,N, trimethylammonium hydroxide</p>	MCM-41 Co- condensation	Transesterificati on	Fine industry	125
 <p>Propylsulfonic acid</p>	SBA-15 , MCM-41 Co- condensation, Grafting	Alkylation of phenol, Coupling of alcohols to ether, Esterification of fatty acids, Bisphenol A synthesis	Industrial reaction, Food , soap and detergents	31, 79-89

 <p>Perfluorosulfonic acid</p>	MCM-41 SBA-15 Co- condensation	Alkylation of alcohols	Food and oil industry	126, 127
 <p>2-(4- Chlorosulfonylphenyl)eth yltr-imethoxysilane</p>	SBA-15 Co- condensation	Fries – rearrangement of phenylacetate	Pharma, dyes and agrochemic als	128

In view of the above applications of SBA-15 with various ligands, our interest emerged to functionalize SBA-15 material with suitable new acidic and basic ligands for various organic transformations. The selection of the ligands and the importance of their products will be discussed in the relevant chapter. However, brief overview of the catalytic reactions studied in the present research work is discussed below.

1.8.1 Acylation of Naphthalene

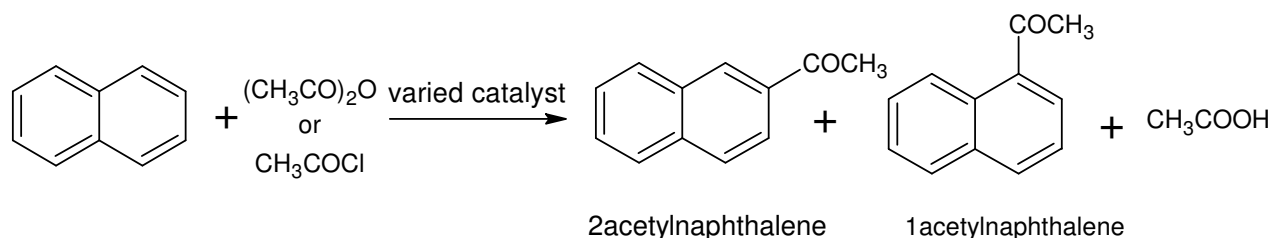
Acylation reactions represent the most important method to synthesize various aromatic ketones, which are valuable intermediates¹²⁹⁻¹³² for the production of fine chemicals such as pharmaceutical, fragrance, flavor, dye¹²⁹, and agrochemical industries¹³³.

A significant effort has been devoted to the acylation of naphthalene and naphthalene derivatives in which several positional isomers can be formed. Acylated product such as 6-acetyl-2-methoxynaphthalene is of particular interest because of its usage in the production of anti-inflammatory drug Naproxen¹³⁴. 2-acetyl naphthalene is important because it is widely used in perfume formulations, mainly in Neroli Orange Blossom, Sweet Pea, Magnolia, Honeysuckle, Wistaria, Narcisse, Jasmin, various exotic florals, Vanilla flavour¹³⁵ etc.

1. Methodology

Conventionally, the electrophilic acylation of naphthalene (Scheme 1.11) were catalyzed by Lewis acids (such as ZnCl₂, AlCl₃, FeCl₃, SnCl₄, and TiCl₄)¹³⁶⁻¹³⁸ or strong protic acids

(such as HF and H₂SO₄). These catalysts were used in stoichiometric amounts and the workup commonly required hydrolysis of the complex, leading to the loss of the catalyst with large amounts of corrosive waste streams. For these reasons, emphases are presently laid on heterogeneous acid-catalysts in liquid phase acylation of naphthalene¹³⁹.



Scheme 1.11 Acylation of Naphthalene

I. Homogeneous Methods

1. Friedel Craft acylation of naphthalene in presence of AlCl₃ with acetyl chloride yields 60% of 2-acetylnaphthalene with 50% product selectivity^{129, 131}.
2. Acylation of naphthalene was also carried out in presence of ZnCl₂, BF₃, H₃PO₄ showing different selectivities of product.^{130, 136}
3. Acylation of naphthalene was also investigated in presence of copper trifluorosulfonate¹⁴⁰.

II. Heterogeneous Methods

1. Liquid phase acylation of naphthalene with acetic anhydride over large pore zeolites faujasite, mordenite and beta was investigated which gave 25% conversion with 80% selectivity¹⁴⁰⁻¹⁴³.
2. Liquid phase reaction of naphthalene with acetic anhydride yield 2-acetyl naphthalene over sulfated zirconia as catalyst which gave very low yields 5-10%^{144, 145}.

Apart from the usage of solid catalyst, the selectivity (2-acetyl naphthalene) of the reaction is the main concern, which has been tackled in the thesis with mild acidic sites.

1.8.2 Nitroaldol Condensation

The Henry or Nitroaldol reaction is particularly useful for carbon-carbon bond-forming reaction giving highly functionalized products of considerable synthetic utility¹⁴⁶.

One of the most important features of this reaction is in its potential products β -nitroalcohols and nitroalkenes^{147, 148}. Nitroalcohols are valuable intermediates for the

synthesis of pharmacologically active¹⁴⁹ β -amino alcohols and α -nitroketones β -amino alcohols the key elements present in β -blockers^{150, 151} and agonists are highly effective in the treatment of cardiovascular disease, asthma, and glaucoma^{152, 153}. Apart from this, β -amino alcohols are of particular significance in the synthesis of biologically important compounds such as epinephrine^{154,155} and anthracycline antibiotics¹⁵⁶. Similarly, Nitroalkenes derived from nitroalcohols possess significant biological activities such as insecticidal, fungicidal, insecticidal¹⁵⁷ fungicidal, bactericidal, rodent-repellent and antitumor agents and are also utilized for the preparation of prostaglandins, pyrroles, and porphyrins¹⁵⁸.

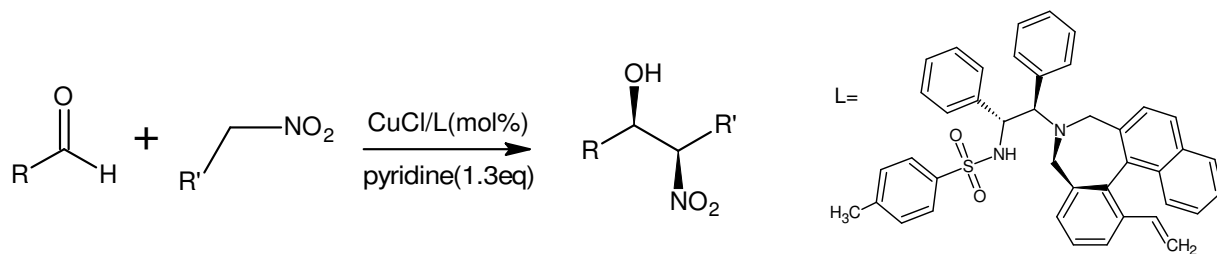
1. Methodology

I. Homogeneous Methods

Traditional synthesis of β -nitroalcohols involves condensation of the carbonyl substrates and a nitroalkane in the presence of an ionic base such as alkali metal hydroxides, alkaline earth oxides, carbonates, bicarbonates, alkoxides, alkaline earth hydroxides, or magnesium and aluminum alkoxides^{148, 149, 159, 160}. All these classical methods are associated with a problem one of which is the formation of side product nitroalkenes by elimination of water which can lead to polymerization and Cannizzaro products in the presence of base^{148, 159}. Furthermore, the acidification required during the work up of reaction may lead to Nef reaction if not done with care¹⁶¹. Therefore attempts were made in overcoming the drawbacks of classical methods wherein heterogeneous catalysts were also employed.

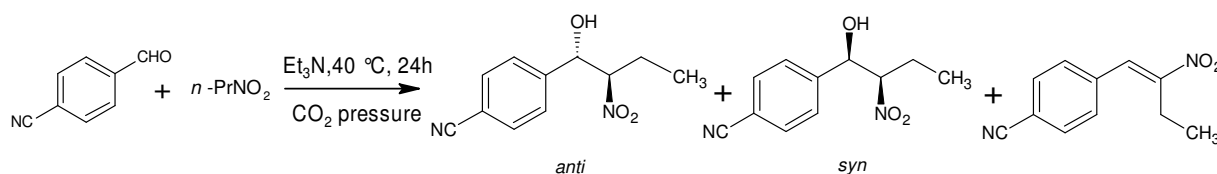
II. Heterogeneous Methods

1. Arai and co-workers reported the synthesis of β -nitroalcohols using binaphthyl-based ligand (Scheme 1.12). Utilizing this ligand with CuCl and with pyridine as an additive with the desired adducts are obtained in high enantiomeric excess (up to 93%)¹⁶².



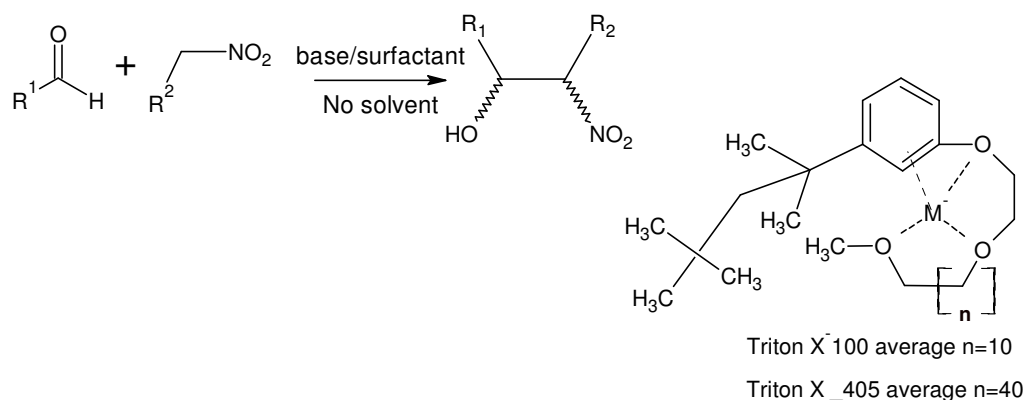
Scheme 1.12 Asymmetric synthesis of β -nitroalcohols

2. Recently supercritical CO_2 was used to carry out nitroaldol condensation for the selective synthesis of nitroalcohols in high yields (Scheme 1.13). The reaction was promoted under very high pressure ~ 8 kbar and triethyl amine as catalyst ¹⁶³.



Scheme 1.13 Nitroaldol condensation under supercritical CO_2

3. Another solvent-free, green technology for the production of nitroalcohols (Scheme 1.14) was reported in literature with dual catalytic system consisting of a mineral base and a Triton surfactant under homogeneous conditions.



Scheme 1.14 Synthesis of β -nitroalcohols in surfactants

The drawbacks of these reactions with different catalyst in literature have led us to develop and design new catalyst. Hence the reaction discussed above will be part of our study in detail over different catalyst in the following chapters.

1.9 Physiochemical Characterization

Characterization methods are critical in evaluating various structural parameters of mesoporous materials. The techniques used to characterize mesoporous materials during the work can be categorized into the following.

1.9.1 Powder X-ray Diffraction (PXRD)

X-ray diffraction (XRD) is an extensively used technique to determine crystallographic and textural properties^{164, 165}. From the diffraction patterns, the uniqueness of mesoporous structure, phase purity, degree of crystallinity and unit cell parameters^{166, 167} of the semi-crystalline hybrid materials can be determined.

In this thesis hydrotalcites (anionic clays) and the ordered mesoporous silica (OMS) were characterized by PXRD technique both at wide angles as well as low angles.

Powder X-ray diffraction (PXRD) for hydrotalcites analysis was performed using wide angle x-ray scattering with Cu K α radiation ($\lambda = 1.5418\text{\AA}$, 40 kV, and 35 mA) using Panalytical's X'Pert Pro XRD over the 2θ range from 5 to 70°. Identification of the crystalline phases were done by comparison with JCPDS files.

SAXS spectrum was recorded on Hecus X-Ray Systems S3 Model using Cu K α radiation ($k = 1.5404\text{\AA}$) from 0-5°. It is performed by focusing an X-ray beam onto a sample and observing a coherent scattering pattern that arises from electron density inhomogeneities within the sample.

1.9.2 Fourier Transform Infra-red spectroscopy (FT-IR)

The FT-IR spectra of samples (as KBr pellets) were recorded using a Shimadzu FTIR spectrophotometer in the range of 400–4000 cm^{-1} . The powdered samples were ground with KBr in 1:20 ratio and pressed into pellets for recording the spectra (recorded with a nominal resolution of 4 cm^{-1}). FT-IR spectroscopy deals with the vibration of chemical bonds in a molecule at various frequencies depending on the elements and types of bonds. FT-IR spectroscopy is useful if there is an oscillating dipole associated with a particular vibrational mode^{168, 169}.

1.9.3 Solid State Nuclear Magnetic Resonance Spectroscopy (SS-NMR)

SS-NMR of samples was recorded on AV500S - 500 MHz High Resolution Multinuclear FT-NMR Spectrometer. Modern high-resolution solid-state NMR spectroscopy allows to elucidate the chemical and structural environment of several atoms (*e.g.* ^{13}C , ^{29}Si , ^{31}P , *etc.*) in a solid matrix like that of porous materials.^{170, 171} The most popular technique to get high-resolution NMR spectra with narrow line width is the magic angle spinning (MAS), where the solid sample is fast rotated about an axis inclined at a "magic" angle $\theta = 54^\circ 44'$ to the direction of B_0 . Cross-polarization (CP) involves indirect excitation of the less abundant nucleus through magnetization transfer from an abundant spin system (*e.g.* ^1H) to ^{13}C .

1.9.4 Microscopy

In catalysis, microscopy aids in studying the surface topography and morphology of particles, composition and crystal arrangement. Scanning electron microscopy (SEM) are important tools in textural analysis of solids^{172, 173}. SEM images were recorded on Digital Scanning Electron Microscope - JSM 6100 (JEOL). Scanning electron microscopy (SEM) is an important tool for morphological characterization of mesoporous molecular sieve materials employed to view synthesized catalysts.

1.9.5 N_2 Adsorption-Desorption Isotherms

Nitrogen adsorption–desorption isotherms were measured by using Micromeritics ASAP 2020 analyzer at -196°C . Before the adsorption measurements, all samples were out gassed for 12 h at 300°C in the degas port of the adsorption analyzer. The specific surface area was calculated by the BET method and the pore size distribution was calculated by Barrett–Joyner–Halenda (BJH) method from the desorption isotherm of the sample. The adsorption-desorption isotherms is a most widely used method for the evaluation of surface area, pore volumes and pore size distributions of porous solids¹⁷⁴. N_2 is often used as an adsorbate because of its inert nature. IUPAC has classified¹⁷⁴ the different shapes of isotherms into six types, and the different types of hysteresis loops into four types to distinguish the porous structure.

1.9.6 Temperature Programmed Desorption studies (TPD)

The number of acidic sites on the catalyst surface was determined by ammonia TPD method on Micrometrics ChemiSoft TPx V1.02 with (20ml min⁻¹) of gas flow. Temperature-Programmed Desorption (TPD) is one of the most widely used and flexible techniques for characterizing the acid and basic sites. Species are adsorbed on the surface of a catalyst at low temperature. A solid is first exposed to an adsorbate gas (NH₃, CO) under well-defined conditions (wide range of pressure and temperature) and then heated under inert conditions with a temperature program. By monitoring the gas phase concentration of species desorbed, due to a linear increase in surface temperature, key information is obtained.

1.9.7 Thermal Analysis

Various thermal analysis such as Thermo gravimetric analysis (TGA) and Differential thermal analysis (DTA), Differential Scanning Calorimetry (DSC) have been widely used to establish the thermal stability of mesoporous materials. Differential Scanning Calorimetry of the samples was recorded on Shimadzu, DSC-60. The differential scanning calorimetry (DSC) have been widely used to establish the thermal stability of mesoporous materials. DSC can be used to study thermal properties and phase changes and hence act as a fingerprint for identification purposes^{175, 176}.

1.9.8 Energy-dispersive X-ray fluorescence (EDXRF)

EDXRF of the samples to find out the content of extra element present in samples was recorded on PANalytical Epsilon-5 EDXRF System. XRF is used normally to determine the concentrations of different elements in a sample with advantages of good sensitivity.

1.10 Organization/Outline of thesis

Mesoporous materials are getting tremendous attention due to their remarkable properties such as large surface area, tunable pore size and flexibility of incorporating organic moieties. These functionalized materials are innovative materials for ion-exchange, adsorption, electronic and mechanical devices, sensors and recyclable stable heterogeneous catalysts.

Mesoporosity can be generated either by particle-particle interaction such as in layered materials (e.g. Layered Double Hydroxides) that show disordered pore systems with broad pore-size distributions or can be tuned through careful choice of surfactant and co-solvents as templating agents as in ordered mesoporous silica (OMS) materials¹⁷⁷. Materials with pores of 2-50 nm possess a potential combination of high surface area and flexibility in pore sizes that will be useful in catalysis. Thus the thesis focus was laid on the synthesis, characterization and catalytic applications of two different types of mesoporous materials particularly hydrotalcites and OMS.

The thesis is divided into eight chapters

Chapter 1 Introduction

Chapter 1 presents the general introduction and summarizes the available literature on heterogeneous catalyst especially nanoporous materials. A brief physiochemical aspect such as synthesis of mesostructured materials (hydrotalcites and ordered mesoporous materials) and their catalytic applications is provided in the chapter. It also describes the characterization techniques used in the characterization of these materials. Based on these reviews, the scope and objective of the present work have been outlined.

Chapter 2 Synthesis, characterization and catalytic applications of calcined M(II)Al hydrotalcites (where M(II)=Mg, Ni, Zn, Co, Cu).

Chapter 2 presents a brief preface on the synthesis and characterization of M(II)Al binary hydrotalcite like materials. The chapter deals with the catalytic application of basic property of M(II)Al HTlc for one step synthesis of phenytoins in the liquid phase. The mechanism for the formation of phenytoins over calcined HTlc are also proposed and explained.

Chapter 3 Synthesis, characterization and catalytic applications of CuM(II)Al-ternary hydrotalcites

Chapter 3 deals with the synthesis, characterization of CuM(II)Al HTlc and the redox property was studied for liquid phase synthesis of vanillic acid and benzil via oxidation of vanillin and benzoin respectively. The detailed catalytic activities for these reactions with plausible mechanism were also investigated.

Chapter 4 Liquid phase one pot multicomponent synthesis of Dihydropyrimidinones (DHPM's) over Aluminated mesoporous SBA-15

Chapter 4 deals with novel heterogeneous system with aluminum impregnated in ordered mesoporous materials SBA-15. These mild acidic nanocomposites are then employed for catalytic studies for biginelli's reaction. Subsequently the synthesized SBA/Al materials are characterized by XRD, N₂ adsorption, FTIR and NH₃ TPD methods.

Chapter5 Synthesis, characterization and catalytic application of SBA-15 Poly-phosphoric acid nanocomposites.

Chapter 5 deals with PPA functionalized via different methodologies such as (in-situ, impregnation methods) into the ordered mesoporous silica framework SBA-15. The chapter aims at introducing mild acidic property in mesoporous material for acylation of naphthalene. The synthesis methods for immobilization and characterization of these heterogeneous catalysts by XRD, N₂ adsorption, FTIR, ³¹P CP MAS NMR, SEM and EDXRF and NH₃ TPD are discussed in detail.

Chapter 6 Synthesis, Characterization and catalytic applications of Chloroacetic acid grafted on to Ordered Mesoporous Silica (OMS)

Chapter 6 deals with post synthetic functionalization of acidic-organic moiety chloroacetic acid on SBA-15. The characterization of chloroacetic acid functionalized SBA-15 by a range of analytical techniques is described. The catalytic application of these materials involves investigation for Knoevenagel Condensation of Cinnamaldehyde with Ethylcyanoacetate.

Chapter7 Synthesis, Characterization of polymer functionalized piperazine nanocomposites for nitroaldol condensation.

This chapter focuses on a novel radical polymerization method for the synthesis of surface modified SBA-15 and functionalization with piperazine. The surface modification is carried out by free radical polymerization of vinyl monomers with different loadings. The detailed characterization of these materials by XRD, N₂ adsorption, FTIR, ³¹P CP MAS NMR, SEM

and NH_3 TPD is discussed. The catalytic activity of these materials is investigated for a selective nitroaldol condensation

Chapter 8 Summary and conclusions

The summary of the results obtained and the basic findings of the present work are presented in this chapter. The scope for future work is also discussed at the end of this chapter.

1.11 References

1. K. Ishizaki, S. Komarneni, M. Nanko, *Porous materials: process technology and applications*, Chapman & Hall, **1998**.
2. G.C. Bond, P.W. Atkins, J.S.E. Holker, A.K. Holliday, *Heterogeneous Catalysis: Principles and Applications*, Clarendon, Oxford, **1987**.
3. K.S.W. Sing, D.H. Everett, R.A.W. Haul, L. Moscou, R.A. Pierotti, J. Rouquerol, T. Siemieniewska, *Pure Appl. Chem* 57 (**1985**) 603–619.
4. A. Corma, *Chem. Rev* 97 (**1997**) 2373-2420.
5. A. Vaccari, *Appl. Clay. Sci.* 14 (**1999**) 161-198.
6. C. Kresge, M. Leonowicz, W. Roth, J. Vartuli, J. Beck, *Nature* 359 (**1992**) 710-712.
7. G. Bachmann, *MST NEWS* (**2001**) 13-14.
8. M.C. Roco, *J. Nanopart. Res.* 3 (**2001**) 353-360.
9. V. Rieke, G. Bachmann, *J. Nanopart. Res.* 6 (**2004**) 435-446.
10. W.T. Reichle, *Solid State Ionics* 22 (**1986**) 135-141.
11. W.T. Reichle, S.Y. Kang, D.S. Everhardt, *J. Catal* 101 (**1986**) 352–359.
12. F. He, A. Vaccari, *Layered double hydroxides: present and future* (**2001**) 323.
13. V. Rives, *Layered double hydroxides: present and future*, Nova Publishers, **2001**.
14. A. Vaccari, *Catal. Today* 41 (**1998**) 53-71.
15. F. Cavani, F. Trifiro, A. Vaccari, *Catal. Today* 11 (**1991**) 173-301.
16. S. Miyata, *Clays Clay Miner.* 31 (**1983**) 305-311.
17. A. Corma, V. Fornés, F. Rey, *J. Catal* 148 (**1994**) 205-212.
18. W.T. Reichle, *Solid State Ionics* 22 (**1986**) 135-141.
19. R. Barrer, *Hydrothermal chemistry of zeolites*, Academic Pr, **1982**.
20. G. Lagaly, *Adv. Colloid Interface Sci.* 11 (**1979**) 105-148.
21. D. Zhao, Q. Huo, J. Feng, B. Chmelka, G. Stucky, *J. Am. Chem. Soc* 120 (**1998**) 6024-6036.
22. V. Alfredsson, M. Anderson, *Chem. Mater* 8 (**1996**) 1141-1146.
23. J. Beck, J. Vartuli, W. Roth, M. Leonowicz, C. Kresge, K. Schmitt, C. Chu, D. Olson, E. Sheppard, *J. Am. Chem. Soc.* 114 (**1992**) 10834-10843.
24. Q. Huo, D. Margolese, U. Ciesla, P. Feng, T. Gier, P. Sieger, R. Leon, P. Petroff, F. Schuth, G. Stucky, *Nature* 368 (**1994**) 317-321.

25. P. Tanev, T. Pinnavaia, *Science* 267 (1995) 865.
26. M. Porter, *Handbook of surfactants*, Chapman & Hall, 1994.
27. D. Karsa, M. Porter, *Biodegradability of surfactants*, Springer, 1995.
28. D. Zhao, J. Feng, Q. Huo, N. Melosh, G. Fredrickson, B. Chmelka, G. Stucky, *Science* 279 (1998) 548.
29. H. Lin, C. Mou, *Acc. Chem. Res* 35 (2002) 927-935.
30. D. Gin, W. Gu, B. Pindzola, W. Zhou, *Acc. Chem. Res* 34 (2001) 973-980.
31. S. Bagshaw, E. Prouzet, T. Pinnavaia, *Science* 269 (1995) 1242.
32. P. Tanev, T. Pinnavaia, *Chem. Mater* 8 (1996) 2068-2079.
33. F. Hoffmann, M. Cornelius, J. Morell, M. Fröba, *Angew. Chem. Int. Ed.* 45 (2006) 3216.
34. J. Clark, D. Macquarrie, S. Tavener, *Dalt. Transc.* 2006 (2006) 4297-4309.
35. D. Brunel, A. Cauvel, F. Fajula, F. DiRenzo, *Stud. Surf. Sci. Catal* 97 (1995) 173.
36. J. Beck, J. Vartuli, G. Kennedy, C. Kresge, W. Roth, S. Schramm, *Chem. Mater.* 6 (1994) 1816-1821.
37. P. Kipkemboi, A. Fogden, V. Alfredsson, K. Flodstrom, *Langmuir* 17 (2001) 5398-5402.
38. A. Stein, B. Melde, R. Schroden, *Adv. Mater.* 12 (2000) 1403-1419.
39. A. Wight, M. Davis, *Chem. Rev.* 102 (2002) 3589-3614.
40. S. Jaenicke, G. Chuah, X. Lin, X. Hu, *Microporous Mesoporous Mater.* 35 (2000) 143-153.
41. M.H. Valkenberg, W.F. Hölderich, *Cat.Rev.* 44 (2002) 321-374.
42. S. Burkett, S. Sims, S. Mann, *Chem. Commun.* 1996 (1996) 1367-1368.
43. D. Loy, K. Shea, *Chem. Rev.* 95 (1995) 1431-1442.
44. S. Inagaki, S. Guan, Y. Fukushima, T. Ohsuna, O. Terasakis, *J. Am. Chem. Soc* 121 (1999) 9611-9614.
45. K. Shea, D. Loy, *Chem. Mater* 13 (2001) 3306-3319.
46. M. Choi, F. Kleitz, D. Liu, H. Lee, W. Ahn, R. Ryoo, *J. Am. Chem. Soc* 127 (2005) 1924-1932.
47. P.T. Anastas, J.C. Warner, *Green chemistry: theory and practice*, Oxford University Press, USA, 2000.
48. D. Debecker, E. Gaigneaux, G. Busca, *Chem. Eur. J.* 15 (2009).

49. K. Takehira, T. Shishido, P. Wang, T. Kosaka, K. Takaki, *J. Catal* 221 (2004) 43-54.
50. M. Climent, A. Corma, S. Iborra, K. Epping, A. Velty, *J. Catal* 225 (2004) 316-326.
51. K. Kaneda, T. Yamashita, T. Matsushita, K. Ebitani, *J. Org. Chem* 63 (1998) 1750-1751.
52. B. Choudhary, S. Madhi, N. Chowdari, M. Kantam, B. Sreedhar, *J. Am. Chem. Soc* 124 (2002) 14127.
53. S. Kannan, *Appl. Clay. Sci.* 13 (1998) 347-362.
54. S. Kannan, *Catal. Surv. Asia.* 10 (2006) 117-137.
55. C. Kelkar, A. Schutz, *Appl. Clay. Sci.* 13 (1998) 417-432.
56. S. Jana, P. Wu, T. Tatsumi, *J. Catal* 240 (2006) 268-274.
57. T. Jyothi, T. Raja, M. Talawar, B. Rao, *Appl. Catal. A. Gen.* 211 (2001) 41-46.
58. M. Climent, A. Corma, S. Iborra, J. Primo, *J. Catal* 151 (1995) 60-66.
59. N. Das, D. Tichit, R. Durand, P. Graffin, B. Coq, *Catal. Lett.* 71 (2001) 181-185.
60. K. Kaneda, S. Ueno, T. Imanaka, *J. Mol. Catal. A: Chem.* 102 (1995) 135-138.
61. A. Dubey, V. Rives, S. Kannan, *J. Mol. Catal. A: Chem.* 181 (2002) 151-160.
62. S. Kannan, A. Dubey, H. Knozinger, *J. Catal* 231 (2005) 381-392.
63. D. Kishore, A. Rodrigues, *Appl. Catal. A. Gen.* 345 (2008) 104-111.
64. D. Kishore, A. Rodrigues, *Catal. Commun.* 10 (2009) 1212-1215.
65. K. Jain, *MedLink Neurology* (2006).
66. P. Bac, P. Maurois, C. Dupont, N. Pages, J. Stables, P. Gressens, P. Evrard, J. Vamecq, *J. Neurosci.* 18 (1998) 4363.
67. J. Engel, *Epilepsia* 42 (2001) 796-803.
68. S. Scholl, A. Koch, D. Henning, G. Kempter, E. Kleinpeter, *Struct. Chem.* 10 (1999) 355-366.
69. J. Knabe, J. Baldauf, A. Ahlhelm, *Die Pharmazie* 52 (1997) 912.
70. M. Meusel, M. Guetschow, *Org. Prep. Proced. Int.* 36 (2004) 391-443.
71. A.K. Silverman, J. Fairley, R.C. Wong, *J. Am. Ac. Derm.* 18 (1988) 721-741.
72. T. Rodgers, M. LaMontagne, A. Markovac, A. Ash, *J. Med. Chem.* 20 (1977) 591-594.
73. M. Brown, G. Brown, W. Brouillette, *J. Med. Chem* 40 (1997) 602-607.
74. M. Bazil, PhD, CW, M. Pedley, TA, *Annu. Rev. Med.* 49 (1998) 135-162.
75. C. Lander, M. Smith, J. Chalk, C. de Wyt, P. Symoniw, I. Livingstone, M. Eadie, *Eur. J. Clin. Pharm.* 27 (1984) 105-110.

76. R. Rosenthal, C. Perkel, P. Singh, O. Anand, C. Miner, *Amer.J.Addict.* 7 (1998) 189-197.
77. E. Ware, *Chem. Rev.* 46 (1950) 403-470.
78. M. Cloyd, W. Lynn, *Virology* 181 (1991) 500-511.
79. R.N. Comber, R.C. Reynolds, J.D. Friedrich, R.A. Manguikian, R.W. Buckheit Jr, J.W. Truss, W.M. Shannon, J.A. Secrist III, *J. Med. Chem.* 35 (1992) 3567-3572.
80. S. Gulati, C. Sriram, V. Kalra, *Ind.Pedi.* 39 (2002) 826-829.
81. S. Shaw, G. Krauss, *Curr.Treat.Options.Neurl.* 10 (2008) 260-268.
82. S. PROFILES, *Chemical Sources International, Inc.* <http://www.chemsources.co>.
83. H. Bucherer, W. Steiner, *J. Prakt. Chem.* 140 (1934) 291-316.
84. H. Bucherer, V. Lieb, *J. Prakt. Chem.* 141 (1934) 5-43.
85. N. Mahmoodi, S. Emadi, *Russ. J. Org. Chem.* 40 (2004) 377-382.
86. E. Gallienne, G. Muccioli, D. Lambert, M. Shipman, *Tetrahedron Lett.* 49 (2008) 6495-6497.
87. N.O. Mahmoodi, Z. Khodae, *ARKIVOC* 3 (2007) 29-36.
88. N.O. Mahmoodi, S. Emadi, *Russ. J. Org. Chem.* 40 (2004) 377-382.
89. G.G. Muccioli, J.H. Poupaert, J. Wouters, B. Norberg, W. Poppitz, G.K.E. Scriba, D.M.Lambert, *Tetrahedron* 59 (2003) 1301-1307.
90. E. Angelescu, O. Pavel, R. Bîrjega, M. Florea, R. Z voianu, *Appl.Catal. A.Gen.* 341 (2008) 50-57.
91. C. Jiménez-Sanchidrián, J. Hidalgo, R. Llamas, J. Ruiz, *Appl.Catal. A.Gen.* 312 (2006) 86-94.
92. P. Delaquis, K. Stanich, P. Toivonen, *J. Food Prot.* 68 (2005) 1472-1476.
93. W.S. Knowles, W.S. Sabacky, B.D.Vineyard, Vineyard, L-Dopa and Intermediates, U. S. Pat. 4, 005,127, 1977.
94. C. Chou, *Ecological studies: analysis and synthesis (USA)* 78 (1990) 105.
95. D. Esiyok, S. Otles, E. Akcicek, *J.Canc.Prevent.* 5 (2004) 334-339.
96. C. Michel, S. Isabelle, , US5686406, 1997.
97. Y. Sazanov, I. Podeshvo, G. Mikhailov, G. Fedorova, M. Goikhman, M. Lebedeva, V. Kudryavtsev, *Russ. J. Appl. Chem.* 75 (2002) 777-780.
98. I.A. Pearl, Synthesis of vanillic acid, in: US 275690 (Ed.).
99. C. Andras, L. Gyoergy, S. Istvan, V. Pal, R. Andras, in: HU19890004337. (Ed.).

100. M. Hocking, *J. Chem. Educ.* 74 (1997) 1055.
101. P.S.J.Cheetham, J.T.Sime, M.L.Gradeley, Flavor/Aroma Materials and their preparation, US 6844019 2005.
102. A. Dausch, G. Pastore, *Quim. Nova* 28 (2005) 642-645.
103. H.R. Bjorsvik, F. Minisci, *Org. Process Res. Dev.* 3 (1999) 330-340.
104. A. Muheim, K. Lerch, *Appl. Microbiol. Biotechnol.* 51 (1999) 456-461.
105. B. Lindgren, T. Nilsson, *Acta Chem. Scand* 27 (1973) 888-890.
106. I. Pearl, *J. Am. Chem. Soc.* 68 (1946) 2180-2181.
107. C. Kathari, P. Pol, S. Nandibewoor, *Turk.J.Chem.* 26 (2002) 229-236.
108. T. Jose, S. Nandibewoor, S. Tuwar, *J. Solution Chem.* 35 (2006) 51-62.
109. C. Fargues, Á. Mathias, J. Silva, A. Rodrigues, *Chem.Eng.Techn.* 19 (2004) 127-136.
110. I. Pearl, *J. Am. Chem. Soc.* 68 (1946) 429-432.
111. H. Bjorsvik, L. Liguori, *Org. Process Res. Dev.* 6 (2002) 279-290.
112. H. Wynberg, H.J. Kooreman, *J. Am. Chem. Soc.* 87 (1965) 1739-1742.
113. S. Buckland, R. Davidson, *Pesticide Science* 19 (2006) 61-66.
114. R. Wadkins, J. Hyatt, X. Wei, K. Yoon, M. Wierdl, C. Edwards, C. Morton, J. Obenauer, K. Damodaran, P. Beroza, *J. Med. Chem* 48 (2005) 2906-2915.
115. T. Hagiwara, A. Horike, Benzil ketal derivatives, US 4,480,094, 1984.
116. W.W. Paudler, J.M. Barton, *J. Org. Chem.* 31 (1966) 1720-1722.
117. W.R. Dunnivant, F.L. James, *J. Am. Chem. Soc.* 78 (1956) 2740-2743.
118. J. Crivello, M. Sangermano, *J. Polym. Sci., Part A: Polym. Chem.* 39 (2000) 343-356.
119. R. Kuhlmann, W. Schnabel, *Polymer* 18 (1977) 1163.
120. J.S. Buck, S.S. Jenkins, *J. Am. Chem. Soc.* 51 (1929) 2163-2167.
121. H. Yamaoka, N. Moriya, M. Ikunaka, *Org. Process Res. Dev.* 8 (2004) 931-938.
122. N. Singh, D. Lee, *Proc. Res. Develop* 5 (2001) 599-603.
123. R. Bhatia, G. Rao, *J. Mol. Catal. A: Chem.* 121 (1997) 171-178.
124. B. El Ali, A.M. El-Ghanam, M. Fettouhi, *J. Mol. Catal. A: Chem.* 165 (2001) 283-290.
125. X. Lin, G. Chuah, S. Jaenicke, *J. Mol. Catal. A: Chem.* 150 (1999) 287-294.
126. M. Alvaro, A. Corma, D. Das, V. Fornés, H. García, *Chem. Commun.* 2004 (2004) 956-957.
127. M. Alvaro, A. Corma, D. Das, V. Fornés, H. García, *J. Catal* 231 (2005) 48-55.
128. J. Melero, G. Stucky, R. Grieken, G. Morales, *J. Mater. Chem.* 12 (2002) 1664-1670.

129. P. Gore, *Chem.Rev.* 55 (1955) 229-281.
130. G. Olah, *Friedel-Crafts Chemistry*, Wiley New York, 1973.
131. G. Olah, J. Olah, *J Am Chem Soc* 98 (1976) 1839-1842.
132. W. Pardee, B. Dodge, *Ind. Eng. Chem.* 35 (1943) 273-278.
133. K. Davenport, C. Linstid III, Acylation of naphthalenes, US Patent 4,593,125, 1986.
134. P. Harrington, E. Lodewijk, *Org. Process Res. Dev* 1 (1997) 72-76.
135. G. Land, J. Maignan, S. Restle, G. Malle, Naphthalene derivatives having retinoid typection, the process for preparation thereof and medicinal and cosmetic compositions containing them, US 4,879,284, 1989.
136. K. Nelson, *Ind. Eng. Chem.* 48 (1956) 1670-1694.
137. H. Brown, H. Pearsall, L. Eddy, W. Wallace, M. Grayson, K. Nelson, *Ind. Eng. Chem.* 45 (1953) 1462-1469.
138. G. Olah, J. Olah, *J. Am. Chem. Soc* 98 (1976) 1839-1842.
139. R. Sheldon, R. Downing, *Appl. Catal. A.Gen.* 189 (1999) 163-183.
140. R. Singh, R. Kamble, K. Chandra, P. Saravanan, V. Singh, *Tetrahedron* 57 (2001) 241-247.
141. L. ervený, K. Mikulcová, J. ejka, *Appl. Catal. A* 223 (2002) 65.
142. K. Gaare, D. Akporiaye, *J. Mol. Catal. A: Chem.* 109 (1996) 177-187.
143. P. Kurek, Acylation of aromatic compounds by acid anhydrides using solid acid catalysts, US 5,126,489, 1992.
144. J. Deutsch, V. Quaschnig, E. Kemnitz, A. Auroux, H. Ehwald, H. Lieske, *Top. Catal.* 13 (2000) 281-285.
145. J. Deutsch, H. Prescott, D. Müller, E. Kemnitz, H. Lieske, *J. Catal* 231 (2005) 269-278.
146. F. Luzzio, *Tetrahedron* 57 (2001) 915-946.
147. G. Rosini, *In Comprehensive Organic Synthesis, Trost, BM Ed*, Pergamon: Oxford, 1991.
148. O. Berner, L. Tedeschi, D. Enders, *Eur. J. Org. Chem.* 2002 (2002) 1877-1894.
149. R. Varma, R. Dahiya, S. Kumar, *Tetrahedron Lett.* 38 (1997) 5131-5134.
150. I. Kudyba, J. Raczko, J. Jurczak, *J. Org. Chem* 69 (2004) 2844-2850.
151. A. Barrett, G. Graboski, *Chem. Rev.* 86 (1986) 751-762.
152. B. Trost, V. Yeh, H. Ito, N. Bremeyer, *Org. Lett* 4 (2002) 2621-2623.

153. R. Looper, R. Williams, *Angew. Chem.* 116 (2004) 2990-2993.
154. M. Karimov, M. Levkovich, V. Leont'ev, A. Sadykov, K. Aslanov, T. Yunusov, A. Sadykov, *Chem. Nat. Compd.* 10 (1974) 490-495.
155. H. Sasai, N. Itoh, T. Suzuki, M. Shibasaki, *Tetrahedron Lett.* 34 (1993) 855-858.
156. E. Takaoka, N. Yoshikawa, Y. Yamada, H. Sasai, M. Shibasaki, *Heterocycles* 46 (1997) 157-163.
157. P. Brian, J. Grove, J. McGowan, *Nature* 158 (1946) 876.
158. M. Sittig, *Pharmaceutical manufacturing encyclopedia*, William Andrew Publishing, 1988.
159. P. Kisanga, J. Verkade, *J. Org. Chem* 64 (1999) 4298-4303.
160. T. Laird, *Org. Process Res. Dev.* 13 (2009) 364-370.
161. J. Melton, J. McMurry, *J. Org. Chem.* 40 (1975) 2138-2139.
162. T. Arai, R. Takashita, Y. Endo, M. Watanabe, A. Yanagisawa, *J. Org. Chem* 73 (2008) 4903-4906.
163. C. Rayner, *Org. Process Res. Dev* 11 (2007) 121-132.
164. W. Callister Jr, *Materials Science and Engineering: An Introduction, 4; Callister, Jr., William D, 1997.*
165. S. Elliott, *The physics and chemistry of solids*, Wiley New York, 1998.
166. S. Biz, M. Occelli, *Cat. Rev. Sci. Eng.* 40 (1998) 329-407.
167. G. Bergeret, P. Gallezot, J. Weitkamp, *VCH, Weinheim* 2 (1997) 439.
168. P. Atkins, *Physical Chemistry*, Oxford, 1998.
169. P. Griffiths, J. De Haseth, *Fourier transform infrared spectrometry*, Wiley-Interscience, 2007.
170. F. Rushworth, D. Tunstall, *Nuclear magnetic resonance*, Gordon & Breach Science Pub, 1973.
171. G. Engelhardt, D. Michel, *High-resolution solid-state NMR of silicates and zeolites*, John Wiley & Sons Chichester, 1988.
172. J. Goldstein, D. Newbury, P. Echlin, C. Lyman, D. Joy, E. Lifshin, L. Sawyer, J. Michael, *Scanning electron microscopy and X-ray microanalysis*, Plenum Pub Corp, 2003.
173. D. Joy, A. Romig, J. Goldstein, *Principles of analytical electron microscopy*, Springer, 1986.

174. F. Rouquerol, J. Rouquerol, K. Sing, *Adsorption by Powders and Porous Solids: Principles (1999)*.
175. E. Lopez-Salinas, E. Torres-Garcia, M. Garcia-Sanchez, *J. Phys. Chem. Solids* 58 (1997) 919-925.
176. L. Pesic, S. Salipurovic, V. Markovic, D. Vucelic, W. Kagunya, W. Jones, *J. Mater. Chem.* 2 (1992) 1069-1073.
177. D. De Vos, M. Dams, B. Sels, P. Jacobs, *Chem.Rev.* 102 (2002) 3615-3640.

Chapter 2
Synthesis, Characterization and
Catalytic Applications of Calcined
M(II)Al-Hydrotalcites, where
M(II)=Mg, Ni, Zn, Co, Cu

2.1 Introduction

Hydrotalcites (HTs) are known to exhibit basic as well as redox properties with different combinations of divalent and trivalent metal ions. Particularly the basic properties of calcined hydrotalcites M(II)Al are universally acknowledged. The calcinations of fresh (as-synthesized) Mg/Al catalysts at different temperatures generate mixed metal oxides with the formation of spinel and inverse spinel phases. With this view in the present chapter, we report the synthesis, characterization of calcined M(II)Al-HTs for one step synthesis of phenytoins in the liquid phase for the first time under milder reaction conditions. The mechanism for the formation of phenytoins over calcined HTs has also been proposed and explained.

2.2 Liquid phase synthesis of phenytoin over Mg/Al-HTs

Phenytoin (dilantin or 5,5-diphenylhydantoin), is a useful pharmacological compound, the vast scope and applications of this compound and its derivatives have been already discussed in introductory section. Many homogeneous methods were developed to synthesize hydantoin and their derivatives¹ such as α -amino amides with triphosgene², amino acids with acetic anhydride and ammonium thiocyanate (thiophenytoin), carbodiimides with α , β -unsaturated carboxylic acids, nitriles with organometallic reagents,³⁻⁵ α -amination of esters by Cu(I)⁶ and gallium (III) salts⁷. In addition, microwave synthesis, solid phase technologies^{8,9} and the esoteric syntheses of hydantoins involving complex rearrangements^{10,11} have also been developed for the synthesis of phenytoins. Very recently, 5,5-diphenyl-2,4-imidazolidinedione (phenytoin) derivatives were synthesized using Almonds¹². However, the use of homogeneous reagents for the synthesis of phenytoins limits their practical utilization because of the difficulties in the product purification, to overcome the effluent treatment problems and environmental concerns. Therefore, the development of heterogeneous catalysts for the one step synthesis of phenytoin still remains a serious challenge and according to the best of literature knowledge no report is available for the synthesis of phenytoins over calcined hydrotalcites. Hence in the present chapter we report the synthesis characterization and the potential use of M(II)/Al (where M(II) = Mg, Ni, Co, Zn) calcined hydrotalcites for the liquid phase synthesis of phenytoins under environmental friendly conditions.

2.3 Synthesis of M(II)Al Calcined Hydrotalcites.

The hydrotalcites were synthesized by co-precipitation method via the low supersaturation technique. Two solutions; solution (I) containing the desired amount of metal nitrates M(II) – Mg, Ni, Zn, Co, Cu and M(III)–Al, and solution (II) having precipitating agents (i.e. NaOH and Na₂CO₃), were added simultaneously, while maintaining the pH around 9-10 under stirring at room temperature. The addition took around 100 minutes and the final pH of the solution was adjusted to 10. The samples were aged at 338K for 18 h, filtered, washed with hot water (until total absence of nitrates and sodium in the washing liquids) , dried in an air oven at 353K for 12 h and the solids synthesized were hand ground. In all cases, the atomic ratio between the divalent and trivalent cations was varied between 5:1 and 1:5. The samples were named as M(II)Al-HT. Similarly ternary hydrotalcites M(II)M'(II)Al-HT, M(II)/M'(II)=3 and (M(II)+M'(II))/Al=3) with different combinations of co-bivalent metal ions were also synthesized to compare the activity and selectivity. The fresh samples were calcined at different temperatures depending upon their decomposition pattern to obtain the mixed oxides with different acid-base properties.

2.4 Physiochemical Characterizations

2.4.1 PXRD

Figure 2.1(A) shows the PXRD pattern of Mg/Al-3 calcined at different temperatures. The calcinations temperatures were chosen depending upon the decomposition pattern of hydrotalcites. At 150°C the dehydroxylation of interlayer occurs and the hydrotalcite phase starts decreasing. At 450°C, dehydroxylation and decarboxylation of the sheet occur and the HTs phase is completely destroyed resulting in the formation of mixed metal oxides (Mg-O-Al). At 600°C and 800°C, the hydrotalcite phase completely disappears and with the formation of mixed oxides (Mg-O-Al) and spinel Mg/Al₂O₄ phase. The peak at $2\theta = 36^\circ$, 42° and 65° can be indexed to the presence of MgO and γ -Al₂O₃ and Mg/Al₂O₄ respectively according to JCPDX classification¹³. Based on the catalytic activity results it was observed that Mg/Al-3 HTs at 600°C exhibits maximum conversion and yield (discussed in detail in catalytic section) and therefore the interest emerged to study the catalytic activity over Mg/Al-HTs with different Mg/Al compositions. (Figure 2.1 (B)) showed the PXRD diffraction pattern of different atomic compositions of Mg/Al and also indicates the

formation of spinel $\text{Mg}/\text{Al}_2\text{O}_4$ and mixed oxides, MgO and $\gamma\text{-Al}_2\text{O}_3$ phases. The formation of spinel phase is facilitated more with the samples having higher concentration of Mg contents.

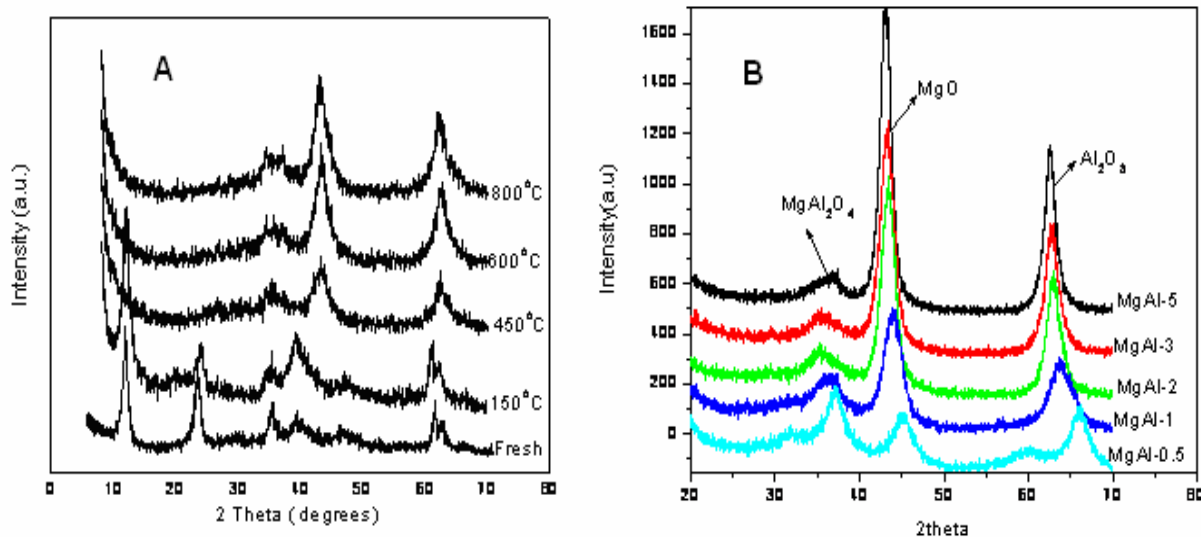


Figure 2.1 PXRD patterns of (A) Mg/Al-3 calcined at different temperatures and (B) with different Mg/Al ratio calcined at 873K.

2.4.2 FT-IR

Figure 2.2 showed the FT-IR spectrum of fresh (as-synthesized) Mg/Al HTs. Generally four kinds of vibrations ν_1 , ν_2 , ν_3 and ν_4 are observed for the hydrotalcite phase in Mg/Al fresh hydrotalcites¹⁴. The ν_1 broad peak at 3560 cm^{-1} is attributed to the vibrations of structural O-H groups or due to the vibrations of O-H---OH stretching. A shoulder peak ν_2 at 3060 cm^{-1} is a characteristic stretching vibrations of CO_3^{2-} ---OH in hydrotalcites. A weak absorption band ν_3 at $1650\text{--}1620\text{ cm}^{-1}$ is due to the deformation mode of interlayer water molecules. The intensity of the band depends upon the amount of water present in the hydrotalcite layers. CO_3^{2-} anion with different symmetries shows different peaks in HTs phase. A sharp intense peak observed at 1360 cm^{-1} is due to the anti-symmetric stretching of interlayer CO_3^{2-} anion that indicates D_{3h} kind of symmetry¹⁵. The symmetry of CO_3^{2-} anion will change from D_{3h} to C_{2v} geometry if a peak at 1080 cm^{-1} was present.

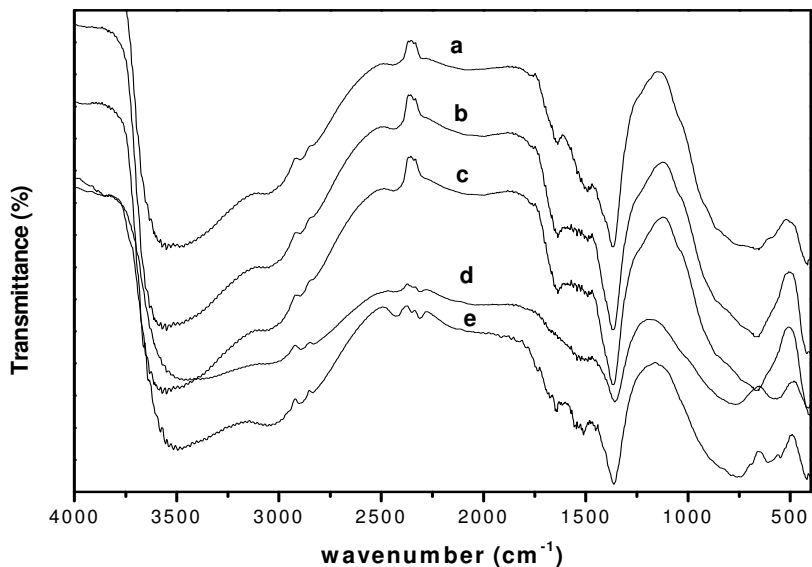


Figure 2.2 FT-IR of fresh (a) Mg/Al-5, (b) Mg/Al-3, (c) Mg/Al-2, (d) Mg/Al-1 (e) Mg/Al-0.2 HTs

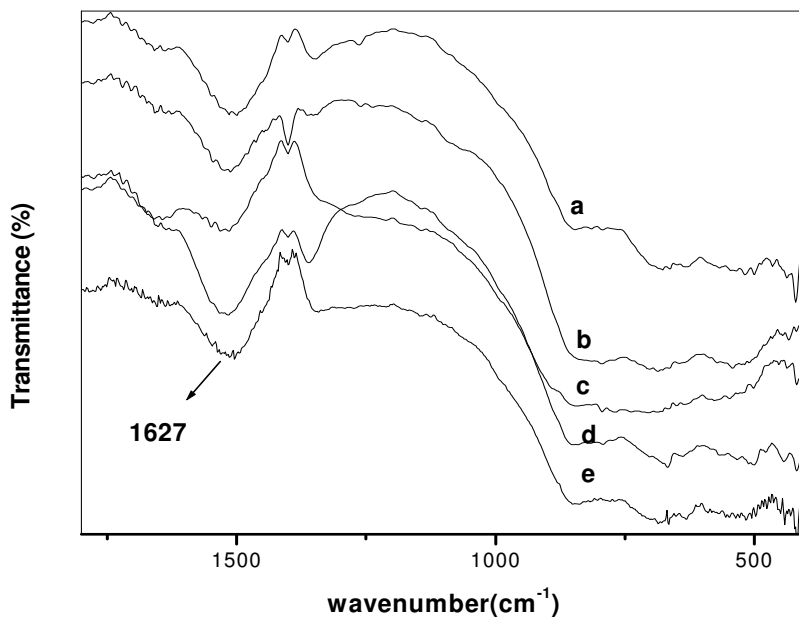


Figure 2.3 FT-IR of (a) Mg/Al -5, (b) Mg/Al-3, (c) Mg/Al-2, (d)Mg/Al-1, (e) Mg/Al-0.2 HTs calcined at 873K.

Figure 2.3 showed the FT-IR spectrum of Mg/Al-HTs with different Mg/Al ratio's calcined at 873K. Despite the complete dehydroxylation of samples at calcination temperature 873 K, peak at 1627 cm^{-1} indicated the deformation mode of O-H stretching of adsorbed water

molecules. And also the disappearance of peak at 1360cm^{-1} indicated complete decarboxylation of hydrotalcite phase in Mg/Al-HTs and resulted in mixed oxides.

2.4.3 Surface area Measurements

Table 2.1 showed the specific surface area, pore volume and pore diameter of mixed oxides Mg/Al-HTs calcined at 873K. The specific surface area increases with increase in Al content and maximum surface area is observed with Mg/Al= 0.2. The surface area and the pore volume of the samples increase with increase in the Al-content for which the reasons were not clear. The increase in the pore volume of Al- rich samples may be due to the formation of porous network.

Table 2.1 Structural parameters of Mg/Al-HTs calcined at 873K

Catalyst	Surface area (m^2/g)	Pore volume ($\text{cm}^3 \text{g}^{-1}$)	Average pore Width (\AA)
Mg/Al-5	41	0.705	710
Mg/Al-3	152	1.19	311
Mg/Al-2	117	0.95	323
Mg/Al-1	171	1.08	248
Mg/Al-0.2	304	0.663	85

2.4.4 Basicity Measurements

Basic strength of the calcined Mg/Al-HTs was qualitatively determined by using Hammett indicators. Bromthymol blue ($H= 7.1$), phenol red ($H= 7.4$), cresol purple ($H= 8.3$), thymol blue ($H= 8.9$), phenolphthalein ($H= 9.7$), and alizarine yellow ($H= 11.0$), 4-nitroaniline ($H=18.4$) and 4-chloroaniline ($H=26.5$) were chosen as Hammett indicators.

1ml of Hammett indicator was added to 25mg of the samples followed by the dilution with 10ml of methanol. The colour of the catalyst was noted after equilibrating the reaction mixture for 4h (Table 2.2).

The soluble basicity was also determined by titration method using 0.02 mol/l anhydrous methanolic solution of benzoic acid. The calcined hydrotalcite (Mg/Al-3) was added to 50ml distilled water and stirred vigorously for 1h and filtered, and then titrated with benzoic acid. The soluble basicity was found to be 0.64mmol/g and is in agreement with the previously reported results^{16, 17}.

Table 2.2 Base strength of Mg/Al HTs calcined at 873K.

Catalyst	Base Strength
Mg/Al-5	$12 < pK_{BH^+} < 18.5$
Mg/Al-3	$18.4 < pK_{BH^+} < 26.5$
Mg/ Al-2	$11 < pK_{BH^+} < 18.4$
Mg/Al-1	$11 < pK_{BH^+} < 18.4$
Mg/ Al-0.2	$11 < pK_{BH^+} < 15$

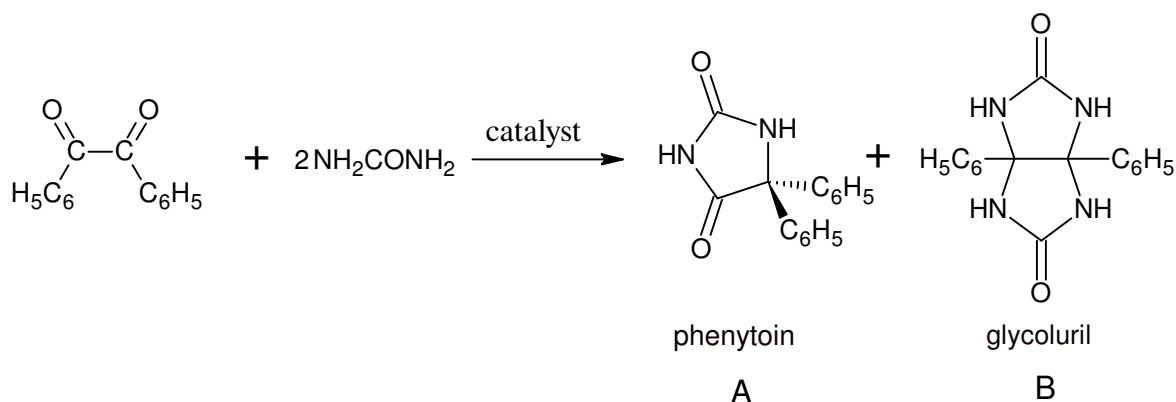
Different ranges of basicity using Hammett indicator of Mg/Al-calcined hydrotalcites shows that basicity is due to (Mg-O pairs), (O^{2-}), and low (OH^- groups). Furthermore, maximum basic strength was attained for Mg/Al molar ratio 3. However with increase in Mg content i.e. (Mg/Al-5) the basicity decreases. These results are in agreement with the which was in consistent with the results obtained on hammett indicators¹⁶ and results in drop of catalytic activity (Table 2.4). Similar trends were also reported by other researchers qualitatively.

Conventionally, the Hammett indicator measurements are performed using non-polar solvent. However, since methanol was employed as both solvent and reactant in the present reaction, so it was appropriate to use methanol and thus giving a better measure of the catalyst basicity under reaction conditions. Additionally, the basicity of Mg/Al-3 was measured at different calcinations temperature and it was found that maximum basicity is achieved at 873 K rather than at 723K.

2.5 Catalytic Studies

2.5.1 Synthesis of phenytoin

2mmol of benzil, 4mmol of urea and 15ml of solvent (methanol) were mixed at desired temperature (298 -373K) in a glass reactor and different amount of catalyst (10-500mg) was added at once to the previously stirred solution. The course of the reaction was monitored by TLC by taking samples periodically for 24h. The product identification was also done by gas chromatography after considering the response factors of the authentic samples. After the completion of the reaction, the catalyst was vacuumed filtered and removed under reduced pressure to isolate the product A (Scheme 2.1) and unreacted benzil by solvent extraction method to account for the mass balance. Finally, the product (A) was recrystallized with ethanol, dried and weighed to calculate the isolated yield.



Scheme 2.1 Synthesis strategy for the production of hydantoin

The product extraction was little difficult due to the solubility constraints of the product with the reactants and therefore comparatively low yield of product (A) was obtained. Similarly benzil was also isolated from the reaction mixture and the total conversion is estimated on the basis of benzil reacted. The product was extracted by adding water from the left over semi-liquid mixture to obtain white colored phenytoin product (A). The product (A) was recrystallized with ethanol, dried and finally the weight of the isolated product was calculated and reported as the isolated yield.

2.5.2 Effect of different bivalent metals in binary M(II)/Al

The catalytic activity (Table 2.3) of the fresh binary hydrotalcites with M(II)/Al-3 (where M (II) = Ni, Zn, Co, Cu) showed very low conversion, yield and the selectivity of the desired product A (Scheme 2.1). It is generally known that the thermal decomposition of hydrotalcites at 873K results in the formation of mixed oxides with enhanced basic properties M(II)-O-Al) and hence the catalytic activity was tested on all the binary calcined M(II)Al-HTs. Table 2.4 showed very high conversion, yield and selectivity of the product (A) in all the calcined hydrotalcites indicating the influence of enhanced acidic-basic properties (bronsted or Lewis)¹⁸⁻²⁰ compared to the fresh hydrotalcites.

Table 2.3 Effect of different fresh hydrotalcites M(II)Al-3 on the conversion of phenytoin.

Catalyst	^a Conversion (%)	Product Selectivity (%)		^b Yield (%)
		(A)	(B)	

Mg/Al	40	100	0	24
Ni/Al	35	93	6	19
Zn/Al	30	95	4	16
Cu/Al	12	92	7	7
Co/Al	0	-	-	-

Conditions: Benzil- 420 mg, Urea-240 mg, Solvent- methanol, Catalyst weight- 50mg, Temperature-338 K, Reaction time -24h.

^aconversion is based on the benzil reacted..

^bbased on isolated phenytoin (A)

Table 2.4 Variation of total conversion, product selectivity and product yield over different catalysts (Hydrotalcites used are calcined at 873K)

Catalyst	Conversion (%)	Product Selectivity (%)		Yield (%)
		(A)	(B)	
Blank	0	-	-	-
MgO	60	71	28	44
Al ₂ O ₃ (basic)	15	80	19	9
KOH	80	77	22	61
Mg/Al-3	94	95	5	73
Ni/Al -3	44	91	8	31
Zn/Al -3	40	90	9	27
Cu/Al -3	18	89	10	12
Co/Al -3	5	90	9	-

Conditions as in Table 2.3

Among all the calcined binary hydrotalcites with different M(II)/Al atomic compositions, highest yield (73%) and the selectivity (95%) of the product (A) was obtained on the Mg/Al-3. It is to be mentioned here that no conversion was obtained in the blank reaction (without catalyst) and very low conversion and selectivity of the desired product (A) was obtained on commercial MgO, Al₂O₃ (basic) and KOH further indicate the necessity of the mixed oxides (both acid-base properties) in controlling the selectivity of the product (Scheme 2.2, proposed mechanism). FT-IR and ¹H-NMR of the sample was compared to prove the structure of phenytoin (Figure 2.4).

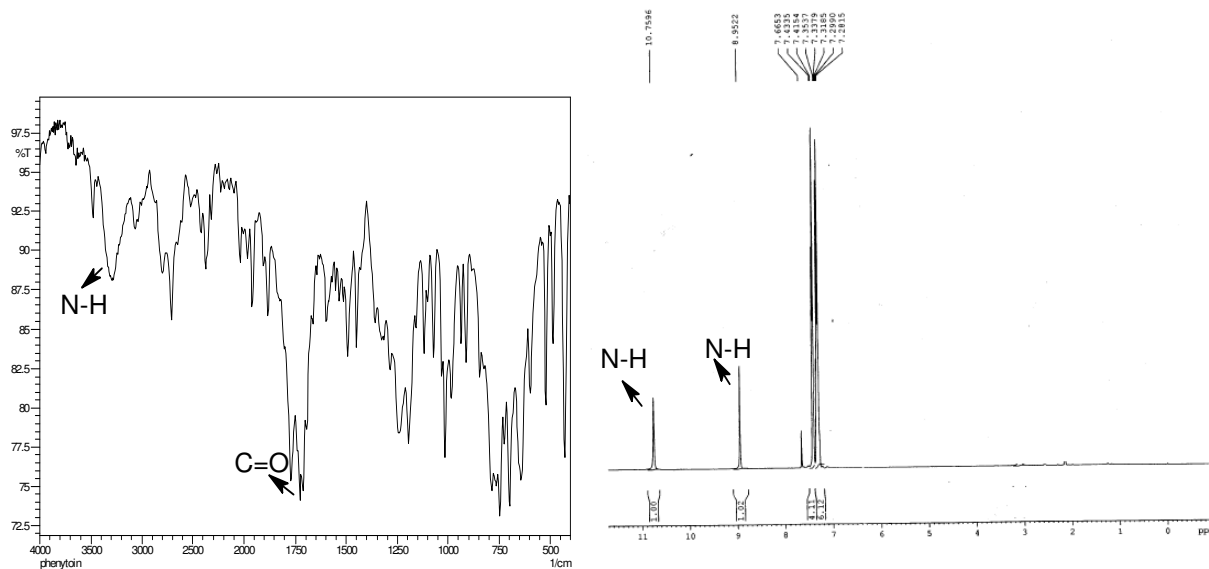


Figure 2.4 FT-IR and ¹H-NMR of the desired product (phenytoin)

2.5.3 Effect of calcined ternary hydrotalcites

The catalytic can be significantly enhanced in the presence of co-bivalent metal ion in ternary HTs. Therefore in order to see the effect of M(II)M'(II)Al HTs (Table 2.5), the catalytic

Table 2.5 Effect of different calcined hydrotalcites on conversion of phenytoin

Catalyst	Conversion (%)	Product Selectivity (%)		Yield (%)
		(A)	(B)	
MgNiAl	35	91	8	26
MgZnAl	56	90	9	43
NiZnAl	18	89	10	10

Conditions as in Table 2.3

activity was also studied on calcined ternary hydrotalcites but very low conversion of phenytoins was observed compared to binary calcined hydrotalcites. These results were similar to the earlier reports¹⁴ and may be due to the formation of different mixed oxide phases responsible for activity and selectivity.

2.5.4 Effect of M(II)/Al catalyst ratio on M(II)/Al-HTs

Although, Mg/Al catalyst calcined at 873K proved to be the most active catalyst at the fixed metal composition (Mg/Al-3) yet the nature of the mixed oxides in each individual series (e.g. Mg/Al, Zn/Al etc) may vary at different metal composition (M(II)/Al).

Table 2.6 Effect of different ratio of M(II)/Al-HTs calcined at 873K on the yield of phenytoin.

M(II)/Al	Mg /Al	Zn/Al	Ni/Al	Co/Al
	Yield (%)	Yield (%)	Yield (%)	Yield (%)
5	53	16	37	-
3	73	27	32	4
2	26	20	27	33
1	19	40	24	41
0.2	17	28	25	-

Conditions as in Table 2.3

Each series of bivalent metal ions exhibited maximum conversion of the desired product at different metal composition and infers the different nature of the mixed oxides with different metal combination (Table 2.6). However, the catalytic results of different atomic compositions on Mg/Al indicates that the catalytic activity increased with increase in the Mg contents up to Mg/Al-3 (Table 2.7) and then decreased with further increase in the Mg concentration at Mg/Al-5. This is due to the decrease in the basicity of the Mg/Al-5 HTs and low surface area compared to Mg/Al-3 (Table 2.1). Therefore, the best catalyst (Mg/Al-3, calcined at 873K) was selected for further detailed catalytic study.

Table 2.7 Variation of the yield of phenytoin over different Mg/Al compositions calcined at 873K.

Catalyst ratio Mg/Al	Conversion (%)	Yield (%)	Surface area (m ² /g)
0.2	20	17	304
1	28	19	171
2	40	26	117
3	94	73	152
5	70	53	41

Conditions as in Table 2.3

2.5.5 Effect of calcinations temperature on Mg/Al-3

The calcinations temperature plays an important role in altering the acid-base properties of the mixed oxides (Mg-O-Al). Therefore the catalyst (Mg/Al-3) was calcined at different temperature (423K, 723K, 873K, and 1073K) in order to seek for better activity and selectivity (Figure 2.1 (A)). It was observed that the catalytic conversion and the yield of the desired product increased with increase in the calcinations temperature up to 873K and slightly decreased at 1073K under our experimental conditions. This reduction in the activity may be due to the decrease in the basicity of the catalyst (Table 2.1). These results (Table 2.8) clearly demonstrate the generation of different acidic-basic properties of the mixed oxides generated at different calcinations temperatures responsible for this reaction. Hence the catalyst calcined at 873K was chosen for further studies.

Table 2.8 Variation of calcination temperature on the conversion of the phenytoin over calcined Mg/Al-3 HT

Calcination temp (K)	Conversion (%)	Yield (%)	Product selectivity (A) (%)
423	24	15	95
723	86	61	95
873	94	73	95
1073	83	63	90

Conditions as in Table 2.3

2.5.6 Effect of the catalyst weight

Figure 2.5 showed the effect of catalyst weight on the conversion and the yield of the product (A). The conversion as well as the yield of the product increased with the increase in the weight of the catalyst up to 75mg and then started decreasing slightly with further increase in the weight of the catalyst. Moreover, the time on stream studies (TOS) indicated that the conversion is kinetically faster initially for higher catalyst concentration but decreased slightly with further course of time compared to the lower catalyst concentration. This may be due to the fact that some amount of the secondary or the interconverted products (although not detected by GC & TLC) might be forming on the catalyst surface which might block the active centers of the catalyst thereby reducing the conversion.

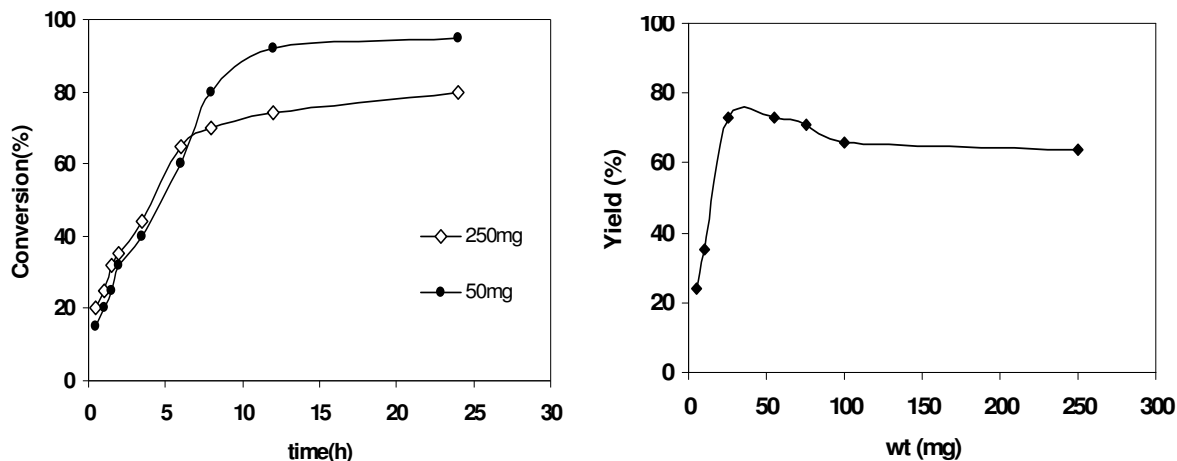


Figure 2.5 Influence of catalyst weight on the conversion of phenytoin over Mg/Al-3 HT

To confirm this, both the catalyst (50mg and 250mg) were filtered after the reaction and washed thoroughly with the acetone, water and again calcined at 873K. The weight of the catalyst (250mg) was observed slightly more (0.02%) whereas no increase in the weight was observed in 50mg of the catalyst. When subjected to fresh reaction for second cycle, small decrease in the conversion (75%) and the product yield (62%) was observed for 250mg of the catalyst but no significant difference in the activity and selectivity was observed for 50mg catalyst. These results explain the cause for the reduction in the conversion at higher catalyst concentration and also confirm the reusability of the catalysts.

2.5.7 Time-on-stream studies (TOS)

In order to compare the activity and selectivity of the desired product, the time-on-stream studies (Figure 2.6, A) were carried out using calcined Mg/Al-3 and KOH. The catalytic results on Mg/Al-3 catalyst indicated the increasing trend on the conversion and the yield of the product (A). Careful examination of the catalytic results showed that the reaction was almost completed within 10h of the reaction time with 95% selectivity of the product. The reaction was allowed to proceed further for 24 h to see the formation of secondary products or the inter conversion of the product(s). However, no difference in the activity and selectivity was noted indicating that the product formed is quite stable under our experimental conditions.

A

B

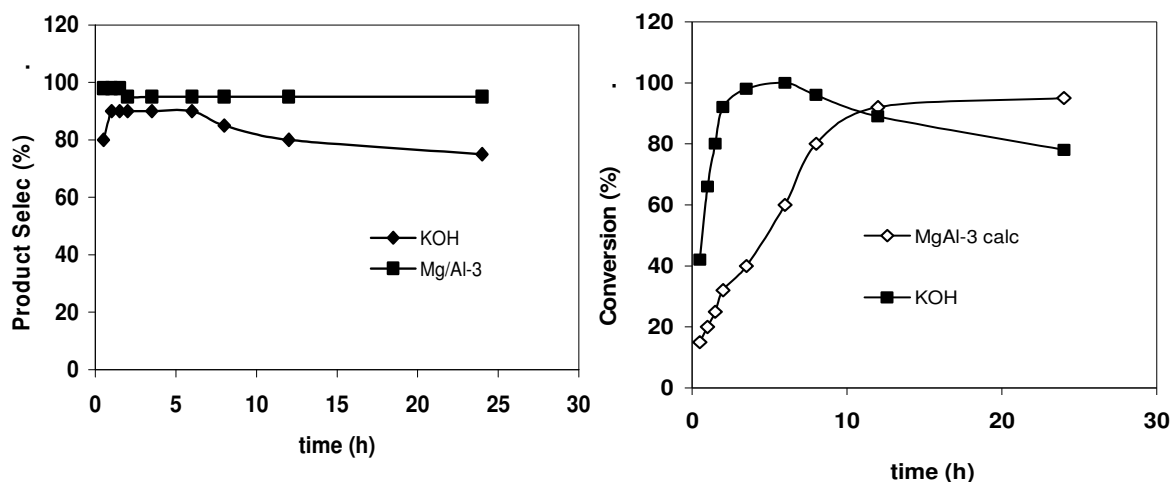


Figure 2.6 Variation of total conversion (A) and product selectivity of phenytoin (B) with the reaction time over KOH and Mg/Al calcined hydrotalcites

On the other hand the initial kinetics of the reaction was observed slightly faster with KOH but the conversion and the selectivity of the product (A) decreased significantly after 6h of the reaction time (Figure 2.6, B) with the formation of other side products (Scheme-2.1, product B) clearly indicating the necessity of both the acid-base properties (solid support) to control the product selectivity (Scheme 2.2).

2.5.8 Effect of substrate: urea molar ratio

Table 2.9 showed that the conversion as well as yield increased with increase in the molar concentration of urea up to 1:2 with 95% selectivity of the desired product (A).

Table 2.9 Effect of the molar ratio (benzil: urea) on the conversion of phenytoin over Mg/Al-3 HTs

Benzil:Urea	Conversion (%)	Yield (%)	Product selectivity (A) (%)
1:1	57	44	95
1:2	94	73	95
1:3	78	57	90

Conditions as in Table 2.3

However, the conversion decreased with further increase in the ratio (1:3) without significantly affecting the selectivity. These results are opposite to the results observed under homogeneous conditions and therefore the present catalyst Mg/Al-HTlc²¹ and hence offers a

significant advantages over homogeneous systems in controlling the selectivity of the product²².

2.5.9 Effect of the reaction temperature

The influence of the reaction temperature indicated (Figure 2.7) that the conversion increased with increase in the temperature from 308K to 338K and the maximum conversion and selectivity of the desired product was observed at 338K. The conversion as well as the yield of the product decreased with further increase in the reaction temperature at 358K with the formation of other side products. This may be due to the cleavage of C-C bond in benzil structure at higher temperature leading to the formation of some secondary products²³.

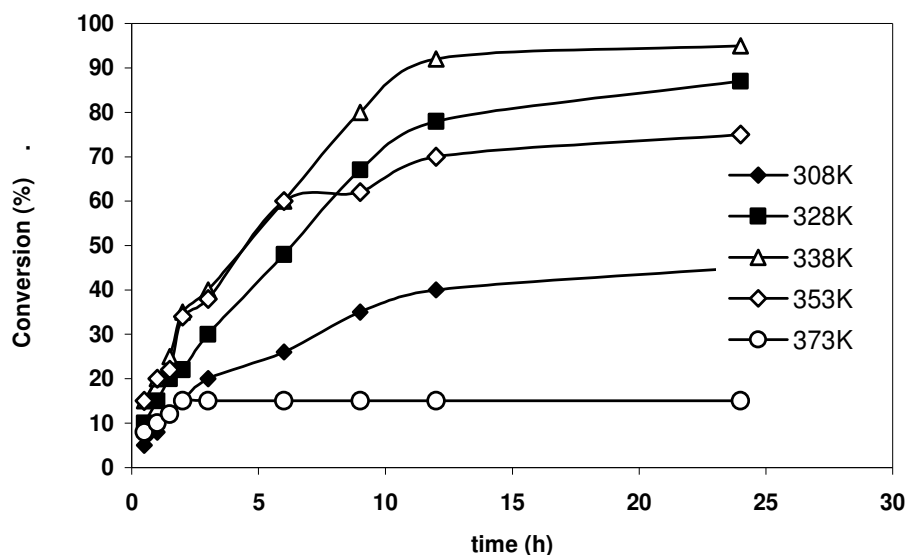


Figure 2.7 Variation of conversion of phenytoin with temperature over Mg/Al-3 HT

2.5.10 Effect of the different Solvent

Figure 2.8 showed the effect of different solvents on the conversion and the yield of the product. Maximum conversion and yield was obtained using methanol as a solvent.

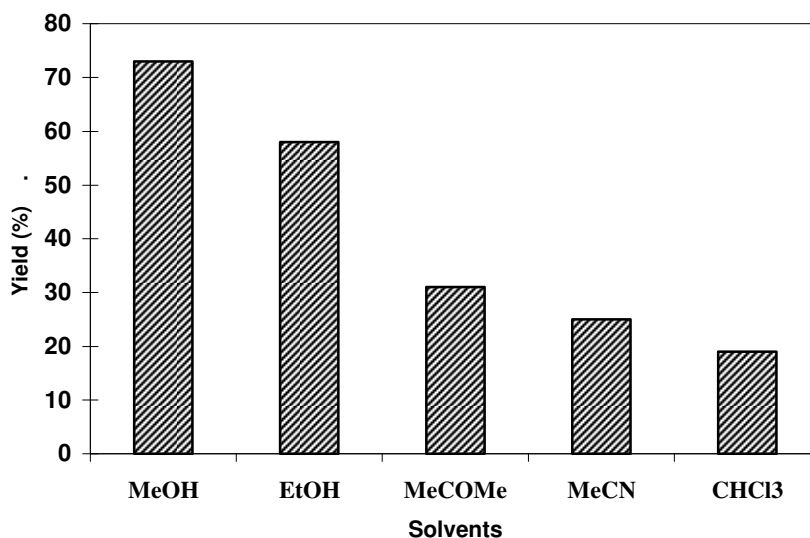


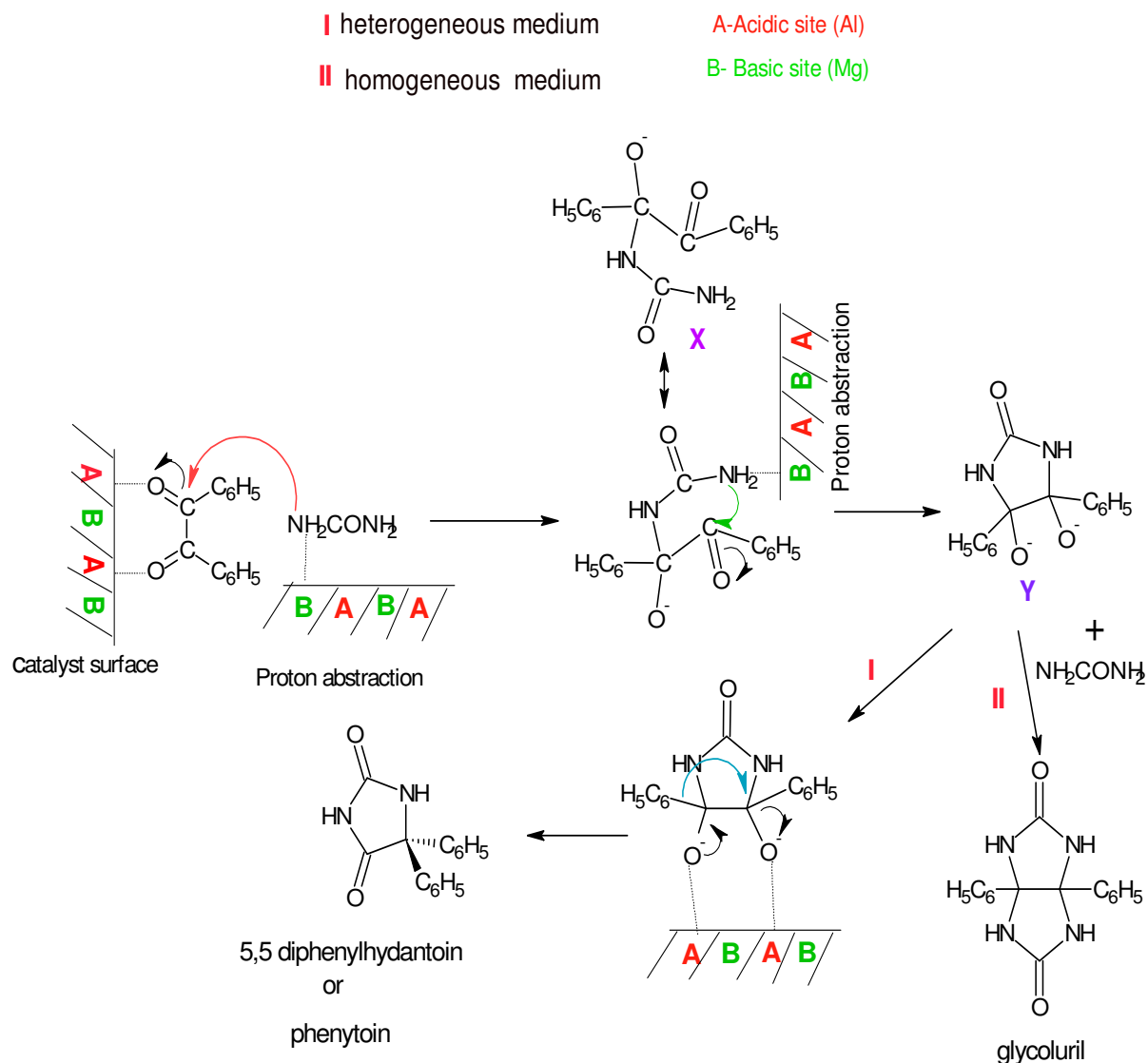
Figure 2.8 Effect of different solvents over Mg/Al HT.

This may be due to the better solubility of the reactants and products in methanol compared to other solvents. It also seems that the conversion of benzil depends directly on the polarity and the nature (protic or aprotic) of the solvent because the hydride transfer is considered to be easier in protic solvent.

2.5.11 Plausible Mechanism of the reaction

The probable reaction mechanism is proposed in Scheme 2.2. Initially the nucleophilic substitution on carbonyl carbon by urea forms an intermediate (X) followed by ring closure via proton abstraction in presence of Mg-O-Al mixed oxide. We believe that the selectivity of the desired product (A) is controlled by the relative stability of the cyclic intermediate (Y) in the presence of the acidic sites on the solid support. Additionally, the presence of this solid support follows the pathway (I) and prevents the reaction pathway (II) which might be possible in homogeneous conditions (KOH). Therefore, the formation of the desired product should essentially proceed via pathway (I) followed by pinacol-rearrangement. Overall the selectivity of the desired product depends on the competitive reaction pathways (I) and (II). Furthermore, the solid support prevents the attack of urea molecule leading to the formation of product (B).

Plausible Mechanism for the synthesis of Phenytoin over MgAl calcined hydrotalcites



Scheme 2.2 Plausible Mechanism

2.5.12 Reusability of the catalysts

In order to see the reusability of the catalysts, the catalyst after the reaction was filtered, washed thoroughly first with methanol, acetone and finally with water. The catalyst was dried, calcined at 873K and finally subjected to fresh reaction. No difference in the activity and selectivity was noted. Subsequently the catalyst was repeated for three cycles without significant loss in the activity indicating the non-leaching behavior of metal oxides from the catalyst during the course of reaction.

2.6 Conclusions

1. Mg/Al calcined HTs were synthesized and characterized by PXRD, FT-IR and surface area measurements. PXRD pattern confirms the formation of mixed oxides without further impurity.
2. Among different atomic compositions of Mg/Al, Mg/Al-3 calcined hydrotalcite showed the highest activity and selectivity for the desired product.
3. Various reaction parameters such as effect of different catalysts, solvent catalyst weight and calcinations temperature etc were studied in detail.
4. The mechanism of the formation of the desired product was proposed and explained.
5. The use of calcined hydrotalcites may pave the new pathways for the synthesis of hydantoin derivatives with multifunctional substitutions for which the efforts are currently underway.

2.7 References

1. N.O. Mahmoodi, Z. Khodaei, *ARKIVOC* 3 (2007) 29-36.
2. D. Zhang, X. Xing, G.D. Cuny, *J. Org. Chem* 71 (2006) 1750-1753.
3. G.G. Muccioli, J.H. Poupaert, J. Wouters, B. Norberg, W. Poppitz, G.K.E. Scriba, D.M. Lambert, *Tetrahedron* 59 (2003) 1301-1307.
4. S. Reyes, K. Burgess, *J. Org. Chem* 71 (2006) 2507-2509.
5. C. Montagne, M. Shipman, *Synlett* 17 (2006) 2203-2206.
6. B. Zhao, H. Du, Y. Shi, *J. Am. Chem. Soc.* 130 (2008) 7220-7221.
7. R.G. Murray, D.M. Whitehead, F.L. Strat, S.J. Conway, *Org. Biomol. Chem.* 6 (2008) 988-991.
8. P.Y. Chong, P.A. Petillo, *Tetrahedron Lett.* 40 (1999) 2493-2496.
9. M.J. Lee, C.M. Sun, *Tetrahedron Lett.* 45 (2004) 437-440.
10. M. Meusel, M. Guetschow, *Org. Prep. Proced. Int.* 36 (2004) 391-443.
11. N. Dieltiens, D.D. Claeys, V.V. Zhdankin, V.N. Nemykin, B. Allaert, F. Verpoort, C.V. Stevens, *Eur. J. Org. Chem.* (2006) 2649-2660.
12. A.G.N. Ashnagar, N. Amini, M., *International Journal of ChemTech Research* 1 (2009) 47-52.
13. V. Rives, *Layered double hydroxides: present and future*, Nova Science Pub Inc, 2001.
14. D. Kishore, S. Kannan, *J. Mol. Catal. A: Chem.* 244 (2006) 83-92.
15. F. Cavani, F. Trifiro, A. Vaccari, *Catal. Today* 11 (1991) 173-301.
16. D.G. Cantrell, L.J. Gillie, A.F. Lee, K. Wilson, *Appl. Catal., A* 287 (2005) 183-190.
17. W. Xie, H. Peng, L. Chen, *J. Mol. Catal. A: Chem.* 246 (2006) 24-32.
18. J.I. Di Cosimo, V.K. Diez, M. Xu, E. Iglesia, C.R. Apesteguia, *J. Catal.* 178 (1998) 499-510.
19. E. Garrone, F.S. Stone, p. III-441. *Dechema, Frankfurt-am-Main* (1984).
20. W.T. Reichle, S.Y. Kang, D.S. Everhardt, *J. Catal.* 101 (1986) 352-359.
21. W.R. Dunnivant, F.L. James, *J. Am. Chem. Soc* 78 (1956) 2740-2743.
22. D. Tichit, B. Coq, *Cattech* 7 (2003) 206-217.
23. E. Takezawa, S. Sakaguchi, Y. Ishii, *Org. Lett* 1 (1999) 713-715.

Chapter 3
Synthesis, Characterization and
Catalytic Applications of CuM(II)Al-
Ternary Hydrotalcites

3.1 Introduction

The basic properties of the calcined MgAl HTs were efficiently utilized in the previous chapter. The interest emerged to explore the catalytic activity of transition metal containing HTs especially Cu-containing HTs, having known their oxidation behavior. It is known in the literature of hydrotalcites that binary CuAl- HTs are difficult to synthesize due to the strong Jahn-Teller distortion associated in the octahedral environment of Cu-complexes. But HT-phase in Cu-HTs can be stabilized in the presence of other co-bivalent metal ions, which itself forms hydrotalcite, resulting in ternary CuM(II)Al-HTlc¹. Therefore in this chapter the copper containing ternary hydrotalcites were synthesized and characterized for the environmentally benign liquid phase oxidations of vanillin and benzoin.

3.2 Synthesis of M(II) Al and CuM (II)Al Hydrotalcites.

M(II)Al-HTs and CuM(II)Al-HTlc, where M(II)-Mg, Ni, Co, Mn, Zn and Cu, were synthesized by co-precipitation method under low supersaturation¹. Two solutions; solution (A) containing the desired amount of metal nitrates and solution (B) having precipitating agents (i.e., NaOH and Na₂CO₃), were added simultaneously, while maintaining the pH around 9-10 under stirring at room temperature. The addition took around 100 minutes and the final pH of the solution was adjusted to 10. The samples were aged at 338K for 18 h, filtered, washed (until total absence of nitrates and sodium in the washing liquids) and dried in an air oven at 353K for 12 h. The samples obtained were powdered and denoted as CuM(II)Al-X, where X stands for Cu/M(II) atomic ratio at fixed composition of (Cu+M(II))/Al=3. In all cases the atomic ratio of (Cu + M(II))/ Al was maintained at 3, while Cu/M (II) was varied from 5:1 to 1:5.

3.3 Physiochemical Characterizations

3.3.1 PXRD

PXRD pattern (Figure 3.1) for as synthesized CuMgAl-HTlc showed sharp, intense peaks at low diffraction angles (peaks close to $2\theta = 11^\circ$, 24° , and 35° ; indicating basal planes at (003), (006), and (009), respectively)². The peaks at $2\theta = 38^\circ$, 46° , and 60° indicates (105), (108), and (110) planes. These peaks confirm the presence of pure hydrotalcite phase without the formation of any impurities². However the sharp peak at 62° due to the average distance between the two cations clearly signifies the presence of hydrotalcite phase.

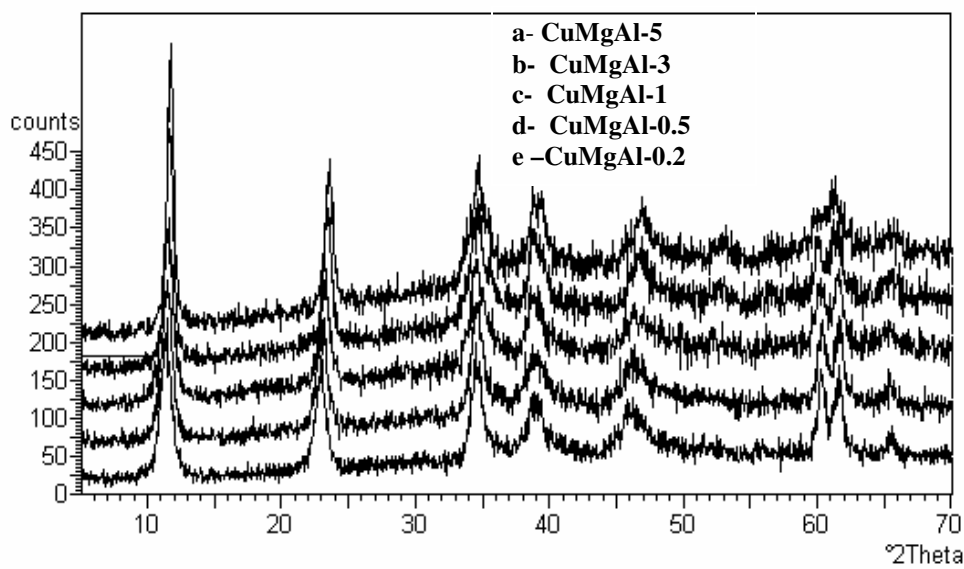


Figure 3.1 PXRD pattern of fresh CuMgAl-HTs, top(a) , bottom (e).

3.3.2 FT-IR

Figure 3.2 showed FT-IR of fresh CuMgAl samples, the peak at 3605cm^{-1} corresponds to the

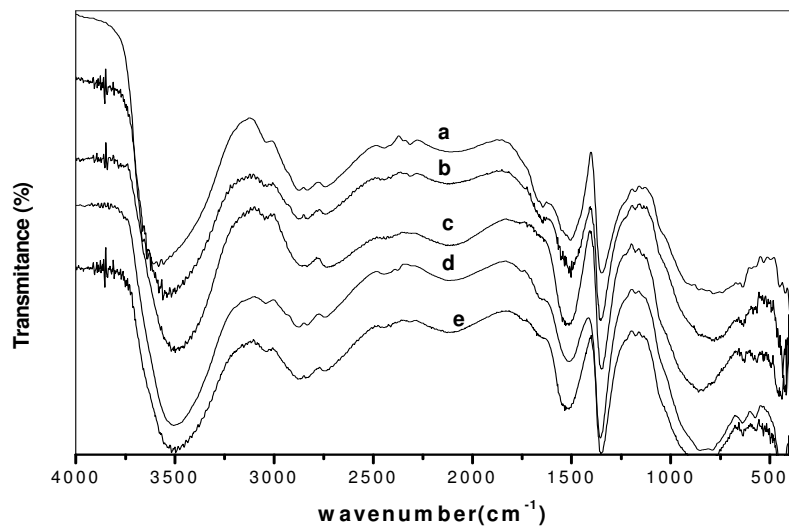


Figure 3.2 FT-IR of (a) CuMgAl-5 (b) CuMgAl-3 (c)CuMgAl-1 (d) CuMgAl-0.5 (e) CuMgAl-0.2 HTs.

$\nu(\text{OH})$ stretching mode of H-bonded hydroxyl groups in the lattice of HTlc and of interlayer water molecules. The broad band at 2865cm^{-1} also indicates the presence of hydrogen bonding between hydroxyl group and interlayer carbonate groups. The water deformation

band was also recorded at 1650cm^{-1} which overlaps with band from 1340 to 1550cm^{-1} . Furthermore, the presence of CO_3^{2-} was indicated by sharp band at 1340cm^{-1} and 1516cm^{-1} which confirms the structure of HTlc²⁻⁴.

3.3.3 Surface Area Measurements

The specific surface area was calculated by the BET method. CuMgAl-HTlc showed increase in surface area with increase in Mg content; this may be attributed to the differences in the morphology arises during the crystallite formation. Furthermore the pore size distribution also varies with Mg content, as it is well known in hydrotalcites that pore formation in hydrotalcites is through interparticle packing, and the distribution of pores is influenced by the crystallite size and packing arrangement of crystallites⁵. The detailed structural parameters of CuMgAl-HTlc are given in Table 3.1.

Table 3.1 Structural parameters of CuMgAl-HTs.

Catalyst	Surface area (m^2/g)	Pore volume ($\text{cm}^3\text{ g}^{-1}$)	Average pore width (Å)
CuMgAl-5	65	0.54	312
CuMgAl-3	77	0.53	223
CuMgAl-1	110	0.76	170
CuMgAl-0.5	120	0.91	210
CuMgAl-0.2	132	0.90	211

The synthesized CuMgAl-HTlc were tested as a catalyst for the liquid phase oxidation of :

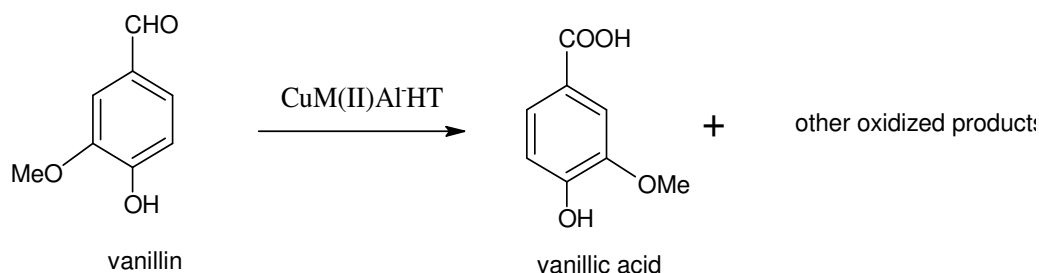
(A) Liquid phase oxidation of vanillin

(B) Liquid phase aerial oxidation of benzoin

(A) Liquid phase oxidation of Vanillin over CuM(II)Al-HTlc

One step catalytic oxidation of vanillin is a very important reaction due to the wide applications of its product vanillic acid (Scheme 3.1). Vanillic acid is a kind of polyphenol which has utility in diverse fields such as chemical, biological, agricultural and medicinal applications⁶⁻¹¹. Very few reports are provided for vanillin oxidation via chemical method such as silver oxide^{10, 12} Hexacyanoferrate(III)¹³, Diperoxidatonickelate(IV)¹⁴ in aqueous alkaline medium, Sodium N-Chloro-p-toluenesulfonamide^{15, 16}. In a quest for a simple process in converting vanillin directly into vanillic acid; hydrotalcites under environmental

friendly conditions were employed. Since no report on oxidation of vanillin over heterogeneous catalyst was found^{17, 18}, and very few reports concerning the effects of pH on the kinetics of vanillin degradation under homogeneous conditions are available.^{19, 20} In this part of the chapter, one step liquid phase oxidation of vanillin is reported for the first time over fresh CuM(II)Al-HTlc, (where M(II) = Ni, Co, Mg and Zn) with different atomic compositions of Cu/M(II) using water and H₂O₂ as a solvent and an oxidant respectively.



Scheme 3.1 Oxidation of vanillin to vanillic acid

3.4 Catalytic Studies

Oxidation of vanillin was carried out in a two-neck glass reactor (50 ml) fitted with a condenser and a septum. Hydrogen peroxide (30%) was added through the septum to the magnetically stirred solution of vanillin (10 mmol) containing catalyst (as-synthesized HTlc) and water (10ml) as solvent kept at the desired reaction temperature. The course of the reaction was monitored periodically drawing small samples (0.05 cm³), which were analyzed by gas chromatography (GC; Shimadzu-14B, Japan) fitted with SE-30 packed column using a flame ionization detector. Quantification was done after considering the response factors of the reagents and products obtained using standard mixtures. The product was extracted from ethyl acetate and dried over Na₂SO₄ to remove the solvent to obtain the desired product. The yield of the product was calculated as isolated yield.

3.4.1 Effect of different co-bivalent metal in CuM(II)Al-HTs

Screening of different binary M(II)Al-HTs showed highest conversion and product yield over CuAl-HTs (although CuAl does not form pure HT phase). Based on our earlier reports, it was concluded that copper containing ternary hydrotalcites exhibit maximum conversion and yield over liquid phase oxidation/hydroxylation of aromatics^{3, 5}, therefore the catalytic

activity of oxidation of vanillin was tested over CuM(II)Al-HTlc. The results showed maximum activity and selectivity for CuMgAl-5 followed by Co, Ni and Zn co-bivalent metal ions (Table3.2). The atomic composition of Cu/M(II) = 5 was found to be the best catalyst for this conversion. In all the samples only vanillic acid was observed as the major product with 100% selectivity.

Table 3.2 Variation of conversion and yield of vanillin over different CuM(II)Al-HTs

Catalyst	Conversion (%)	Yield (%)	Product selectivity (%)
CuAl-3	57.2	50.2	100
CoAl-3	22.5	18.2	100
NiAl-3	17.2	15.3	100
ZnAl-3	15.8	13.9	100
CuCoAl-5	77.2	69.2	100
CuNiAl-5	80.4	76.3	100
CuZnAl-5	67.4	30.2	100
CuMgAl-5	90.2	82.5	100

Reaction conditions: catalyst–10 mg, substrate-vanillin (10 mmol), solvent-H₂O, Temp.–313 K, reaction time–6 h, sub:oxi–1:1 (molar ratio).

The higher activity and selectivity of these catalysts suggest that although copper is acting as the active centers but the overall activity and selectivity of these catalysts is influenced by geometric and electronic factors around the active centers i.e. the influence of co-bivalent metal (Co, Ni, Zn, Mg) ions in ternary hydrotalcites. We attempted variation of different solvents (THF, acetonitrile, MeOH CHCl₃) and oxidants, to our delight H₂O and H₂O₂ were the best solvent and oxidant for this reaction proving to be quite significant for industrial applications. Based on the screening observations on various co-bivalent metals, CuMgAl-5 was selected for further study.

3.4.2 Effect of the substrate:catalyst ratio

In order to see the effect of catalyst weight on the conversion of vanillin, different amount of catalyst weight were chosen (Figure 3.3). It was observed that the catalytic activity decreases with increase in the weight of the catalyst. This may be due to the coke formation (the reaction mixture turns black) during the reaction which blocks the active centers of the catalyst thereby reducing the overall conversion. The maximum conversion was noted with

10 mg weight of the reaction. To verify, we have estimated the coke formed for the reaction having substrate: catalyst ratio of 10:1 and observed around 0.1–0.2 g of coke per gram of catalyst (calculated after taking due consideration of weight loss due to catalyst upon calcination in air). We believe, once coke is formed in the reaction, it masks the active centers of the catalyst thereby inhibiting the access of the reactant molecule to further undergo the reaction.

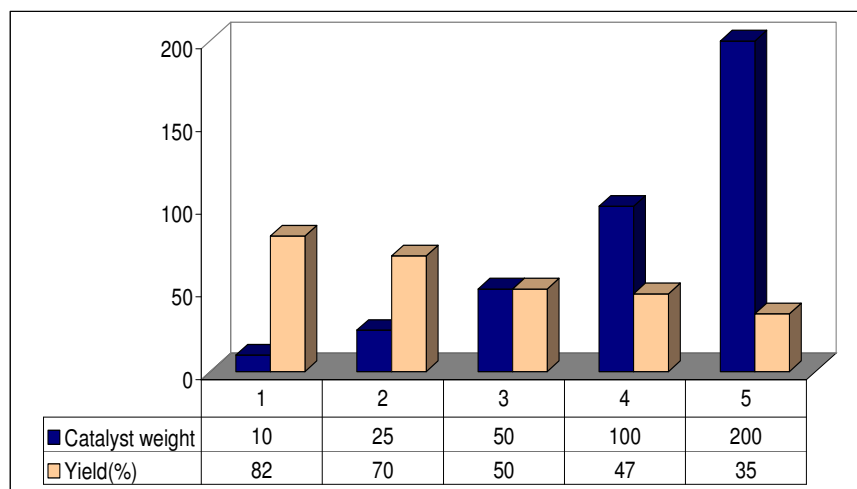


Figure 3.3 Effect of catalyst weight on the conversion of vanillin over CuMgAl-5 HT.

3.4.3 Effect of the reaction time

In order to see the influence of the reaction time, samples were carefully withdrawn from the reaction mixture at different intervals using syringe filters and analyzed (Figure 3.4). It was observed that the conversion increased with increase in the reaction time and the reaction was completed within 3 h of the reaction time and then became constant with further increase in the reaction time. The reaction was then allowed to proceed for 24 h to see the formation of other secondary products or inter conversions of the products (due to the possibility of formation of over oxidized products). However, no difference in the activity and selectivity of the product was observed.

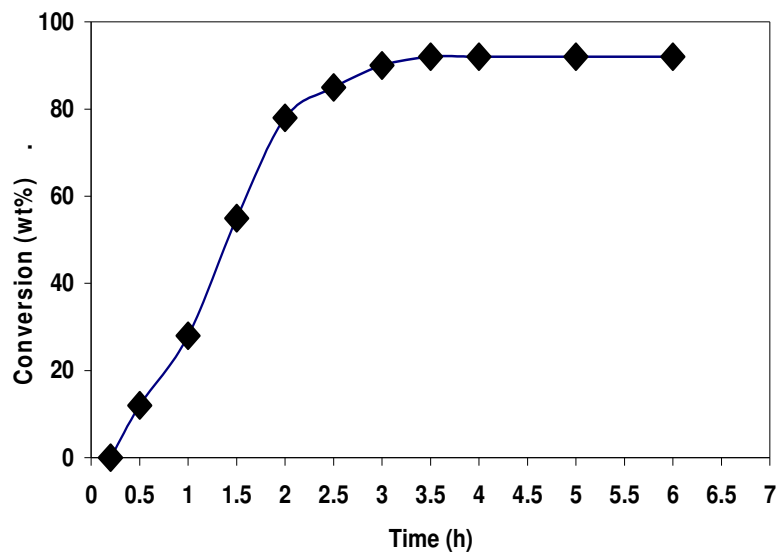


Figure 3.4 Effect of the reaction time on the conversion of vanillin over CuMgAl-5 HT

3.4.4 Effect of the substrate:oxidant ratio

Table 3.3 showed the variation of the conversion of vanillin with substrate:oxidant ratio. The results indicated that the conversion as well as yield increased with increase in H₂O₂ concentration. This proportionate increase in the conversion and yield inferred that the H₂O₂ is essentially used for the desired product vanillic acid only.

Table 3.3 Effect of subs:oxidant ratio on the conversion of vanillin over CuMgAl-5 HT

Sub:Oxi	Conversion (%)	Yield (%)	Product Selectivity (%)
1:1	90.2	80.2	100
2:1	44.2	38.2	100
3:1	27.2	23.8	100
5:1	18.2	17.7	100
10:1	9.4	9.2	100

Conditions as in Table 3.2

3.4.5 Effect of pH on the reaction

Effect of pH on the reaction was studied to determine the participation of the radicals in the mechanism of this reaction. The catalytic activity results showed that there is no effect of the pH on the conversion of vanillin from pH 5.2 (which is the original pH of the reaction) up to

pH 7 but completely dropped at pH 9. This could be due to the better stabilization of the hydroxyl radicals at this pH range (5.2–7) and further drop in the conversion at higher pH may be due to generation of OH⁻ species, which would approach the active centre thereby inhibiting the adsorption of hydrogen peroxide, and in turn affecting the generation of hydroxy radicals^{2,3}.

3.4.6 Effect of ethanol addition

In order to verify the participation of hydroxyl radicals further, ethanol (which is a very good scavenger for hydroxyl radicals) was used as a co-solvent with water.

Table 3.4 Effect of C₂H₅OH:H₂O (molar ratio) on conversion of vanillin over CuMgAl-5

C ₂ H ₅ OH:H ₂ O	Conversion (wt%)	Yield (%)	Product Selectivity (%)
Pure H ₂ O	90.2	82.5	100
0.02	70.5	62.5	100
0.04	55.4	46.4	100
0.06	28.3	18.4	100
0.08	15.2	6.4	100
Pure ethanol	0	0	0

Conditions as in Table 3.2

The results showed (Table 3.4) that the conversion decreased with increase in the ethanol concentration and no conversion was observed with pure ethanol confirming the participation of the hydroxyl radicals in bringing this conversion.

3.4.7 Effect of the calcination temperature

The catalysts used for the catalytic reaction were dried at 353K and 383K depending on the metal composition. The effect of calcination temperature (673K, 873K and 1073K) studies showed the decreasing trend in the activity with increase in the calcinations temperature. This may be due to the loss of hydrotalcite phase (due to the dehydroxylation and decarboxylation of the layers at higher temperatures) and structural order responsible for the activity. However, no difference in the activity was noted up to 423K (near to first weight loss transition during thermal analysis) indicated that major drop in activity at higher calcinations temperature necessitates the presence of hydrotalcite.

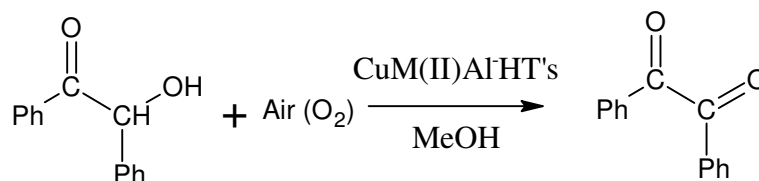
3.4.8 Reusability of the catalysts

In order to see the reusability of the catalysts, the catalyst after the reaction is filtered, washed thoroughly first with methanol, acetone, water and then dried in air and finally subjected to fresh reaction. The catalytic yield is slightly reduced to 78% with 100% selectivity of the product.

Furthermore, no leaching of active metal ions from the catalyst during the course of reaction was observed that was confirmed by several experiments according to the earlier reports^{21,22}. In order to see the leaching of the metal ions during course of the reaction; initially the catalyst along with the solvent and oxidant was stirred for 24h at the reaction temperature. The catalyst was filtered from the reaction mixture and was subjected to fresh reaction with both filtrate and solvent. No measurable conversion was obtained with the filtrate indicating the non-leaching behavior of the metal ions in the hydrotalcite framework²²

(B)Liquid Phase Aerial Oxidation of benzoin over CuM(II)Al-HTlc

Benzil, an alpha diketone, is one of the important organic intermediates, has received an enormous attention (Scheme 3.2). Various homogeneous reagents such as nitric acid²³, Fehling's solution²³, thallium nitrate²⁴, ammonium nitrate–copper acetate²⁵, bismuth nitrate–copperacetate²⁶ and ferric chloride²⁷ were employed in stoichiometric amounts for oxidation of benzoin to benzil. However, the use of these reagents limits their practical utilizations over heterogeneous catalysts in terms of product recovery, product selectivity and environmental concerns.



Scheme 3.2 Aerial Oxidation of Benzoin in presence of CuMgAl-3 catalyst

In continuation, many heterogeneous catalysts such as zeolite²⁸, VOCl₃²⁹, ferric nitrate on graphite³⁰, wet carbon-potassium bromate³¹ and Amberlite IRA 400 resin³² were exploited to overcome these difficulties. Very recently, transition metal doped MCM-41 mesoporous material is also reported for one step oxidation of benzoin to benzil³³ but the desired product selectivity still remains a challenge for this interesting reaction and in the current industrial

scenario, efforts are highly acknowledged in order to develop for simpler, efficient and recyclable heterogeneous catalyst. Among the heterogeneous catalysts, hydrotalcite catalysts are one of such materials whose potential has been exploited for various redox-mediated catalytic transformations^{21, 34, 35}.

Therefore, in this section, CuM(II)Al is reported for the first time in the liquid phase oxidation of benzoin under milder reaction conditions. The possible reaction mechanism of was also proposed and discussed.

3.5 Catalytic Studies

Oxidation of benzoin was carried out in liquid phase conditions using air as an oxidant (Scheme 3.2). Typically, 212mg (1mmol) of the substrate (benzoin) and 10ml of solvent was added in a glass reactor at desired temperature (298-363K) under stirring conditions. Different amount of the catalyst weights (5-500mg) was added at once to the reaction mixture. The products of the reaction mixture were analyzed through TLC with authentic benzil sample. The product was extracted from the reaction mixture using petroleum ether and finally the yield of the pure product was reported as isolated yield.

3.5.1 Effect of the different metal ion concentration

Table 3.5 showed the catalytic activity results on various binary hydrotalcites. In all, only benzil was formed as a major product with 100% product selectivity.

No conversion was obtained on blank reaction (i.e. without catalyst) infers the necessity of the catalyst to drive this transformation. Based on our earlier studies on hydrotalcites, it was also concluded that the binary hydrotalcites are generally inactive for liquid phase oxidation of aromatics but are significantly active when combined with other bivalent metal ions in ternary hydrotalcites^{2, 21}.

Table 3.5 Effect of different binary M(II)/Al=3 HTs on the conversion of benzoin.

Catalyst	^a Conversion (%)	^b Yield(%)	Product Selectivity (%)
NiAl	10	7	100
CoAl	18	14	100
MnAl	20	15	100
ZnAl	14	10	100

CuAl	15	12	100
MgAl	0	0	-

Reaction Conditions: (benzoin-214mg, air-1atm, catalyst-10mg, solvent- methanol (15ml), temp.-325K, Time-24h)

^a % based on the product benzil.

^b % based on product isolated.

Therefore, the interest emerged to see the effect of Cu (having known its redox properties) as co-bivalent metal ion in ternary CuM(II)Al-HTs with (CuM(II)/Al=3 and different compositions of Cu/M (II). The catalytic activity results (Table 3.6) showed remarkably high conversion and the product yield (10-90%), with 100% selectivity of the product corroborating our endeavor and hence the subsequent detailed study was carried out on CuM(II)Al-ternary hydrotalcites.

Table 3.6 Variation of the product yield with different solvents on CuMgAl HTs

Cu/M(II)	CuMgAl	CuNiAl	CuCoAl	CuZnAl	CuMnAl	Product Sel(%)
	Yield (%)	Yield (%)	Yield (%)	Yield (%)	Yield (%)	
5	51	28	67	46	76	100
3	90	62	57	70	74	100
1	66	70	69	82	64	100
0.5	44	55	35	52	37	100
0.2	13	32	31	25.7	11	100

Conditions as in Table 3.5, (Cu+M(II))/Al=3

Among the screening of different co-bivalent metal ions, maximum conversion and yield was obtained on CuMgAl-3 catalyst. This difference in the higher activity of CuMgAl-3 catalyst is due to the higher surface area of the catalyst compared to other CuM(II)Al catalysts (Table 3.7 and 3.8)^{2, 21}.

Table 3.7 Variation of different CuM(II)Al-3 HTs on the yield of benzil

Catalyst	Conversion (%)	Yield (%)	S _{BET} (m ² /g)
CuMgAl-3	98	90	77
CuNiAl-3	74	62	48
CuCoAl-3	65	57	38
CuZnAl-3	81	70	n.d
CuMnAl-3	84	74	n.d

Conditions as in Table 3.5

Table 3.8 Variation of different Cu/Mg composition on the conversion of benzil

Catalyst	Conversion (%)	Yield (%)	S _{BET} (m ² /g)	^a TON (w.r.t Cu as active site)
CuMgAl-5	60	51	65	1324
CuMgAl- 3	98	90	77	2513
CuMgAl- 1	72	66	110	2441
CuMgAl- 0.5	51	44	120	2443
CuMgAl- 0.2	20	13	132	1203

Conditions as in Table 3.5

^aTON = no of moles of reactant / no of moles of active center (Cu) times the % yield of the product.

Owing to the inherent properties of the calcined hydrotalcites (mixed oxides); the catalytic activity was also tested on calcined hydrotalcites but the catalytic activity was found to be lower than the fresh hydrotalcites clearly demonstrating the necessity of hydrotalcite phase². These results on CuMgAl-HTlc have advantages over some of the Cu-MCM-41 mesoporous materials³³ indicating that the desired activity and selectivity over CuMgAl-3 catalyst does not essentially depend on the Cu as active centers but also on the overall geometric and electronic environment around the catalyst (Table 3.8).

3.5.2 Effect of the weight of the catalyst

Table 3.9 showed the effect of the weight of the catalyst on the conversion and yield of the product. The yield of the product decreased with the increase in the weight of the catalyst up to 200mg of the samples but remained constant with further increase in the weight up to 500mg of the catalyst. This may be due to the different amount of tar (coke) formation (reaction mixture turns black) at higher catalyst concentration which selectively blocks the active centers of the catalyst thereby reducing the activity. We tried to estimate the tar formation with 500mg of the catalyst and it was observed that only 0.001g coke was formed per gm of the catalyst.

Table 3.9 Effect of the weight of the catalyst on the product yield over CuMgAl-3 HTs

Catalyst Wt (mg)	Yield (%)	Product Selectivity (%)
5	64	100

10	90	100
20	75	100
50	60	100
100	56	100
200	55	100
500	54	100

Conditions as in Table 3.5

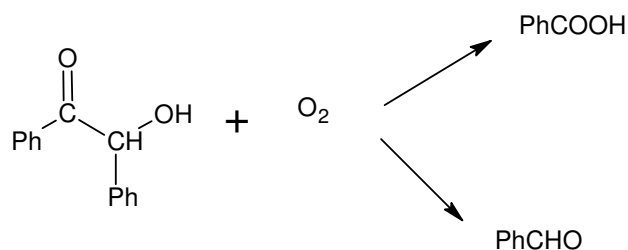
3.5.3 Effect of the reaction temperature

Table 3.10 showed the effect of the catalytic conversion of benzoin on the reaction temperature. The results indicated that the conversion and the yield increased with increase in

Table 3.10 Effect of the reaction temperature on the product yield over CuMgAl-3 HTs

Temp. (K)	Yield (%)	Product Selectivity (%)
298	60	100
308	65	100
325	90	100
345	46	100
363	28	80

Conditions as in Table 3.5.



Scheme 3.3 Cleavage of Benzoin at high temperature.

temperature up to 328K but decreased with further increase in temperature. This decrease in the yield may be due to the cleavage of carbon – carbon bond (Scheme3.3) in the reactant at higher temperatures^{36, 37}.

3.5.4 Effect of the solvent

Figure 3.5 showed the conversion of benzoin on different solvents and maximum conversion and yield was obtained using methanol as a solvent.

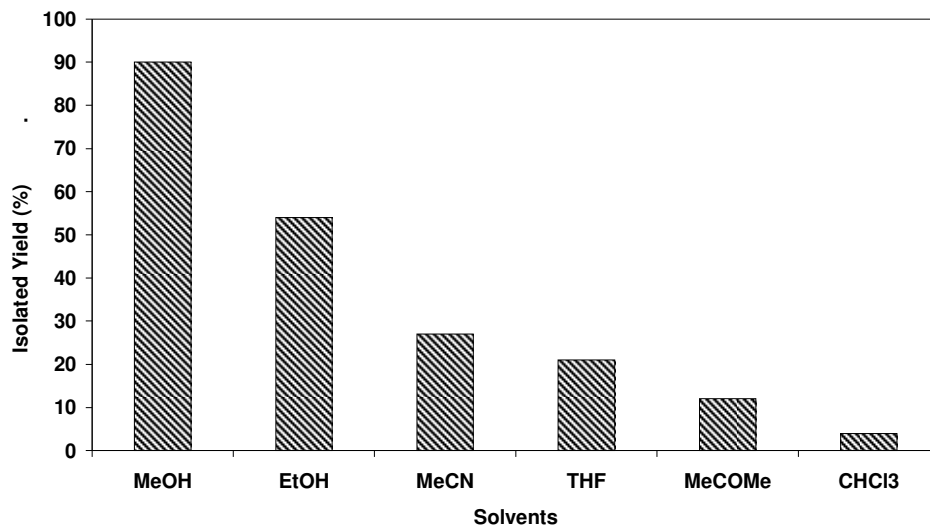


Figure 3.5 Effect of different solvent on conversion of benzil over CuMgAl-3 catalyst.

It seems that the conversion of benzil depends directly on the polarity and the nature (protic or aprotic) of the solvent because benzoin is more polar and hence making the hydride transfer easier in protic solvent.

3.5.5 Effect of different oxidants with oxidant: substrate molar ratio

Among the various oxidants (H_2O_2 , m-perchlorobenzoic acid and air), it was concluded that the best activity and selectivity can be achieved by air itself under optimized reaction conditions (Table 3.11). We further observed that air present inside the reaction mixture itself is sufficient enough to derive this reaction and hence no additional supply of the air was pumped into the reaction mixture. Moreover, in order to see the effect of the air present in the reaction mixture, different reactions with increased amount of the substrate (Table 3.12) were carried out under similar experimental conditions.

Table 3.11 Effect of different oxidants on the product yield over CuMgAl-3 HTs

H_2O_2 :benzoin	Conversion (%)	m-chloroperbenzoic acid: benzoin	Conversion (%)
2:1	81	2:1	75
1:1	70	1:1	66
0.5:1	63	0.5:1	52

Conditions as in Table 3.5

Table 3.12 Variation of different Cu/Mg composition on the product yield

Reactant wt. (g)	Yield (%)	^aTON (w.r.t Cu as active site)	Product Selectivity (%)
0.106	96	1340	100
0.212	90	2513	100
0.424	77	4301	100
1.060	22	3072	100
2.120	18	5027	100

Conditions as in Table 3.5

^aTON = no of moles of reactant / no of moles of active catalyst times the %yield of the product

The results showed that the conversion and the product yield decreased with increase in the amount of the reactants but no difference in the product selectivity was observed. This decrease in the conversion and yield is obvious because the air present in the reaction mixture is not sufficient for the conversion of increased amount of reactants. Furthermore higher conversion (100%) and the yield (96%) were obtained using higher oxygen concentration (0.2 atm) under our reaction conditions. Here we have not used the external supply of the air and optimum concentration of the reactant was chosen for further study

3.5.6 Time on stream studies (TOS)

TOS studies (Figure3.6) showed that the catalytic activity of the reactant increased continuously up to 18 h and then became constant with further increase in the reaction time. No difference in the product selectivity was noted during the course of reaction time. Further, to calculate the yield of the product with time, separate eight batches (to take the samples at different times) of the reactions were put under similar reaction conditions. The yield of the products was calculated periodically up to 48hrs to see the formation of secondary or-

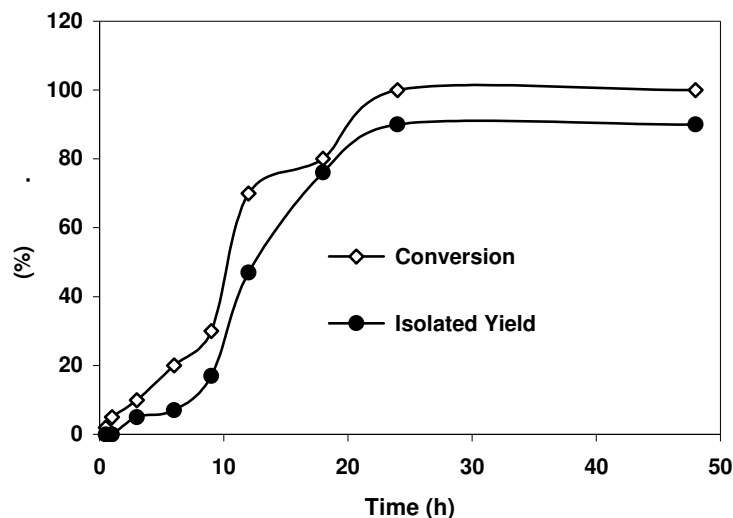


Figure 3.6 Variation of the product yield with time over CuMgAl-3 catalyst

interconverted products. However no difference in the conversion, yield and selectivity of the products was observed indicating the product formed is quite stable and thus may be beneficial industrially.

3.5.7 Effect of the pH on the reaction and plausible mechanism

In order to see the influence of the pH on the reaction, different experiments were performed at different pH (6-13) range. Figure 3.7 showed that the reaction is feasible both at lower as-

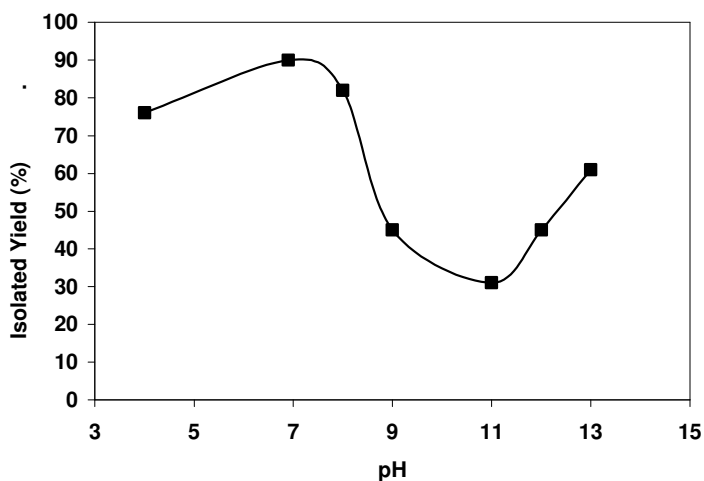


Figure 3.7 Variation of the product yield with pH of the reaction over CuMgAl-3 catalyst

well as in the high pH range than the original (without adjustment) pH ~6.8 of the reaction. However some interesting trend is observed at relatively higher pH range wherein the conversion decreased initially with the pH (7-10) and then again increased with pH~12. These observations were repeated and found reproducible under our reaction conditions. Mechanistically, we believe this peculiar behavior may be due to the better stabilization of the reactive intermediate (A) and (B) either in radical or ionic form (Scheme 3.4) responsible for the formation of product^{38, 39}.

Table 3.13 Effect of molar ratio of methanol: ethanol at different pH

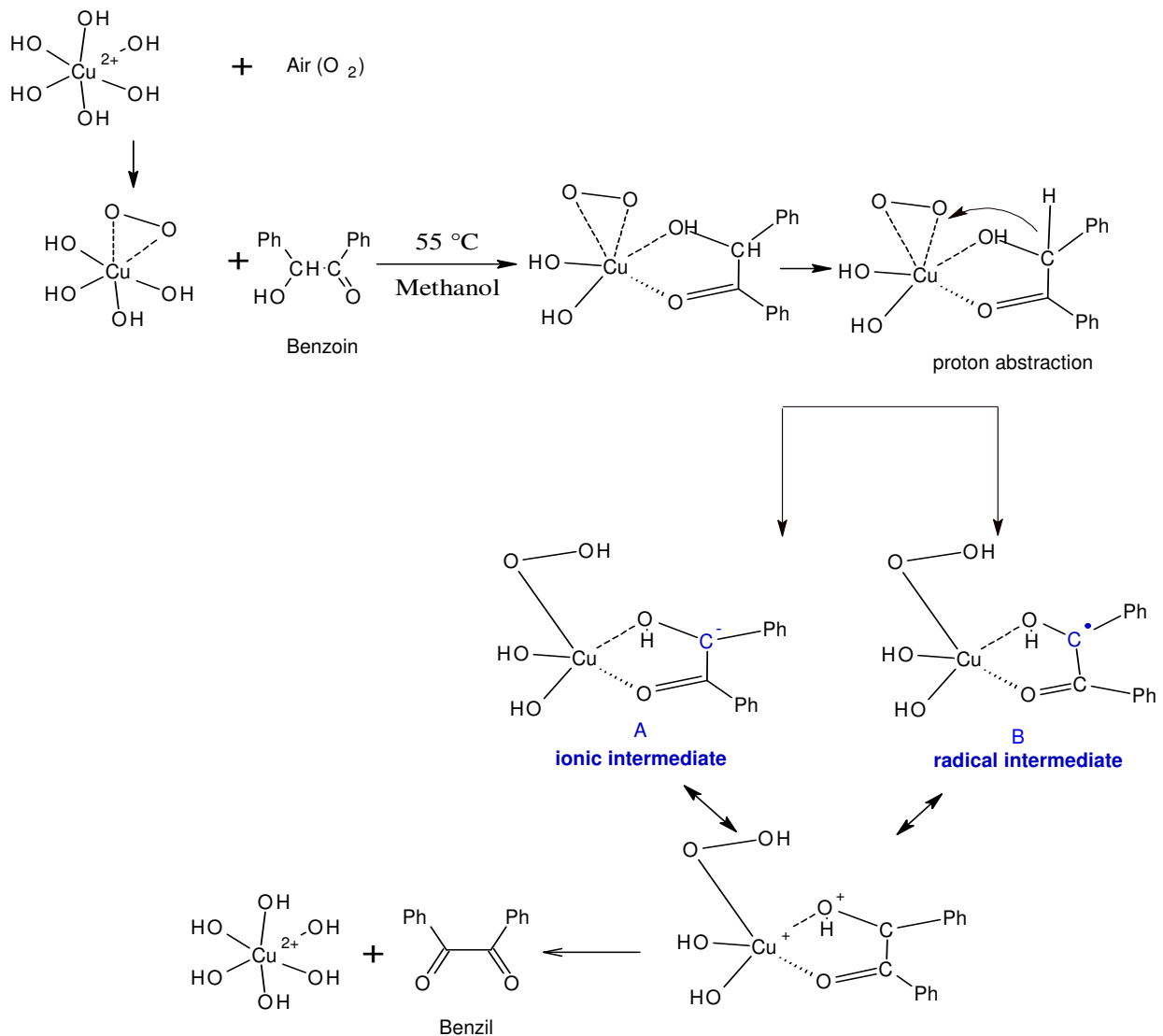
Methanol:ethanol	pH=4 Yield (%)	pH=13 Yield (%)
0.25: 0	76	61
0.22 : 0.01	56	58
0.12 : 0.10	35	55
0.02 : 0.16	19	57
0 : 0.18	6	60

Conditions as in Table 3.5

In order to investigate the presence of radical or ionic mechanism, the reactions were carried out using ethanol (well known radical scavenger) as a co-solvent at both higher pH ~13 and lower pH ~ 4 (Table 3.13). Interestingly the conversion as well as the yield of the products decreased at lower pH but no significant difference in the activity was observed at higher pH indicating the influence of radical mechanism at lower pH and possibility of the ionic mechanism at higher pH.

The presence of the intermediates was chemically identified with the formation of purple color (semiquinone species) under alkaline conditions³⁸. Therefore, we believe, the interaction of the oxidant with the catalyst surface generates the peroxy compounds which via proton abstraction leads to the formation of the resonance stabilized intermediates (A) and (B) (Scheme 3.4). Finally, the competitive transformation of these intermediates into the stabilized semiquinone species under different reaction conditions leads to the formation of the product^{25, 38}.

Plausible Mechanism for aerial oxidation of benzoin over CuMgAl-HT's



Scheme 3.4 Plausible mechanism

3.5.8 Effect of calcinations temperature

It is known that the thermal decomposition of hydrotalcites at different temperatures results in mixed oxides of different acid-base properties. Having known the inherent reactivity of these mixed oxides, the catalyst CuMgAl was calcined at 423K, 673K, 873K and 1073K according to the thermal decomposition pattern of the hydrotalcites. The catalytic activity of these mixed oxides was found to lower than the fresh hydrotalcites. These results further

indicate that the optimum concentration of the active species and proper hydrotalcite phase is responsible for the conversion and selectivity.

3.5.9 Reusability of the catalysts

In order to see the reusability of the catalyst CuMgAl-3; redox-catalysts for benzoin oxidation, after the first run, catalyst was filtered, washed thoroughly with excess water and acetone, dried completely at 120 °C and again subjected to fresh reaction. The catalytic activity reduced slightly to 85% but remained constant for almost four cycles indicating their promise use in this interesting conversion. This small reduction in the activity may be attributed to slight decrease in the crystallinity of the catalyst after the first cycle or due to the absorption of the tar during the reaction, which block the active center of the catalyst. Subsequently the catalyst was repeated for three cycles without any significant loss in the activity. Also no leaching of the metal ion Cu from CuMgAl-3 was observed which was confirmed by the experiment already discussed in section 3.4.8.

3.6 Conclusions

1. CuM(II)Al-HTs were synthesized by co-precipitation method and characterized by PXRD, FT-IR, surface area measurements. PXRD pattern confirmed the presence of hydrotalcite phase without the formation of any impurities.
2. CuM(II)Al as heterogeneous catalyst were employed for the oxidation of vanillin and benzoin in liquid phase.
3. Various parameters such as effect of catalyst, weight, solvent, pH etc. were investigated for the oxidation of vanillin and benzoin over these CuM(II)Al-HTs.
4. Among the CuM(II)Al catalyst with different co-bivalent metal ions, CuMgAl-5 showed highest activity and selectivity for oxidation of vanillin using water as solvent and hydrogen peroxide as oxidant.
5. Among the various CuM(II)Al catalyst for aerial oxidation of benzoin, CuMgAl-3 showed highest activity and selectivity of the product benzil in liquid phase.

3.7 References

1. F. Cavani, F. Trifiro, *Catal. Today* 24 (1995) 307-313.
2. S. Kannan, A. Dubey, H. Knozinger, *J. Catal.* 231 (2005) 381-392.
3. A. Dubey, S. Kannan, S. Velu, K. Suzuki, *Appl.Chem.A.Gen.* 238 (2003) 319-326.
4. A. Dubey, V. Rives, S. Kannan, *J. Mol. Catal. A: Chem.* 181 (2002) 151-160.
5. A. Dubey, S. Kannan, *Catal. Commun.* 6 (2005) 394-398.
6. C. Chou, *The role of allelopathy in agroecosystems: studies from tropical Taiwan*, 1990.
7. D. Esiyok, S. Otlis, E. Akcicek, *J. Canc.Prev.* 5 (2004) 334-339.
8. Michael.C, Isabelle.S, US5686406, USA, 1997.
9. I.A.Pearl, ed., US 275690, 1952.
10. I. Pearl, D. Beyer, *Ind. Eng. Chem.* 44 (1952) 2893-2894.
11. X. Feng, J. Liu, G.E. Fryxell, Surface functionalized mesoporous material and method of making same, US Patent 6,326,326, 2001.
12. D. Englis, M. Manchester, *Anal. Chem.* 21 (1949) 591-593.
13. T. Jose, S. Nandibewoor, S. Tuwar, *J. Solution Chem.* 35 (2006) 51-62.
14. C. Kathari, P. Pol, S. Nandibewoor, *Turk. J. Chem.* 26 (2002) 229-236.
15. N. Suresha, R. Jagadeesh, N. Vaz, *Synth. React. Inorg. Met.-Org. Nano. Met. Chem.* 35 (2005) 845-854.
16. B. Deganatti, N. Shetti, S. Nandibewoor, *Transition Met. Chem.* 34 (2009) 143-152.
17. W. Hoelderich, *Catal. Today* 62 (2000) 115-130.
18. R. Sheldon, *Green Chem.* 7 (2005) 267-278.
19. C. Fargues, Á. Mathias, J. Silva, A. Rodrigues, *Chem. Eng. Tch.* 19 (2004) 127-136.
20. S. Wallick, K. Sarkanen, *Wood.Sci. Tech.* 17 (1983) 107-116.
21. D. Sachdev, A. Dubey, B.G. Mishra, S. Kannan, *Catal. Commun.* 9 (2008) 391-394.
22. R. Sheldon, M. Wallau, I. Arends, U. Schuchardt, *Acc. Chem. Res* 31 (1998) 485-493.
23. J.S. Buck, S.S. Jenkins, *J. Am. Chem. Soc.* 51 (1929) 2163-2167.
24. A. McKillop, B.P. Swann, M.E. Ford, E.C. Taylor, *J. Am. Chem. Soc.* 95 (1973) 3641-3645.
25. M. Weiss, M. Appel, *J. Am. Chem. Soc.* 70 (1948) 3666-3667.
26. S. Balalaie, M. Golizeh, M.S. Hashtroudi, *Green Chem.* 2 (2000) 277-278.
27. B. El Ali, A.M. El-Ghanam, M. Fettouhi, *J. Mol. Catal. A: Chem.* 165 (2001) 283-290.

28. C. Zhebin, S. Zhengui, *Chin.J.Org.Chem.* 22 (2002) 446-449.
29. V. Choudhary, P. Chaudhari, V. Narkhede, *Catal. Commun.* 4 (2003) 171-175.
30. J.D. Lou, M.H. Piao, F. Li, L. Li, C.L. Gao, *Synth. React. Inorg. Met.-Org. Nano. Met. Chem.* 37 (2007) 553-555.
31. A. Zali, A. Shokrolahi, *Synth. Commun.* 38 (2008) 1064-1069.
32. N. Bhati, K. Sarma, A. Goswami, *Synth. Commun.* 38 (2008) 1416-1424.
33. B. Li, J. Wang, J. Fu, J. Wang, C. Zou, *Catal. Commun.* 9 (2008) 2000-2002.
34. V. Rives, *Layered double hydroxides: present and future*, Nova Science Pub Inc, 2001.
35. V. Rives, A. Dubey, S. Kannan, *PCCP* 3 (2001) 4826-4836.
36. H. Tse-Lok, *Synthesis* 1972 (1972) 560-561.
37. E. Takezawa, S. Sakaguchi, Y. Ishii, *Org. Lett.* 1 (1999) 713-715.
38. A. Weissberger, J. LuValle, D. Thomas, *J. Am. Chem. Soc.* 65 (1943) 1934.
39. G. Hammond, C. Wu, W. Waddell, A. Schaffer, R. Becker, A. Allerhand, R. Komoroski, R. Roy, R. Robinson, R. Bates, *J. Am. Chem. Soc.* 95 (1973) 8215-8494.

Chapter 4

Liquid Phase One Pot Multicomponent

Synthesis of Dihydropyrimidinones

(DHPM's) over Aluminated

Mesoporous SBA-15

4.1 Introduction

The basic and redox properties of binary and ternary hydrotalcites have been exclusively employed in previous chapters. In the coming chapters the attempts have been devoted to functionalize the ordered mesoporous SBA-15 materials as mild acid and base catalyst for significant organic transformations. In this chapter, SBA-15 is functionalized with different amount of aluminum by simple post-impregnation method for one pot multicomponent synthesis of 3,4-dihydropyrimidin-2(1H)-ones.

4.2 Liquid phase synthesis of 3,4-dihydropyrimidin-2(1H)-ones

3,4-dihydropyrimidine-2(1H)-ones (DHPM's) and their derivatives show an indispensable pharmacological and biological profile including antiviral, antitumor, antibacterial, and anti-inflammatory effects¹⁻³. A number of marine alkaloids with broad spectrum of biological activities contain DHPM framework as a part of their structures^{1,4}. Moreover functionalized DHPM's have emerged as antihypertensive agents due to their metabolism in vivo to the potent calcium channel blockers⁵⁻⁷. Monastrol is the only cell-permeable molecule currently known to block mitosis by specifically inhibiting the motor activity of the mitotic kinesin Eg5 for the development of new anticancer drugs⁸. The dihydro-pyrimidine-5-carboxylate core unit is also found in many natural marine products including batzelladine alkaloids that are found to be potent HIVgp-120-CD4 inhibitors⁹. The syntheses of DHPMs is carried out by Biginelli reaction involving acid catalyzed three-component condensation of 1,3-dicarbonyl compound, aldehyde and urea^{3, 4, 10}. Several homogeneous reagents including Lewis and Bronsted acids such as Cu(OTf)₂, CuCl₂, Ag₃PW₁₂O₄₀, FeCl₃·6H₂O, Me₃SiCl¹¹⁻¹⁴, NH₂SO₃H, NH₄Cl¹⁵ were employed for the synthesis of DHPM's. In addition, ionic liquids, microwave irradiation, trimethylsilyl-triflate, heteropolyacids L-proline and I₂ were also tested¹⁶⁻²⁰ for these transformations. With this view aluminated SBA-15 (SBA/Al) is tested as the heterogeneous catalysts for this interesting conversion in liquid phase.

4.3 Synthesis of SBA-15

The synthesis of SBA-15 is carried out using Pluronic (P123) (EO₂₀PO₇₀EO₂₀, MW = 5800, Aldrich) and TEOS as the surfactant and silica source respectively. In a typical synthesis batch with TEOS, 3 g of P123 was dissolved in 100 g of distilled water and 5.9 g of conc. HCl (35%). After stirring for 1h 7.3 g of TEOS (ACROS, 98%) was added at 35°C

maintaining the molar ratio of P123: H₂O: HCl: TEOS as 1: 5562.9: 86.29: 42.51 and stirring for 24h²¹. Subsequently the mixture was heated for 24 h at 100 °C under static conditions in a closed polypropylene bottle. The solid product obtained after the hydrothermal treatment was filtered and dried at 80 °C. The template was removed by calcinations at 550 °C for 6h.

4.4 Synthesis of Al/SBA-15 catalyst

Aluminum contents were incorporated into the SBA-15 framework via impregnation method. Different amounts of AlCl₃ (5, 10 and 15 wt(%)) were impregnated to 1 g of calcined SBA-15 material using acetone as solvent. Typically for 15wt%, 270mg of AlCl₃ was dissolved in 20 ml acetone and stirred at 50°C for 24h to impregnate AlCl₃ into 1g of SBA-15 material. After complete impregnation, the samples were dried and characterized using standard characterization techniques. The samples were named as SBA/xAl where x denotes the percentage of Al in SBA-15.

4.5 Physiochemical Characterizations

4.5.1 PXRD

PXRD pattern of Al/SBA-15 (Figure 4.1) at low angle showed the characteristic peaks at-

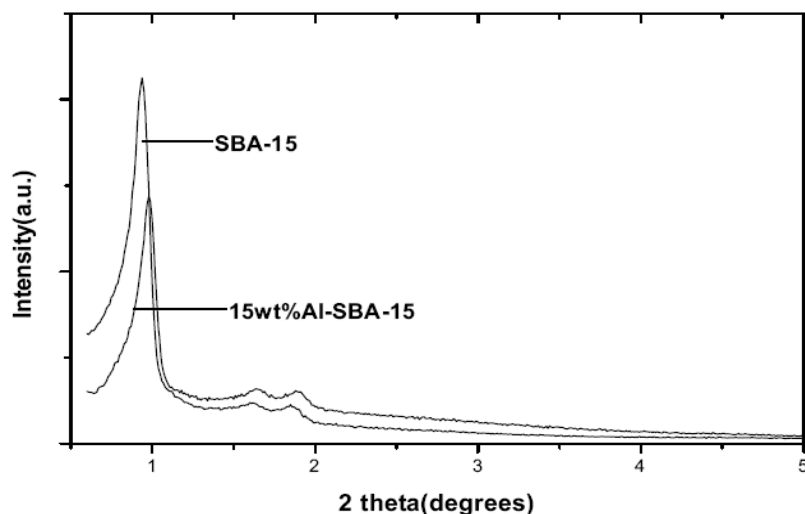


Figure 4.1 PXRD patterns of SBA-15 and 15 wt.% Al/SBA-15

(100), (110), and (200), similar to SBA-15 material. The base peak intensity in the case of Al/SBA-15 was reduced compared to SBA-15 indicating that the Al was uniformly incorporated inside the pores of SBA-15²¹

4.5.2 N₂ Adsorption-Desorption Studies

N₂ Adsorption-Desorption (Figure 4.2 and 4.3) showed type IV adsorption isotherm according to IUPAC classification²² with sharp capillary condensation step at P/P₀= 0.5-0.6 region and H1 hysteresis loop indicates the mesoporous nature of the samples.

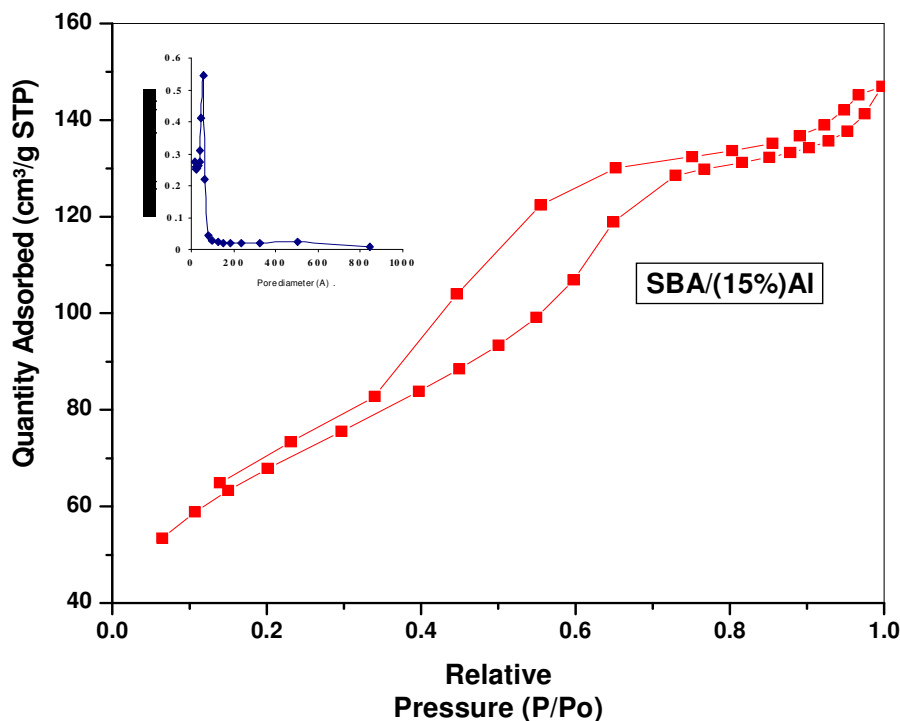


Figure 4.2 N₂-adsorption –desorption isotherm of SBA/(15%)Al. (Inset: Pore size distribution (BJH, desorption branch of isotherm)).

Table 4.1 Structural Parameters of Al/SBA-15 samples

Entry	Materials	Surface area (m ² /g)	Pore Volume (cm ³ /g)	Pore Size BJH _{Ads} (nm)	No of acidic sites (μmol/g)
1.	SBA-15	672	1.2	8.1	-
2.	SBA/(15%)Al	244	0.21	4.0	670
3.	SBA/(5%)Al	668	0.66	4.5	8.8

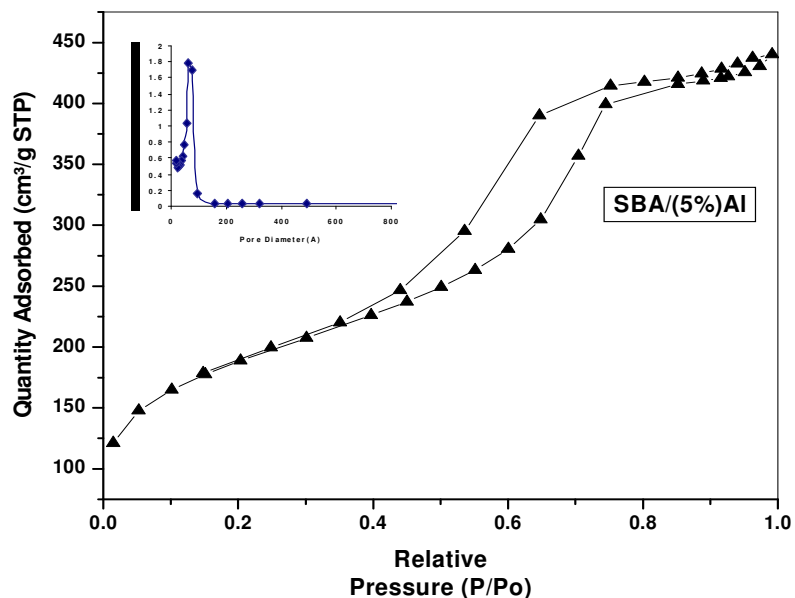


Figure 4.3 N₂-adsorption –desorption isotherm of SBA/(5)Al. (Inset: Pore size distribution (BJH, desorption branch of isotherm).

The pore size distribution curves were computed from the BJH model (shown as an inset). It was observed that the pore size distribution of the Al/SBA-15 samples (Table 4.1) were quite narrow indicating the uniform distribution of aluminum in mesopores. Total pore size, pore volume decreases with increase in aluminum content.

4.5.3 TPD of Al/SBA-15

NH₃ Temperature Programmed Desorption (TPD) spectra of Al/SBA-15 samples Figure 4.4 showed that most of the acidic sites are centered at temperature around 222⁰C. The peaks become sharper with increase in the Al contents (Table 4.1).

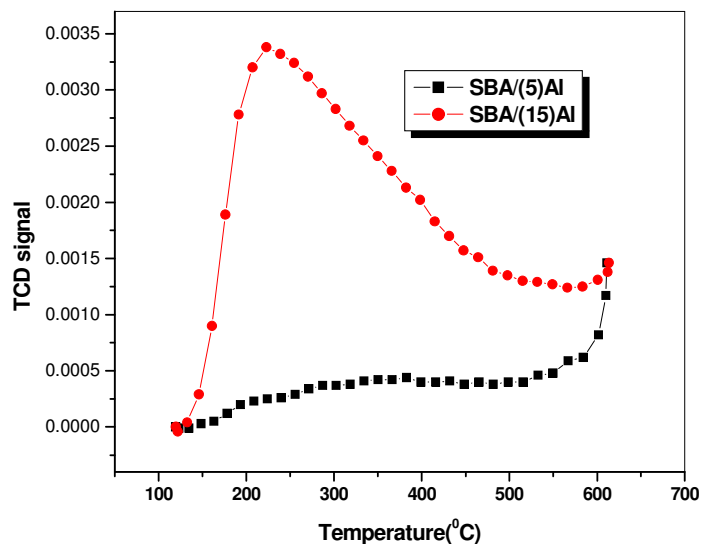


Figure 4.4 Temperature Programmed Desorption (TPD) of SBA/Al

4.5.4 FT-IR

FT-IR spectrum of the samples showed characteristic peaks similar to SBA-15. Careful examination of the spectrum Figure 4.5 (B) showed a slight variation in the vibrational frequencies ($\nu_1, \nu_2, \nu_3, \nu_4, \nu_5$) of Al/SBA-15 samples as compared to SBA-15 in the wavenumber region of $1300-400\text{cm}^{-1}$.

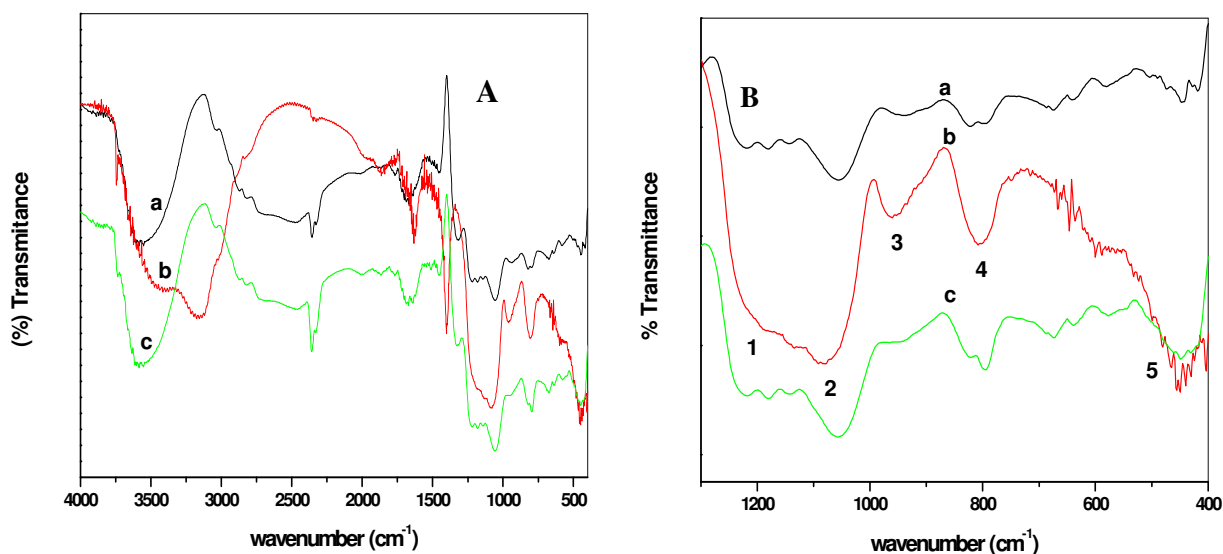


Figure 4.5 FT-IR spectra of (a) SBA-15, (b) SBA(15)Al and (c) SBA(5)Al samples.

The shift in the vibration bands (Table 4.2) may be due to the change in silica bond length (Si-O) with the substitution of Al where ($r \text{ Si}^{4+} = 0.26 \text{ \AA}$) and ($r \text{ Al}^{3+} = 0.39 \text{ \AA}$) are the atomic sizes.

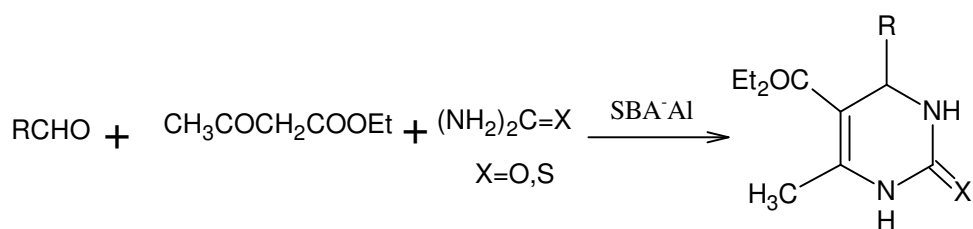
Table 4.2 Vibrational Frequencies of SBA/Al samples

Samples	Wave number (cm^{-1})				
	ν_1	ν_2	ν_3	ν_4	ν_5
SBA-15	1229	1055	928	799	443
SBA/(15)Al	1210	1076	944	794	445
SBA/(5)Al	1222	1053	956	808	455

4.6 Catalytic Studies

4.6.1 Synthesis of 3,4-dihydropyrimidin-2(1H)-ones

The catalytic activities of SBA/Al as heterogeneous catalyst was investigated for the synthesis of 3,4-dihydropyrimidin-2(1H)-ones in liquid phase. The catalytic reactions were optimized for the model reaction where $R=\text{Ph}$ in Scheme 4.1 and further extended to a wide variety of aromatic aldehydes. The liquid phase reactions were carried out in a glass reactor. Aryl aldehyde (1 mmol), ethylacetoacetate (1 mmol) and urea (2 mmol) were kept at the desired temperature under stirring, and the catalyst was added to the stirred solution under an inert atmosphere using ethanol as solvent.



Scheme 4.1 Synthetic strategy for the 3,4-dihydropyrimidin-2(1H)-ones (DHPM's).

The progress of the reaction was monitored by TLC from 1 to 6 h. The yield of the product was calculated after 24 h. After the completion of reaction, catalyst was filtered and washed thoroughly with solvent. Solvent is evaporated from the reaction mixture and the product was extracted with ethyl acetate. Ethyl acetate was dried over anhydrous Na_2SO_4 and

concentrated in vacuum, to obtain the solid product which was recrystallized from hot ethanol.

4.6.2 Effect of the different catalysts

The catalytic activity studies (Table 4.3) showed an increasing trend with increase in the aluminum concentration and maximum yield of 80% was observed with 15% Al incorporated in SBA-15 framework. However, the product yield decreases with decrease in the aluminum content and no conversion was obtained with SBA-15 indicating that the acidic centers are required for further conversion. Therefore SBA/(15) Al was selected for further studies.

Table 4.3 Variation of different amount of catalyst loading on the yield of DHPM's

Catalyst	Yield (%)
SBA-15	0
SBA/(5)Al	14
SBA/(10)Al	54
SBA/(15)Al	80

Reaction conditions: aryl aldehyde (1 mmol), ethyl acetoacetate (1 mmol), urea (2 mmol), catalyst- 65mg, Time-24 h

4.6.3 Effect of the solvents

Variation of different solvents (Table 4.4) indicates that the conversion as well as the yield of 3,4 Dihydropyrimidin-2(1H)-ones increases with polar protic solvents and the maximum yield was obtained with ethanol as solvent. It seems that the transition state obtained during the reaction is more stabilized in protic solvent than in aprotic or non-polar solvent.

Table 4.4 Variation of solvent on the yield of DHPM's over SBA/(15)Al catalyst

Solvent	Yield(%)
Ethanol	80
Methanol	78
No solvent	66
Acetonitrile	58
Chloroform	27
Hexane	18

Conditions as in Table 4.3

4.6.4 Effect of the temperature

Table 4.5 showed the variation of temperature on the yield of 3,4-Dihydropyrimidin-2(1H)-ones and it was observed that maximum yield (80%) was obtained at 80°C . Further increase in temperature decrease the yield of 3,4-Dihydropyrimidin-2(1H)-ones which may be due to the decomposition of benzaldehyde at higher temperature. Variation of amount of catalyst showed that maximum conversion was achieved with 65mg of SBA/(15)Al catalyst.

Table 4.5 Variation of temperature on the yield of DHPM's over SBA/15Al catalyst

Temp (°C)	Conversion (%)	Yield (%)
35	10	7
55	50	34
65	60	52
80	85	80
100	64	55

Conditions as in Table 4.3

4.6.5 Time on Stream Studies

The time on stream studies (Figure 4.6) for the synthesis of 3,4-Dihydropyrimidin-2(1H)-ones indicates that the reaction is completed within 6-12h of the reaction time.

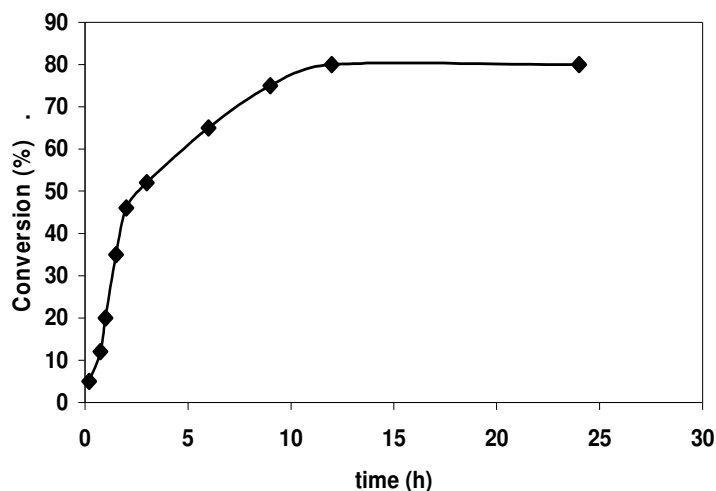
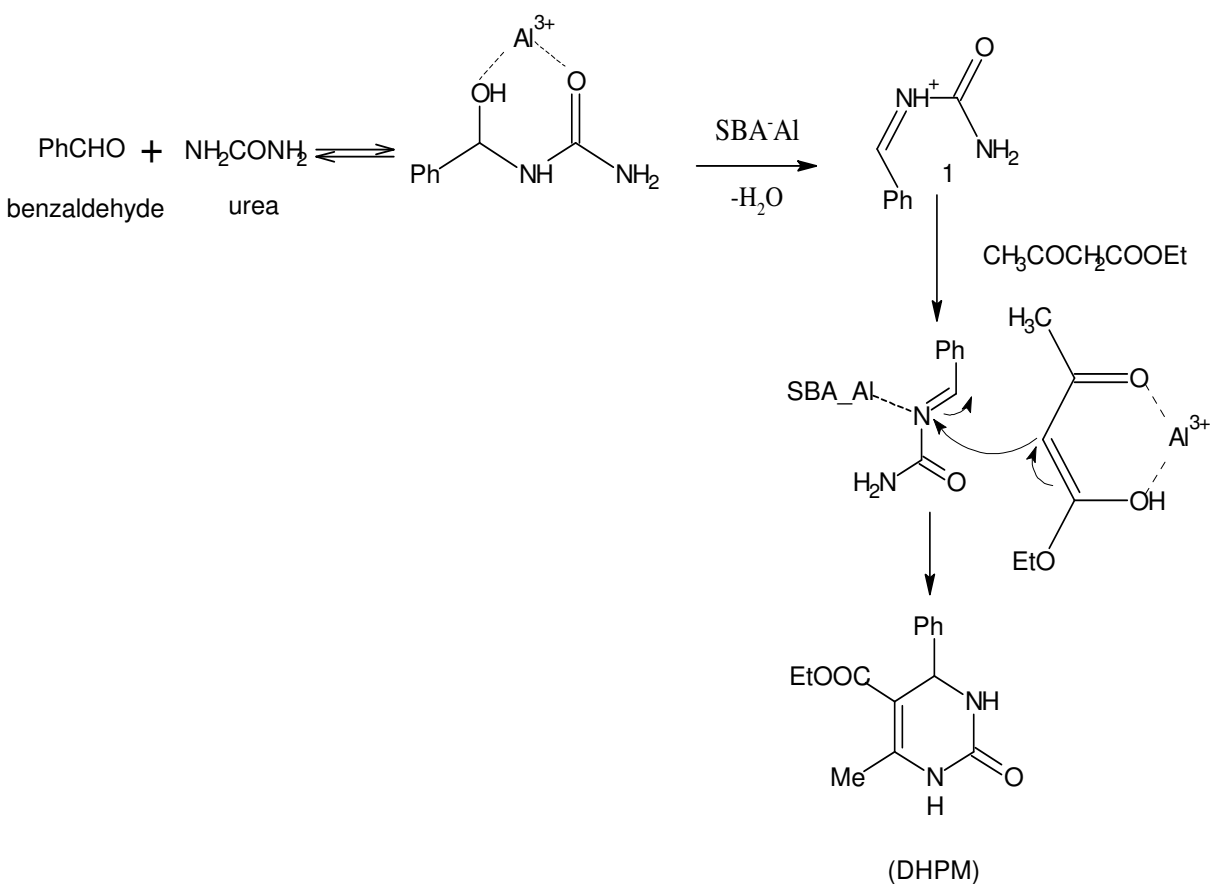


Figure 4.6 Effect of the reaction time on conversion of product over SBA/(15)Al catalyst

No further increase in the yield was observed with increase in reaction time indicating the product formed is stable under the reaction conditions.

4.6.6 Plausible Mechanism

Synthesis of DHPM's involves the reaction between benzaldehyde and urea to form a schiff's base which in presence of acid results in the formation of N-acylium ion²³(1) (Scheme 4.2). Mechanistically the bimolecular reaction involves the interaction of this inium ion (1) with ethylacetoacetate in presence of SBA-Al which results in cyclization of product and form DHPM's.



Scheme 4.2 Plausible mechanism for the synthesis of DHPM's

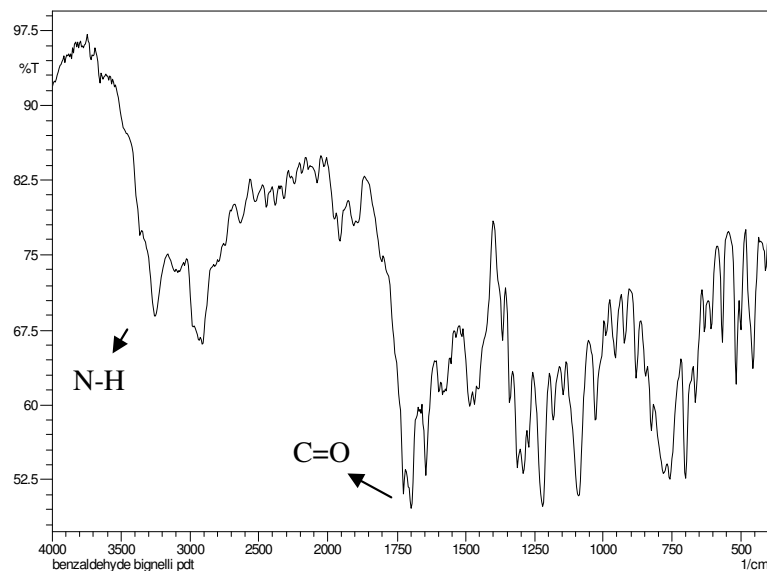
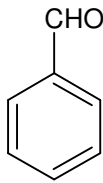
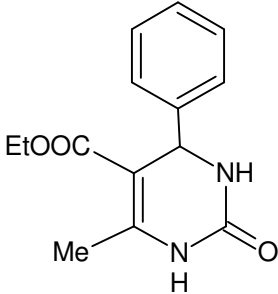
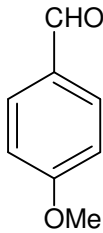
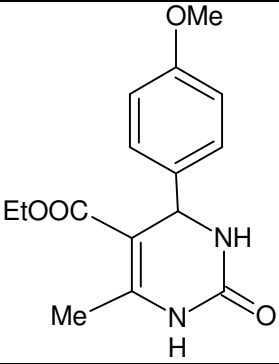
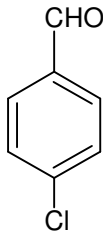
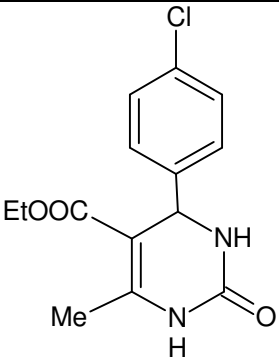
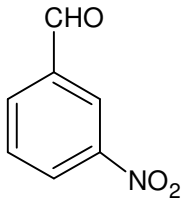
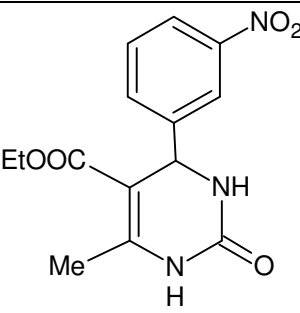
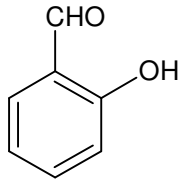
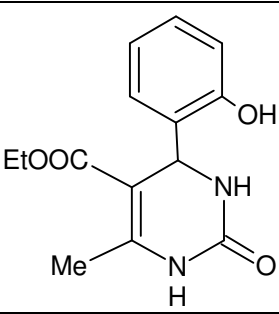


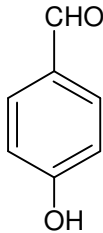
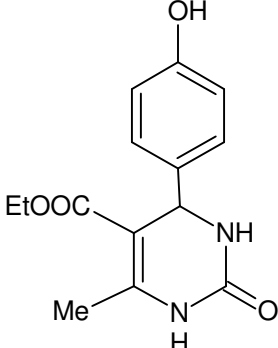
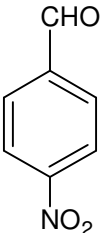
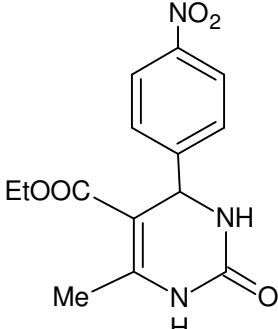
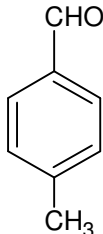
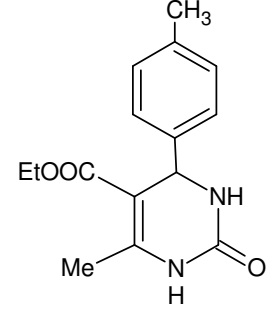
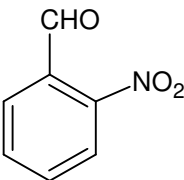
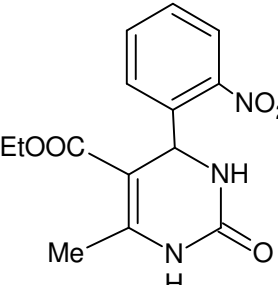
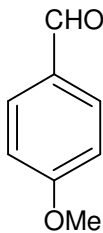
Figure 4.7 FT-IR of DHPM

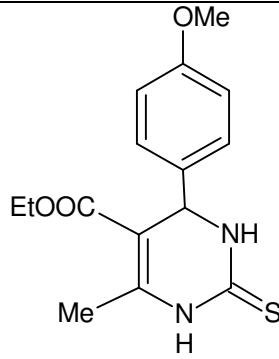
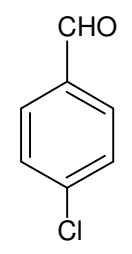
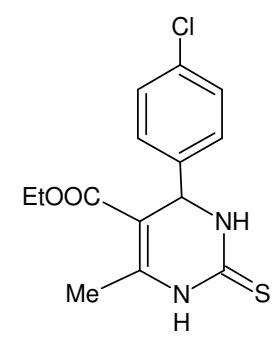
The product structure was further confirmed by FT-IR (Figure 4.7). The same methodology was extended to substituted aldehydes but no direct correlation was found for the substituent effect on the yield (Table 4.6). The melting point of the products was confirmed from the literature¹⁷.

Table 4.6 Effect of substituted aldehydes on the yield of DHPM's over SBA/(15)Al catalyst

S.No.	Substituted aldehydes	Reactant	Product	Yield (%)
1.		NH_2CONH_2 + $\text{CH}_3\text{COCH}_2\text{COOEt}$		80 ¹⁷

2.		NH_2CONH_2 $+$ $\text{CH}_3\text{COCH}_2\text{COOEt}$		81 ¹⁷
3		NH_2CONH_2 $+$ $\text{CH}_3\text{COCH}_2\text{COOEt}$		85 ¹⁷
4		NH_2CONH_2 $+$ $\text{CH}_3\text{COCH}_2\text{COOEt}$		82 ¹⁷
5		NH_2CONH_2 $+$ $\text{CH}_3\text{COCH}_2\text{COOEt}$		70 ¹⁷

6		NH_2CONH_2 $+$ $\text{CH}_3\text{COCH}_2\text{COOEt}$		94 ¹⁷
7		NH_2CONH_2 $+$ $\text{CH}_3\text{COCH}_2\text{COOEt}$		90 ¹⁷
8		NH_2CONH_2 $+$ $\text{CH}_3\text{COCH}_2\text{COOEt}$		61 ¹⁷
9		NH_2CONH_2 $+$ $\text{CH}_3\text{COCH}_2\text{COOEt}$		80 ¹⁷
10		NH_2CSNH_2 $+$ $\text{CH}_3\text{COCH}_2\text{COOEt}$		68 ¹⁷

				
11		NH_2CSNH_2 $+$ $\text{CH}_3\text{COCH}_2\text{COOEt}$		75 ²⁴

Conditions as in Table 4.3

4.6.7 Reusability

The catalyst was filtered from the reaction mixture and washed thoroughly with acetone, water and finally dried in vacuum. The catalysts were reused for the model reaction and it was observed that the product yield is slightly reduced to 75% for the first cycle and further reduced to 60% in second cycle, this indicates that minor leaching of Al may be occurring during the catalytic process.

4.7 Conclusions

1. Al-SBA-15 was functionalized by post impregnation method with the view to induce mild acidity in SBA-15 framework (SBA-15/Al). Different amounts of aluminum were incorporated inside the silica framework.
2. SBA/Al catalysts were characterized by PXRD, N₂ adsorption desorption, FT-IR and TPD techniques.
3. The catalytic activity studies of SBA/Al were tested for the synthesis of 3,4-dihydropyrimidine-2(1H)-ones in the liquid phase. Various reaction parameters were optimized. The catalytic activity and the product yield increased with increase in the

aluminum contents. Based on these results, the catalytic activity was extended to other substituted derivatives.

4.8 References

1. C.O. Kappe, *Eur.J.Med.Chem.* 35 (2000) 1043-1052.
2. K. Folkers, T. Johnson, *J. Am. Chem. Soc.* 55 (1933) 3784-3791.
3. C. Oliver Kappe, *Tetrahedron* 49 (1993) 6937-6963.
4. C. Kappe, *Acc. Chem. Res* 33 (2000) 879-888.
5. K. Atwal, B. Swanson, S. Unger, D. Floyd, S. Moreland, A. Hedberg, B. O'Reilly, *J. Med. Chem.* 34 (1991) 806-811.
6. G. Grover, S. Dzwonczyk, D. McMullen, D. Normandin, C. Parham, P. Sleph, S. Moreland, *J. Cardiovasc. Pharmacol.* 26 (1995) 289.
7. D. Nagarathnam, S. Miao, B. Lagu, G. Chiu, J. Fang, T. Dhar, J. Zhang, S. Tyagarajan, M. Marzabadi, F. Zhang, *J. Med. Chem* 42 (1999) 4764-4777.
8. T. Mayer, T. Kapoor, S. Haggarty, R. King, S. Schreiber, T. Mitchison, *Science* 286 (1999) 971.
9. A. Patil, N. Kumar, W. Kokke, M. Bean, A. Freyer, C. Brosse, S. Mai, A. Truneh, B. Carte, *J. Org. Chem.* 60 (1995) 1182-1188.
10. I. Ugi, A. Dömling, W. Hörl, *Endeavour* 18 (1994) 115-122.
11. A. Manjula, B. Rao, P. Neelakantan, *Synth. Commun.* 34 (2004) 2665-2671.
12. L. Xu, Z. Wang, C. Xia, L. Li, P. Zhao, *Helv. Chim. Acta* 87 (2004) 2608-2612.
13. J. Yadav, B. Reddy, R. Srinivas, C. Venugopal, T. Ramalingam, *Synthesis* 2001 (2001) 1341-1345.
14. A. Paraskar, G. Dewkar, A. Sudalai, *Tetrahedron Lett.* 44 (2003) 3305-3308.
15. J. Li, J. Han, J. Yang, T. Li, *Ultrason. Sonochem.* 10 (2003) 119-122.
16. A. Shaabani, A. Bazgir, F. Teimouri, *Tetrahedron Lett* 44 (2003) 2757.
17. M. Zhang, Y. Li, *Synth. Commun.* 36 (2006) 835-841.
18. Y. Yu, D. Liu, C. Liu, G. Luo, *Bioorg. Med. Chem. Lett.* 17 (2007) 3508-3510.
19. C. Kappe, D. Kumar, R. Varma, *Synthesis* 1999 (1999) 1799-1803.
20. B. Mishra, D. Kumar, V. Rao, *Catal. Commun.* 7 (2006) 457-459.
21. M. Kruk, M. Jaroniec, C. Ko, R. Ryoo, *Chem. Mater* 12 (2000) 1961-1968.
22. F. Rouquerol, J. Rouquerol, K. Sing, *Adsorption by Powders and Porous Solids: Principles* (1999).
23. X. Wang, K.S.K. Lin, J.C.C. Chan, S. Cheng, *J. Phys. Chem. B* 109 (2005) 1763-1769.

24. M. Lei, D. Wu, H. Wei, Y. Wang, *Synth. Commun.* 39 (2009) 475-483.

Chapter 5
Synthesis, Characterization and
Catalytic Application of Ordered
Mesoporous Silica Functionalized with
Polyphosphoric acid (SBA-15/PPA).

5.1 Introduction

The present chapter deals with functionalization of SBA-15 material with polyphosphoric acid (PPA) inside the silica framework by direct (in-situ) and impregnation methods. The interest stems to heterogenize PPA because of the intricate problems associated with neat PPA (viscous liquid, solubility problems)¹. Moreover according to the best of the literature knowledge, no report is available to functionalize PPA into the ordered mesoporous SBA-15. With this view the present chapter aims at the synthesis and characterization of SBA/PPA for acylation of naphthalene in the liquid phase.

5.2 Liquid phase acylation of naphthalene over SBA/PPA.

Friedel Craft's acylation of naphthalene is an important process in chemical industry for the production of intermediates in pharmaceuticals, agrochemicals, dyes and in petrochemical sectors²⁻⁵. Various heterogeneous catalysts such as clay^{6, 7}, zeolites⁸⁻¹⁰, Nafion on silica¹¹, sulphated zirconia¹²⁻¹⁵ and heteropolyacids¹⁶ have been employed for the acylation of naphthalene and their substituted derivatives but the selectivity of the desired product i.e. 2-acyl naphthalene still remains a serious challenge. Hence, there is a need to develop non-corrosive heterogeneous acid catalysts that can greatly improve the environmental impact of commercial production of acylated products. Several researchers have modified the catalytic properties of ordered mesoporous silica (OMS) by incorporating different acidic moieties such as propylsulfonic acid¹⁷⁻¹⁹, perfluoroalkylsulfonic acid²⁰, inorganic metals (Al, Ti, W)²¹⁻²⁵ and heteropolyacids^{26, 27} into the different silica matrix²⁸. However, not much attention has been paid to develop the catalyst having low to moderate acidity. Polyphosphoric acid (PPA) because of its mild acidity ($pK_a=2.1$)²⁹ and versatile use in^{30, 31} alkylation, acylation, cyclization, halogenation, dehydration, hydrolysis, polymerization and phosphorylation reactions^{32, 33} can be one of the options to induce milder acidity into the silica frame work. The use of silica gel-supported polyphosphoric acid (PPA/SiO₂) has been reported for the conversion of carbonyl compounds to oxathioacetals³⁴, Knoevenagel condensation³⁵ and for the synthesis of 2*H*-indazolo³⁶phthalazine-1,6,11(13*H*)-trione derivatives^{36, 37}.

5.3 Synthesis of SBA-15

The synthesis of SBA-15 is carried out using Pluronic (P123) (EO₂₀PO₇₀EO₂₀, MW = 5800, Aldrich) and TEOS as the surfactant and silica source respectively. In a typical synthesis

batch with TEOS, 3 g of P123 was dissolved in 100 g of distilled water and 5.9 g of conc. HCl (35%)³⁸. After stirring for 1h, 7.3 g of TEOS (ACROS, 98%) was added at 35°C maintaining the molar ratio and stirring for 24h. Subsequently the mixture was heated for 24 h at 100°C under static conditions in a closed polypropylene bottle. The solid product obtained after the hydrothermal treatment was filtered and dried at 80°C. The template was removed by calcinations at 550°C for 6h.

5.4 Direct synthesis of SBA/PPA(d) catalysts

The direct synthesis of SBA/PPA is carried out by incorporating PPA directly during the SBA-15 synthesis by using Pluronic P₁₂₃(EO₂₀PO₇₀EO₂₀, MW = 5800, Aldrich) as the surfactant and TEOS (tetraethylorthosilicate) as silica source. For the direct SBA/PPA (d) synthesis, 7.3 g of P123 was dissolved in 100 g of distilled water and 4 g of conc. HCl (35%)³⁸. After stirring for 3h, 11.6 g of TEOS (ACROS, 98%) and 2g of PPA was added together at 35°C maintaining the molar ratio of P123: H₂O: HCl: TEOS: PPA as 1: 5562.9::86.29: 42.51: 4.645 respectively. The mixture was left under stirring for 24 h at 35°C, and subsequently heated for 24 h at 100°C under static conditions in a closed polypropylene bottle. The solid product obtained after the hydrothermal treatment was filtered and dried at 80°C. The template was removed by calcining at 550°C for 6h and finally the solid obtained was grinded and named as SBA/x(d) where x represents the wt% of PPA incorporated. Similarly, the catalysts with different amounts of PPA were also synthesized under similar conditions.

5.5 Post-impregnated synthesis of SBA/PPA(I) catalysts

In the post-synthetic impregnation method, PPA is incorporated by impregnation method after calcining the SBA-15 materials at 550 °C. Typically for 15wt%, 450mg of PPA (calculation is based on the 85 wt% of P₂O₅ in PPA) was dissolved in 20 ml of methanol and impregnated into 1g of SBA-15 material. After the impregnation the solution was kept at reflux temperature for 24h. The mixture was cooled, filtered and washed with excess of methanol to remove the residual PPA and dried at 80°C for 12h. The samples were named as SBA/x(I), where x represents the wt% of PPA incorporated.

5.6 Physiochemical Characterization

5.6.1 PXRD

Powder X-ray diffraction pattern of SBA/PPA samples (Figure 5.1) at low angles showed the characteristic peaks at (100), (110), and (200) similar to the SBA-15 materials³⁸ indicating that the PPA has been incorporated uniformly inside the silica framework.

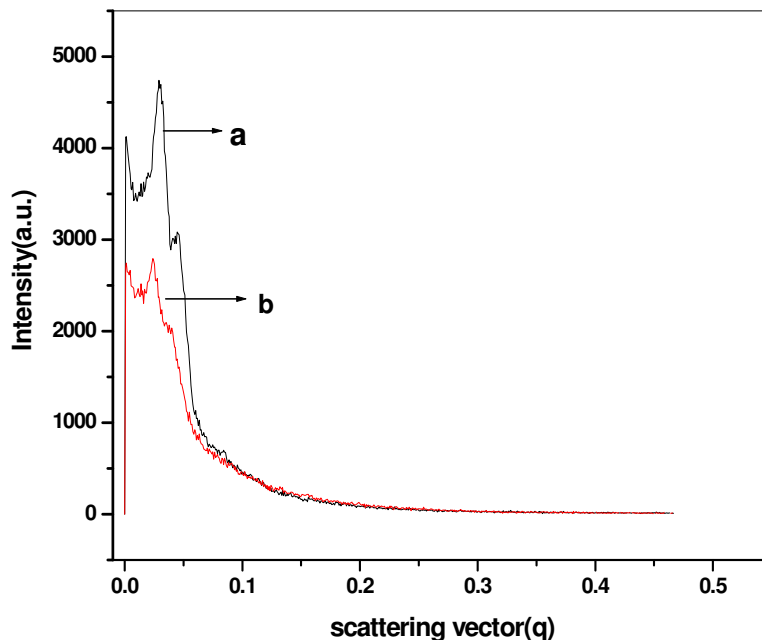


Figure 5.1 PXRD pattern of (a) SBA/15(d) and (b) SBA/15(I) catalysts

5.6.2 N₂ Adsorption-Desorption Studies

N₂ adsorption-desorption isotherms were measured at -196 °C using a Quantachrome AS-1MP volumetric adsorption analyzer. Before the adsorption measurements, all samples were out gassed for 12 h at 300°C in the degas port of the adsorption analyzer. The adsorption-desorption isotherm of the samples (Figure 5.2) showed a type IV adsorption isotherm indicating the mesoporous nature of the samples according to the IUPAC classification³⁹.

Table 5.1 Structural parameters of SBA/PPA catalysts

Materials	Surface area (m ² /g)	Pore Volume (cm ³ /g)	Pore Size (nm)	P (%)	P ₂ O ₅ (%)
-----------	----------------------------------	----------------------------------	----------------	-------	-----------------------------------

SBA-15	678	1.2	8.2	0	0
SBA/15(d)	473	0.36	3.6	1.21	21.54
SBA/10(d)	391	0.43	4.7	n.d	n.d
SBA/15(I)	390	0.44	4.6	8.34	14.01

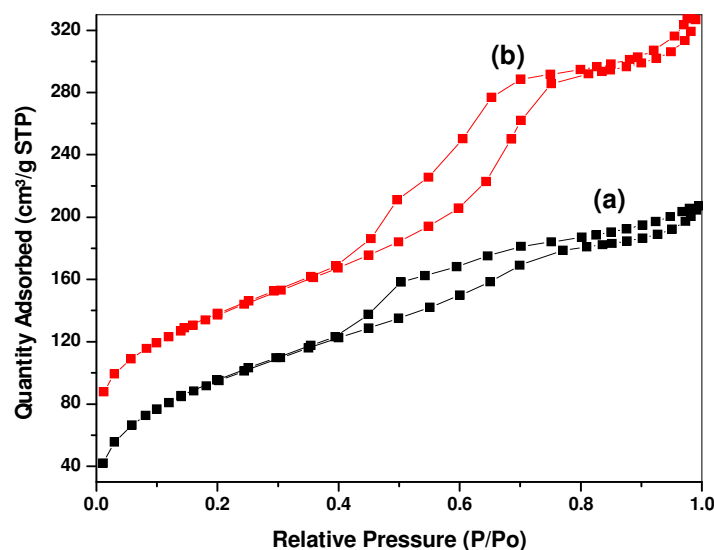


Figure 5.2 Nitrogen adsorption-desorption isotherms of (a) SBA/15(d) and (b) SBA/15(I) catalysts

A sharp capillary condensation step at relatively high pressure with an H1 hysteresis loop indicates the presence of large mesopores with narrow pore size distributions. The shape of the isotherms is slightly twisted compared to pure SBA-15 samples because of the strain generated during the incorporation of PPA inside SBA-15 framework in both SBA(d) and SBA(I) samples. The surface area, pore volume and pore diameter decreased with the incorporation of PPA indicating that the PPA has been incorporated inside the SBA-framework. All the structural parameters are included in Table 5.1.

5.6.3 SS-NMR

The incorporation of the PPA into the silica framework was further identified by ^{31}P magic angle spinning (MAS) SS-NMR. NMR spectrum of the samples (Figure 5.3) exhibits two different peaks at -0.2 and -11.44 ppm indicating the two types of phosphorus incorporated inside the silica framework⁴⁰.

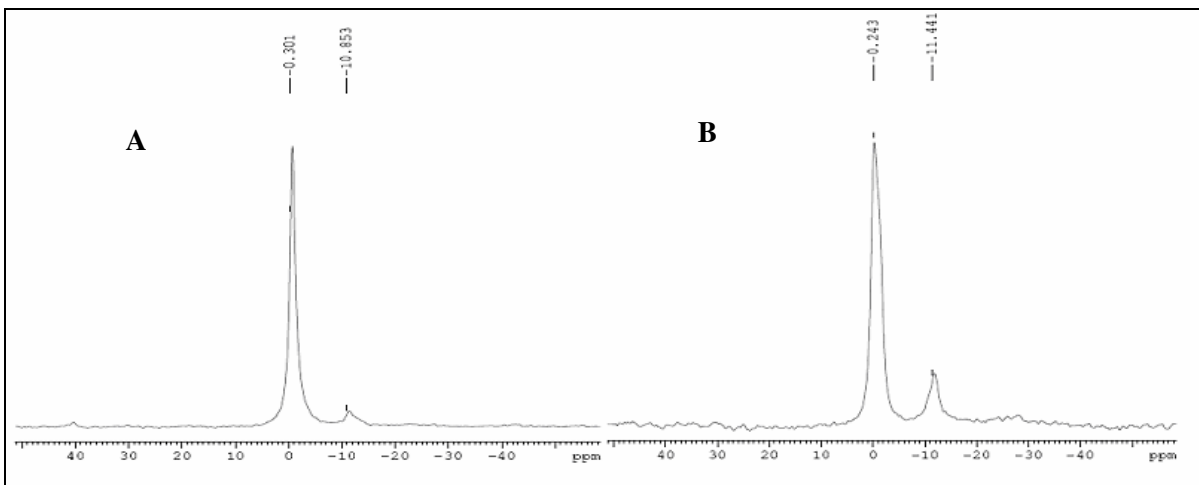


Figure 5.3 ^{31}P spectra of (A) SBA/PPA (I) and (B) SBA/PPA (d)

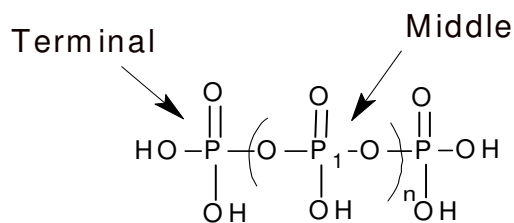


Figure 5.4 Distinct nature of phosphorus in PPA.

The intense peak around -0.2 ppm is due to the presence of phosphorus (P_1) in the middle of PPA chain whereas the signal at -11.44 ppm is attributed to phosphorus (P) present at the terminals of the PPA chain (Figure 5.4) ⁴⁰.

5.6.4 Energy Dispersive X-ray Fluorescence Spectrometry (EDXRF)

The loading of PPA, in terms of pure phosphorous and in P_2O_5 form in SBA-15 was estimated by EDXRF (Table 5.1). The spectrum (Figure 5.5) was analyzed to obtain the number of P $\text{K}\alpha$ counts per second and to determine the phosphorus content in SBA/PPA catalysts.

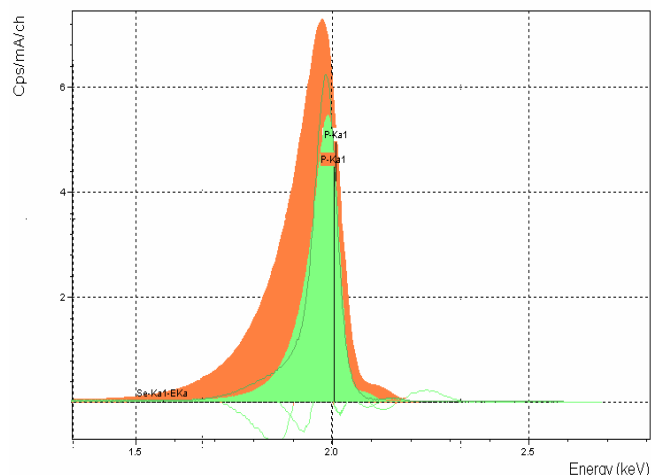


Figure 5.5 EDXRF spectrum of P in SBA/PPA (I) “orange” and SBA/PPA (d) “green”

5.6.5 Scanning Electron Microscopy (SEM)

The SEM images (Figure 5.6) of SBA-PPA (in-situ) shows rod shape particles with relatively 1 μ m uniform size. These rod shaped structures are uniformly aggregated into macro-structures due to the polymerization of PPA along with silica during the synthesis of ordered mesoporous silica material.

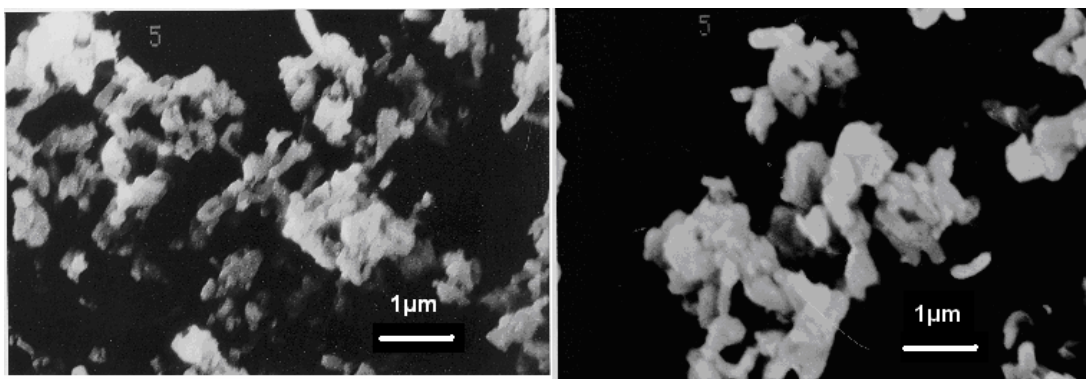


Figure 5.6 SEM images of SBA/PPA (I)

This is a clear indication that PPA is tightly restored within the silica framework during its synthesis and assist in recyclability.

5.6.6 FT-IR

FT-IR spectrum of the samples (Figure 5.7) showed the vibrational frequencies of the functionalized SBA-PPA samples in accordance to neat PPA, clearly indicating the uniform

nature of PPA inside the SBA-15 mesopores. The shift in vibrations frequencies from the original PPA (Table 5.2) indicates that PPA is polymerized with in the silica framework.

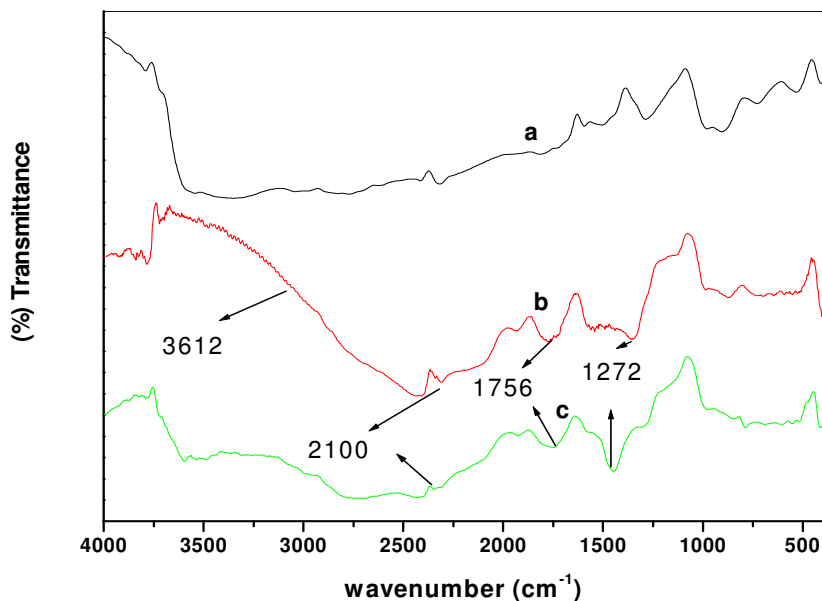


Figure 5.7 FT-IR spectra of (a) Neat PPA (b) SBA/10(d) (c) SBA/15(d) samples.

Table 5.2 FT-IR peaks of the samples

Peaks	PPA(neat) (cm ⁻¹)	SBA-PPA (10%) (cm ⁻¹)	SBA-PPA (15%) (cm ⁻¹)
O-H (str)	3612-3120	3603-3300	No peak
PO-H	3120-2100	3300-2100	3006-2100
P-O	933	912	913
P=O	1272	1436 (b)	1436 (b)
P-O-P (bending)	720	737	737

5.6.7 TPD of SBA/PPA

NH₃-Temperature Programmed Desorption (TPD) spectra of samples (Figure 5.8) showed the desorption pattern centred at T_{max} 228°C and 136°C indicating two different types of acidic sites in PPA, which can be ascribed to the terminal proton and the central proton of PPA structure (Figure 5.3).

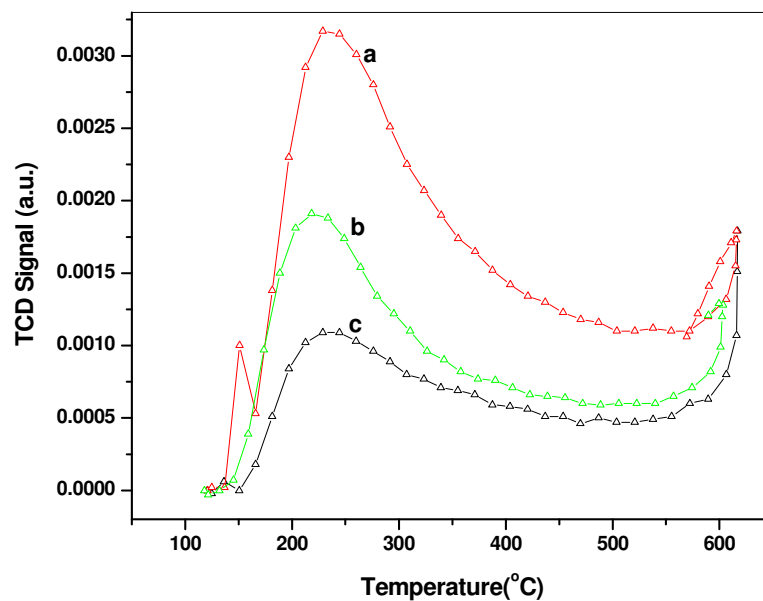


Figure 5.8 Temperature programmed desorption (TPD) of a) SBA/15(I) (b) SBA/15(d) (c) SBA/10(d) samples

Furthermore the presence of two types of acidic sites in SBA-15 functionalized PPA was confirmed by differential calorimetric scanning (DSC) (Figure 5.9). The total number of acidic sites is higher for SBA/15(I) - 87.0 $\mu\text{mol/g}$ compared to SBA/15(d) - 35.3 $\mu\text{mol/g}$ and SBA/10(d) - 11.0 $\mu\text{mol/g}$.

5.6.8 Differential Scanning Calorimetry (DSC)

Figure 5.9 showed the DSC pattern of SBA/PPA (d) catalyst. The catalyst is fairly stable upto 600°C and the two peaks at $T_1=386^\circ\text{C}$ and $T_2=512^\circ\text{C}$ indicates that there are two types of acidic sites available in SBA/PPA catalyst.

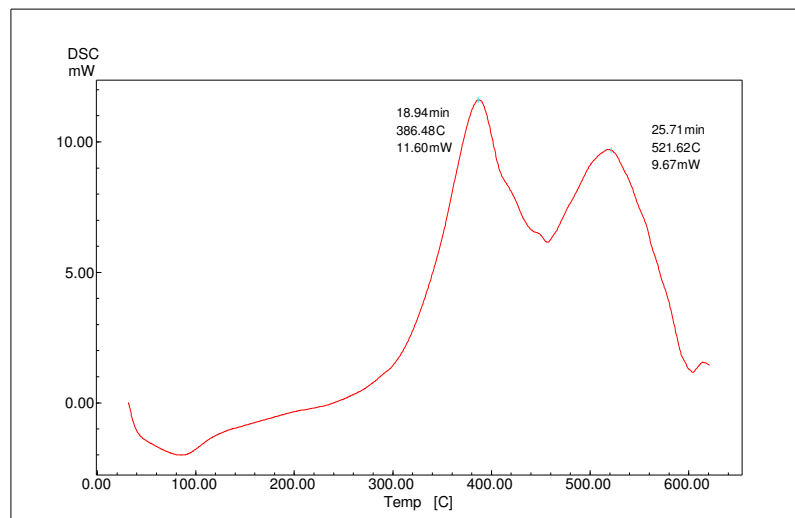
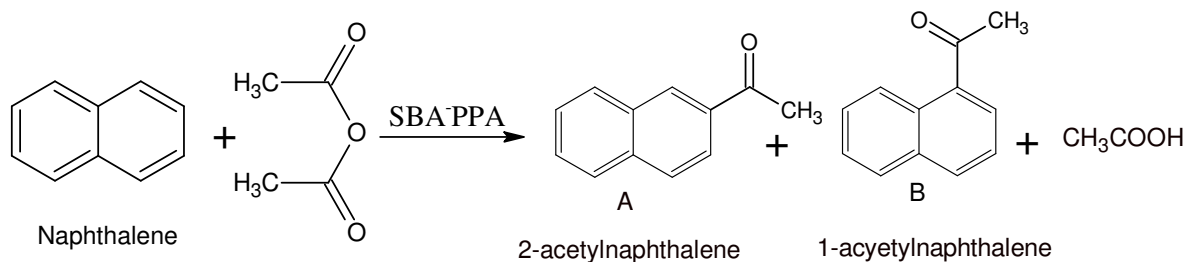


Figure 5.9 Differential Scanning Calorimetry of SBA/PPA(d)

5.7 Catalytic Studies

To test the catalytic activity of this mild catalyst, we selected acylation of naphthalene (Scheme 5.1) as a model reaction.

Acylation of naphthalene was carried out in the liquid phase using acetic anhydride as the acylating agent. Typically, 2 mmol of naphthalene, 2mmol of acetic anhydride were mixed in specially designed glass reactor. The desired amount of (SBA/PPA) catalyst was added to the reaction mixture at 90 °C under stirring conditions and the catalytic activity was monitored for 24 h by TLC. The products of the reaction were analyzed first by TLC and then later confirmed by gas chromatography after considering the response factors of the authentic samples using n-decane as internal standard.



Scheme 5.1 Acylation of Naphthalene

5.7.1 Effect of the different Catalysts

The catalytic activity results for acylation of naphthalene (Scheme 5.1) using acetonitrile as a solvent and acetic anhydride as acetylating agent showed around 23-25% conversion of 2-acetylnaphthalene (Table 5.3) on both the SBA/PPA catalysts, but very high selectivity (95%) of the 2-acetylnaphthalene (A) was obtained on the SBA/PPA (d) catalyst compared to 75% selectivity in the SBA/PPA (I) catalyst.

Table 5.3 Effect of different catalyst on the conversion and selectivity of acylation of naphthalene

Catalyst	^a Conversion (%)	Product Selectivity (%)	
		A	B
SBA-15	0	0	0
PPA (neat)	20	64	27
SBA/15(d)	23	94	6
SBA/10(d)	15	95	5
SBA/5(d)	0	0	0
SBA/15(I)	24	75	24

Conditions: Naphthalene- 2mmol, acetic anhydride-2mmol, Temp.-90 °C, acetonitrile (15ml), Catalyst 100mg

^a (%) conversion is based on both the products(A+B)

This difference in the selectivity of the 2-acylated product may be due to the better dispersion of PPA into SBA-15 framework coupled with high surface area of the SBA/PPA (d) catalysts (Table 5.1). Furthermore, no conversion was obtained for 5wt% SBA/PPA (d) catalyst infers that the minimum concentration of the active centres is required to achieve the conversion.

5.7.2 Effect of the different Solvents

Variation of the solvents showed high activity and selectivity using acetonitrile as a solvent (Table 5.4) under our experimental conditions. In order to see the influence of acetic acid generated during the reaction, the catalytic activity was also tested using acetic acid as a solvent, but no conversion of naphthalene was obtained indicating that the acetic acid generated during the reaction (Scheme 5.1) has no effect on the conversion and the selectivity of the desired product. In spite of having lower acidity of PPA (pKa = 2.1) the catalytic activity results of SBA/PPA catalysts can be compared with other heterogeneous catalysts such as sulphated zirconia, large pore zeolites and beta-zeolites already reported in

the literature⁸⁻¹³. Additionally, these results have advantages in terms of better selectivity of 2-acylated product over 1-acylated product. The catalyst SBA/15(d) was selected for further studies

Table 5.4 Variation of conversion of naphthalene with different solvents

Solvent	Conversion (%)	Product Selectivity (%)	
		A	B
Ethanol	0	0	0
1,2dichloroethane	7	97	3
Carbontetrachloride	7	96	3
cyclohexane	14	95	3
Decalin	16	92	7
1,4 Dioxane	21	94	5
Acetonitrile	23	94	6
Acetic acid	0	-	-

(Conditions as in Table 5.3)

5.7.3 Effect of the weight of catalyst

Figure 5.10 showed the effect of the catalyst weight on the total conversion of the products with time. The total conversion of naphthalene increased with increase in the weight of the catalyst (100mg) but no change in the selectivity was observed indicating that the uniform-

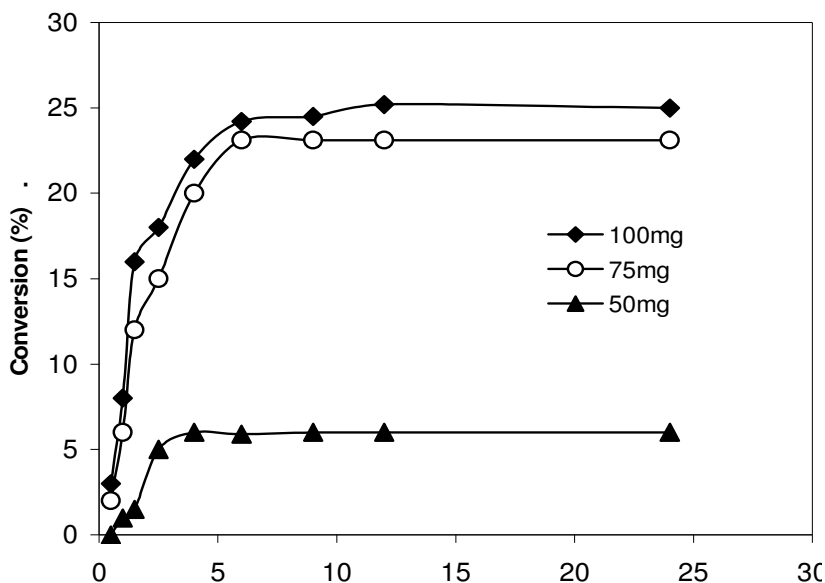


Figure 5.10 Effect of weight of the SBA/15(d) catalyst on the conversion of naphthalene

incorporation of PPA inside the SBA-15 catalysts is responsible for the selectivity of 2-acylated product.

5.7.4 Time on Stream studies

The time on stream studies (TOS) indicates that the maximum conversion can be achieved within 12h of the reaction time (Figure 5.11) but the reaction was allowed to proceed for 24h to see the stability of the product and the variation in the product selectivity.

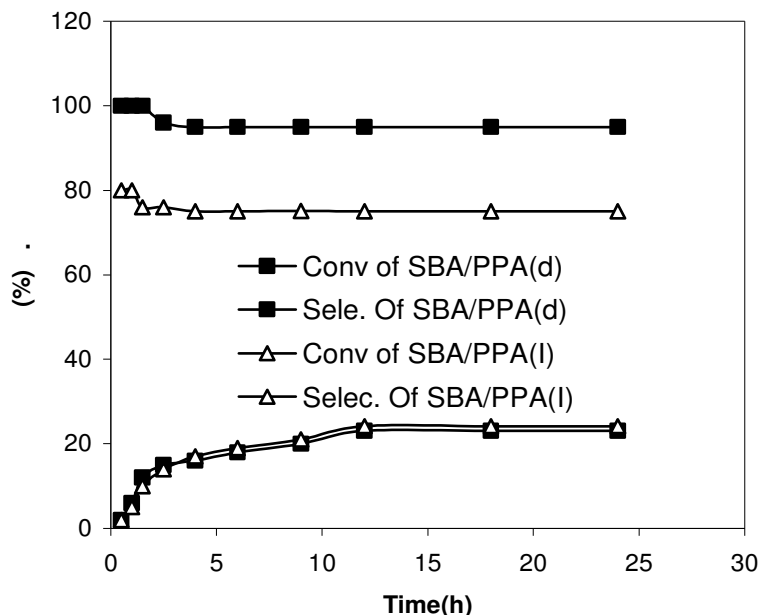


Figure 5.11 Effect of time on the conversion and product selectivity of 2-acetyl naphthalene over SBA/PPA (d) and SBA/PPA (I) catalysts

However no difference in the total conversion and selectivity of the 2-acetylated product was observed with time indicating that the products formed are stable and can be further scaled up industrially.

5.7.5 Effect of the amount of acetic anhydride

Variation of molar ratio of naphthalene: acetic anhydride indicated that the conversion increased with increase in the concentration of acetic anhydride initially (Table 5.5) and then decreased with further increase in the ratio infers that the use of excess acetic anhydride may block the active sites of the catalyst, reducing the accessibility of the reactants to the catalytic surface.

Table 5.5 Effect of different amount of acetic anhydride on the conversion and selectivity of acylation of naphthalene

Naphthalene:Acetic anhydride	Conversion (%)	Product Selectivity (%)	
		A	B
1:1	23	94	6
1:2	11	95	5
1:0.5	5.2	95	5

Conditions as in Table 5.3

5.7.6 Reusability

In order to see the reusability of the catalyst SBA/PPA (in-situ), the catalyst after first cycle was filtered washed thoroughly with solvent acetone and finally with water, dried at 150°C in the air oven and subjected to fresh reaction under identical reaction conditions. No difference in the activity and selectivity was observed up to three cycles (not tested further) indicating the promising use of these catalysts. The structure of the catalyst was retained after the reaction which was evident from the comparison of FT-IR spectrum (Figure 5.12) of the used catalyst with the starting one.

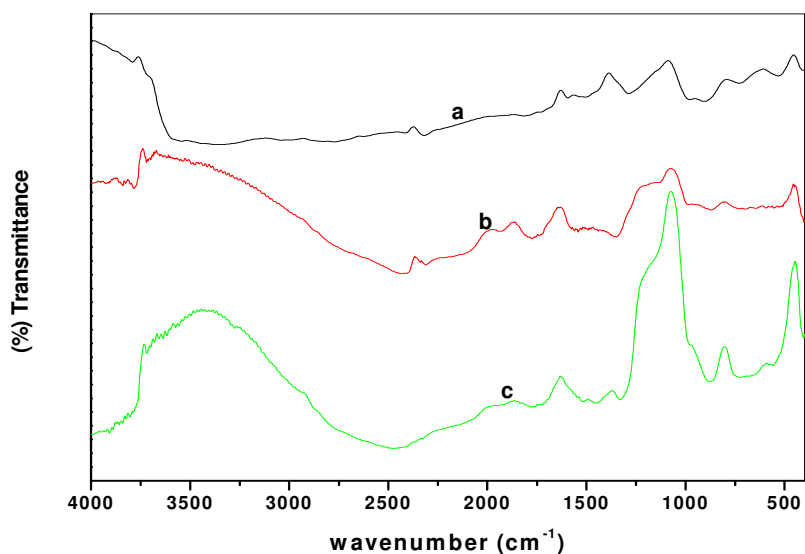
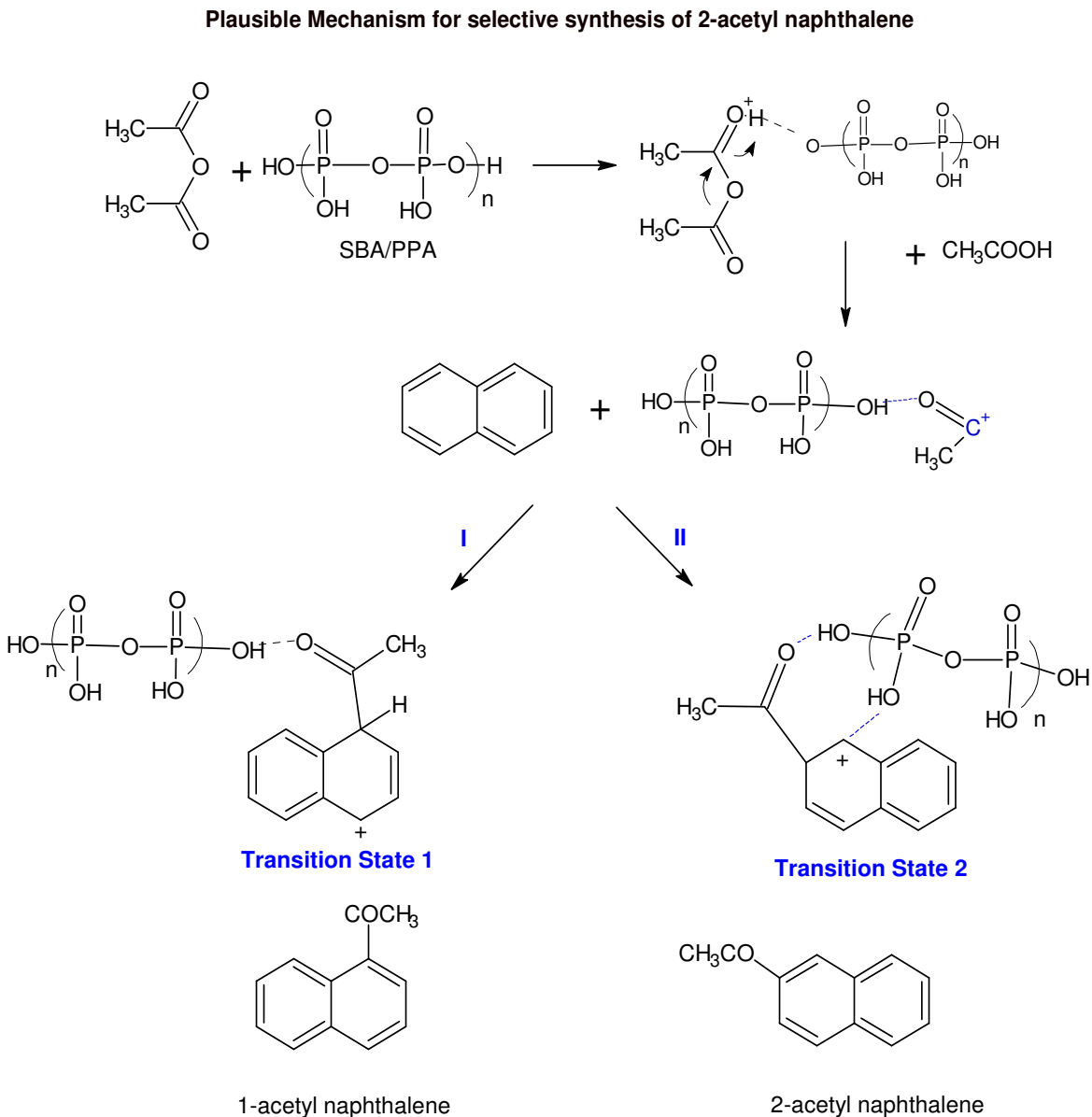


Figure 5.12 FT-IR spectra of (a) PPA (b) After first run and (c) after second run of SBA/15(d) catalyst

5.7.7 Plausible Mechanism

The mechanism of acylation of naphthalene (Scheme 5.2) proceeds via protonation of acetic anhydride which cleaves to form acylium ion.



Scheme 5.2 Plausible Mechanism

We presume that acylium ion formed gets stabilized by polymeric PPA via H-bonding and reacts with the nucleophilic center of naphthalene i.e. at 1 or 2-position. Moreover the reaction can follow two pathways either I or II but the pathway II is the major one that is followed in the present catalytic studies. This may be due to the better stability of the transition state2 due to ring like structure. However Pathway I can also be adopted by the

reaction because of the allylic carbocation stability of transition state I which is also confirmed by product selectivity. Furthermore this acylation reaction at β or 2-position is believed to be a second order reaction.

5.8 Conclusions

1. SBA/PPA nanocomposites with different amount of acidity were synthesized by two different methodologies by direct in-situ and post impregnation methods.
2. SBA/PPA catalysts were characterized by PXRD, N_2 adsorption desorption, EDXRF, FT-IR, SS-NMR, TPD, SEM and DSC techniques which showed that PPA was uniformly incorporated inside the framework of SBA-15.
3. The catalytic activity results for liquid phase acylation of naphthalene over SBA/PPA nanocomposites synthesized by in-situ method showed very high activity and selectivity of the 2-acylated product.
4. Proper tuning of these SBA/PPA, mild acid catalyst may pave the way for other acid catalyzed reaction which are commercially important.

5.9 References

1. K. Mikami, Y. Motoyama, L.A. Paquette, *Encyclopedia of Reagents for Organic Synthesis*, **1995**.
2. P. Gore, *Chem.Rev.* 55 (**1955**) 229-281.
3. G. Olah, J. Olah, *J Am Chem Soc* 98 (**1976**) 1839-1842.
4. G. Olah, *Friedel-Crafts Chemistry*, Wiley New York, **1973**.
5. W. Pardee, B. Dodge, *Ind. Eng. Chem.* 35 (**1943**) 273-278.
6. T.W. Bastock, J.H. Clark, P. Landon, K. Martin, *J. Chem. Res., Synop.* (**1994**) 104-105.
7. B.M. Choudary, M. Sateesh, M.L. Kantam, K.V.R. Prasad, *App.Catal., A* 171 (**1998**) 155-160.
8. M. Climent, A. Corma, H. García, J. Primo, *App.Catal.*, (**1989**) 113-125.
9. K. Gaare, D. Akporiaye, *J. Mol. Catal. A: Chem.* 109 (**1996**) 177-187.
10. D. Rohan, C. Canaff, E. Fromentin, M. Guisnet, *J. Catal.* 177 (**1998**) 296-305.
11. A. Heidekum, M.A. Harmer, W.F. Hoelderich, *J. Catal.* 188 (**1999**) 230-232.
12. V. Quaschnig, J. Deutsch, P. Druska, H. Niclas, E. Kemnitz, *J. Catal.* 177 (**1998**) 164-174.
13. J. Deutsch, V. Quaschnig, E. Kemnitz, A. Auroux, H. Ehwald, H. Lieske, *Top. Catal.* 13 (**2000**) 281-285.
14. V. Quaschnig, A. Auroux, J. Deutsch, H. Lieske, E. Kemnitz, *J. Catal.* 203 (**2001**) 426-433.
15. A. Trunschke, J. Deutsch, D. Müller, H. Lieske, V. Quaschnig, E. Kemnitz, *Catal. Lett.* 83 (**2002**) 271-279.
16. I. Kozhevnikov, *App.Catal., A* 256 (**2003**) 3-18.
17. S. Sreevardhan Reddy, B. David Raju, V. Siva Kumar, A. Padmasri, S. Narayanan, K. Rama Rao, *Catal. Commun.* 8 (**2007**) 261-266.
18. Y. Wan, D. Zhang, N. Hao, D. Zhao, *Int.J. Nanot.* 4 (**2007**) 66-99.
19. A. Wight, M. Davis, *Chem.Rev.* 102 (**2002**) 3589-3614.
20. M. Alvaro, A. Corma, D. Das, V. Fornés, H. García, *Chem. Commun.* 2004 (**2004**) 956-957.
21. B. Newalkar, J. Olanrewaju, S. Komarneni, *Chem. Mater* 13 (**2001**) 552-557.
22. Y. Ooi, R. Zakaria, A. Mohamed, S. Bhatia, *Catal. Commun.* 5 (**2004**) 441-445.

23. Y. Li, W. Zhang, L. Zhang, Q. Yang, Z. Wei, Z. Feng, C. Li, *J. Phys. Chem. B* 108 (2004) 9739-9744.
24. X. Yang, W. Dai, H. Chen, Y. Cao, H. Li, H. He, K. Fan, *J. Catal.* 229 (2005) 259-263.
25. Q.Y. Liu, W.L. Wu, J. Wang, X.Q. Ren, Y.R. Wang, *Microporous Mesoporous Mater.* 76 (2004) 51-60.
26. H. Jin, Q. Wu, P. Zhang, W. Pang, *Solid State Sci.* 7 (2005) 333-337.
27. J. Wang, H. Zhu, *Catal. Lett.* 93 (2004) 209-212.
28. I. Mbaraka, B. Shanks, *J. Catal.* 229 (2005) 365-373.
29. H. Kawamoto, M. Murayama, S. Saka, *J. Wood. Sci.* 49 (2003) 469-473.
30. Y. Sun, H. Wang, R. Prins, *Tetrahedron Lett.* 49 (2008) 2063-2065.
31. A.V. Aksenov, A.S. Lyahovnenko, I.V. Aksenova, O.N. Nadein, *Tetrahedron Lett.* 49 (2008) 1808-1811.
32. F. Popp, W. McEwen, *Chem.Rev.* 58 (1958) 321-401.
33. J. Zhang, R. Hertzler, E. Holt, T. Vickstrom, E. Eisenbraun, *J. Org. Chem.* 58 (1993) 556-559.
34. T. Aoyama, T. Takido, M. Kodomari, *Synlett* 15 (2004) 2307-2310.
35. S. Kantevari, R. Bantu, L. Nagarapu, *J. Mol. Catal. A: Chem.* 269 (2007) 53-57.
36. H. Shaterian, A. Hosseinian, M. Ghashang, *ARKIVOC* 2 (2009) 59-67.
37. H. Shaterian, A. Hosseinian, M. Ghashang, *Synth. Commun.* 38 (2008) 3375-3389.
38. M. Kruk, M. Jaroniec, C. Ko, R. Ryoo, *Chem. Mater* 12 (2000) 1961-1968.
39. F. Rouquerol, J. Rouquerol, K. Sing, *Adsorption by Powders and Porous Solids: Principles* (1999).
40. Y. So, J. Heeschen, *J. Org. Chem* 62 (1997) 3552-3561.

Chapter 6
Synthesis, Characterization and
Catalytic Applications of Chloroacetic
acid Grafted on Ordered Mesoporous
Silica (OMS)

6.1 Introduction

In continuation of our work to develop solid mild acid catalyst, SBA-15 was functionalized with chloroacetic acid via post-synthetic grafting method¹. Grafting of chloroacetic moiety on to the surface permits more accessibility of catalyst to the reactants and provides better activity and selectivity in a reaction^{2, 3}. In addition the covalent nature of the attachment achieved by grafting method can be exploited to increase the catalyst's stability. Therefore the present chapter aims at the synthesis and characterization of chloroacetic acid functionalized catalyst for the Knoevenagel condensation of cinnamaldehyde with ethylcyanoacetate.

6.2 Knoevenagel Condensation of cinnamaldehyde with ethylcyanoacetate

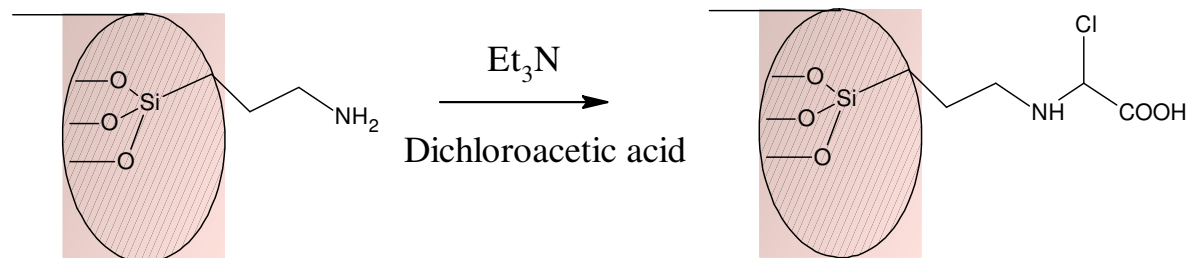
Knoevenagel condensation was chosen as a model reaction for investigating the catalytic property of SBA-15 functionalized with chloroacetic was chosen. Knoevenagel condensation is one of the most useful C–C bond forming reactions for the production of fine chemicals⁴. The products of this reaction⁵ e.g. ethyl (4*E*)-2-cyano-3-hydroxy-5-phenylpent-4-enoate have important applications in photosensitive composition and act as an intermediate for plant growth regulators⁶. Ethyl α -cyanocinnamates or phenylcinnamate's with alkoxy or hydroxyl substituents in the arenes are used in ultraviolet filters composition for protecting light-sensitive foods, wood-products⁷, paper, dyes, fibers, plastics, cosmetics and fragrances⁸⁻¹⁰. Several heterogeneous catalysts including oxides, zeolites¹¹, ammonia, organic amines¹², hydrotalcite in ionic liquid media¹³, 1,8-diazabicycloxx[5.4.0]undec-7-ene (DBU)¹⁴, ZnCl₂¹⁵, CdI₂¹⁶, KSF montmorillonite¹⁷ and KF-Al₂O₃¹⁸ have been reported for this interesting reaction. However, no report is available for chloroacetic acid (pKa = 2.85) functionalized SBA-15 mesoporous materials for the selective synthesis of phenylcinnamate's (A, Scheme-2).

6.3 Synthesis of chloroacetic functionalized SBA-15 (SBA/CA)

The synthesis of SBA was carried out in accordance to the earlier reports¹⁹ using Pluronic (P123) (EO₂₀PO₇₀EO₂₀, MW = 5800, Aldrich) as surfactant and TEOS as the silica source in Chapter 3²⁰.

Chloroacetic acid was incorporated via post synthetic grafting technique into the silica framework (Scheme 6.1). Typically, to 1g of SBA-15, 10ml of amino-propyltriethoxysilane

(APTS) was stirred in dry toluene (20ml) under inert atmosphere (Scheme 1). The product SBA/APTS was filtered and exhaustively washed with ethanol in Soxhlet extractor for 24h. SBA-15 functionalized with APTS was dried under vacuum and used further for functionalization with dichloroacetic acid. Typically, 1g of SBA/APTS was mixed with 1ml of dichloroacetic acid (equivalent amount) in 15 ml of triethylamine (acts as a solvent for neutralizing HCl generated during the functionalization) and refluxed for 24h under stirring conditions. Finally chloroacetic acid functionalized SBA-15 (light brown coloured) was filtrated and washing thoroughly with dil HCl and water. No color change was observed in Ninhydrin test confirms the functionalization of SBA-15 with chloroacetic (absence of free primary amines). The sample was named as SBA/CA.



Scheme 6.1 Functionalization of SBA-15 with chloroacetic acid

6.4 Physiochemical Characterizations

6.4.1 PXRD

PXRD pattern of the samples at low angles (Figure 6.1) showed the diffraction pattern similar to SBA-15 sample. The diffraction at (100), (110), and (200) planes can be indexed to reflections comprising of hexagonal $p6mm$ space group indicating that the materials possess the ordered mesoporous structure^{3, 19}. The intensity of the base peak in SBA/CA was lowered compared to pure SBA-15 indicating that chloroacetic acid has been incorporated into the silica framework.

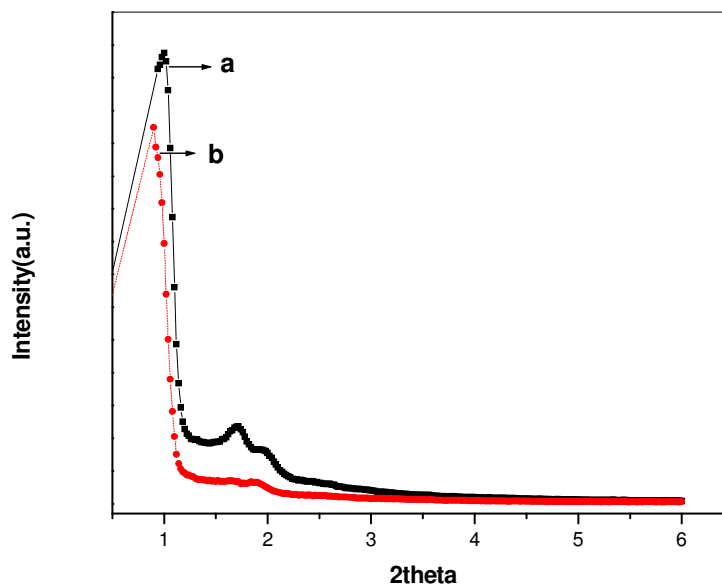


Figure 6.1 PXRD pattern of a) SBA-15 and b) SBA/CA catalysts.

6.4.2 N₂ Adsorption-Desorption studies

The specific surface area was calculated by the BET method and the pore size distribution was calculated by Barrett–Joyner–Halenda (BJH) method from the desorption isotherm of the sample.

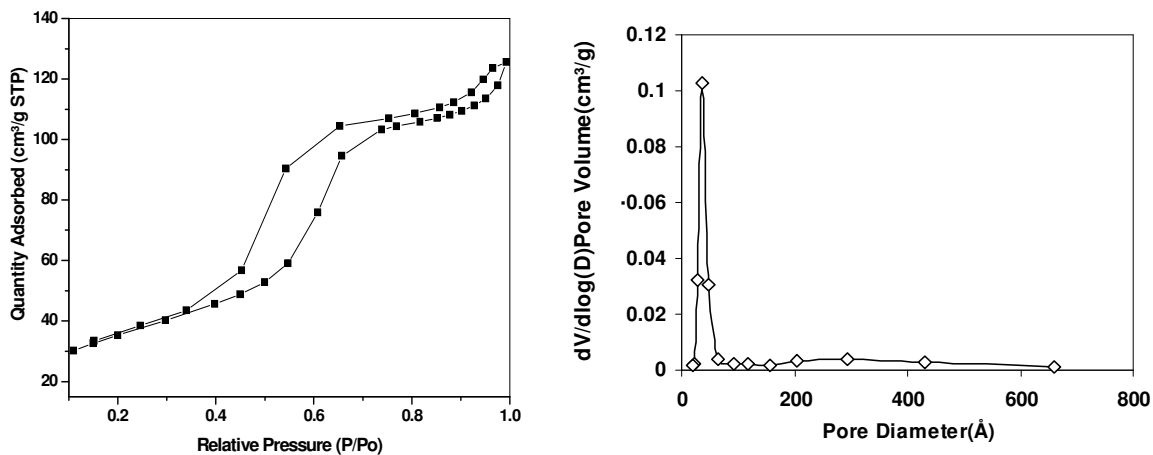


Figure 6.2 N₂-adsorption –desorption isotherm and pore size distribution of SBA/CA

The nitrogen adsorption-desorption isotherm (Figure 6.2) of the catalysts showed a type IV adsorption isotherm according to IUPAC classification^{3, 21}, with a sharp capillary condensation step at relatively high pressure with an H1 hysteresis loop indicative of mesoporous nature of the samples.

Table 6.1 Structural parameters of SBA/CA catalyst

Catalyst	Pore Size BJH _{Ads} (nm)	Pore Volume (cm ³ /g)	Surfacearea (m ² /g)
SBA-15	8.4	1.2	656
SBA/CA	5.6	0.18	129

The shape of the isotherm is slightly tilted indicative of little strain generated during incorporation of chloroacetic acid inside the silica framework. The surface area, pore volume and pore diameter decreased with the incorporation of chloroacetic acid, indicating that the chloroacetic acid has been incorporated inside the SBA-framework (Figure 6.2 and Table 6.1). The particle size of the SBA/CA is 46nm. All the structural parameters of the catalysts are included in Table 6.1.

6.4.3 SS-NMR

The incorporation of chloroacetic acid into the silica framework was further confirmed by ¹³C CPMAS SS-NMR (Figure 6.3). The spectrum of SBA/CA showed five types of carbon. The peak at 173 ppm indicates the presence of deshielded carbon due to the carboxylic acid carbon. The peak at 66ppm with low intensity indicates the presence of C₁ in chloroacetic acid group. Furthermore, the three peaks at 41,20 and 8 ppm indicates the presence of aminopropyl group to which chloroacetic acid group is attached.

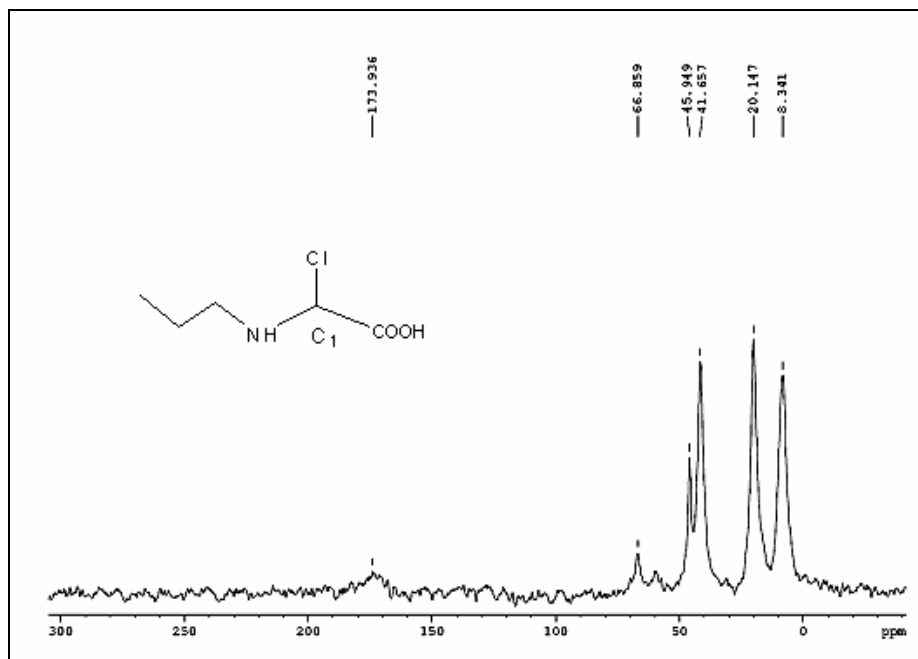


Figure 6.3 ^{13}C CPMAS NMR spectra of SBA/CA catalyst.

6.4.4 Energy Dispersive X-ray Fluorescence Spectrometry (EDXRF)

The amount of loading of chloroacetic acid in SBA-15 was estimated by EDXRF. The spectrum (Figure 6.4) was analyzed to obtain the number of Cl K α counts per second and to determine the chlorine content in SBA/CA catalysts.

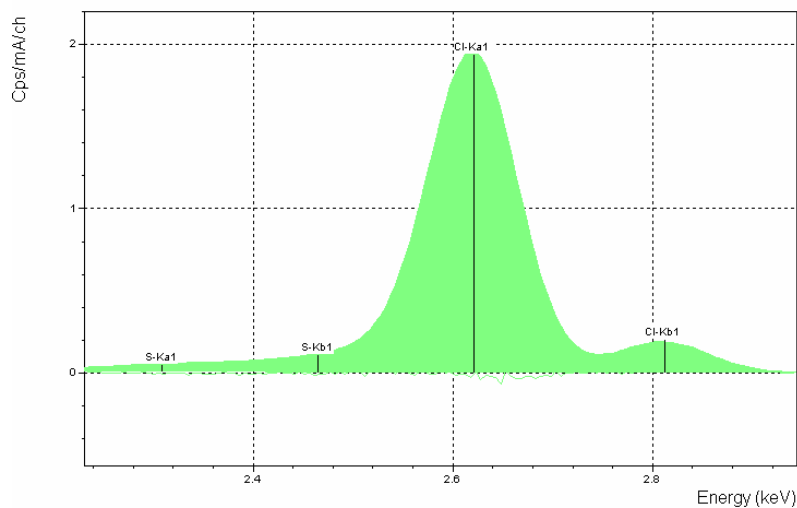


Figure 6.4 EDXRF spectrum of chlorine in SBA/CA.

The chlorine content present in the SBA/CA was 0.329% and is in agreement with the theoretical calculations

6.4.5 FT-IR

The FT-IR spectrum (Figure 6.5) of the SBA/CA showed the presence of the peak at 3604 cm^{-1} for O-H stretching in COOH group while peak at 1674 cm^{-1} indicates the presence of C=O stretching similar to chloroacetic acid (CA). Furthermore the peak at 1250 cm^{-1} confirms the presence of C-Cl stretching bond. The stretching frequencies were well correlated with neat chloroacetic acid indicating the incorporation of acidic moiety inside the silica framework.

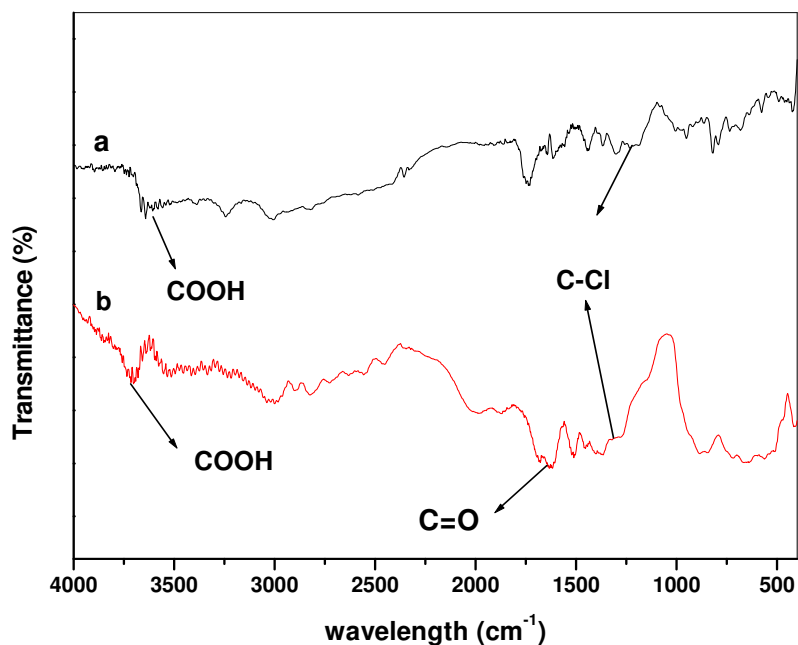


Figure 6.5 FT-IR spectra of a) chloroacetic acid and b) SBA/CA.

6.4.6 Temperature Programmed Desorption (TPD) of SBA/CA

Acidity of the catalyst was measured by TPD (NH₃) method and the number of acidic sites (Figure 6.6) was found to be $24.2\mu\text{mol/g}$ indicating the low acidity content on SBA/CA catalyst.

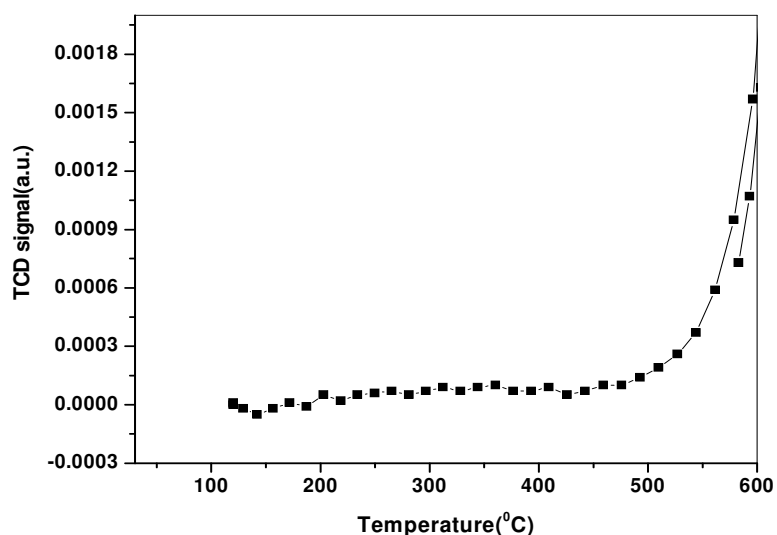
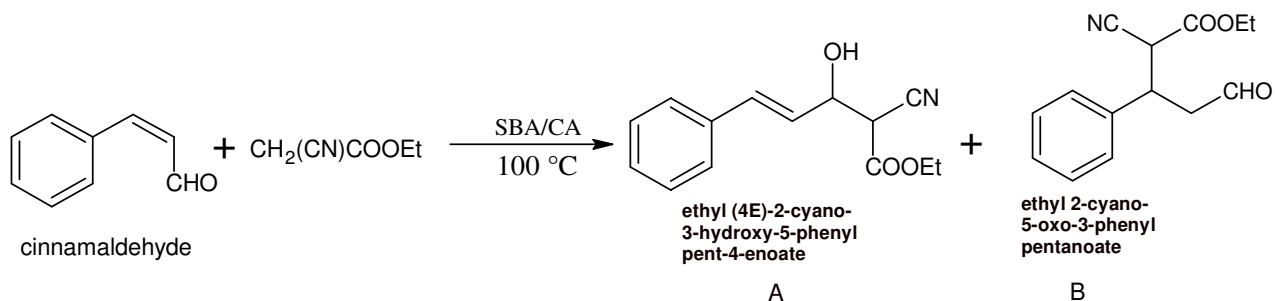


Figure 6.6 Temperature Programmed Desorption (TPD) of SBA/CA.

6.5 Catalytic Studies

The catalytic activity studies were carried out in the liquid phase for Knoevenagel condensation (Scheme 6.2). 1mmol of cinnamaldehyde and 1.2 mmol of ethylcyanoacetate were stirred at 100⁰C in glass reactor. The desired amount of the catalyst (10-200mg) was added to the reaction mixture under inert atmosphere and the reaction was monitored for 12h. The products of the reactions were confirmed with authentic samples (prepared under homogeneous conditions) on TLC. After the completion of the reaction, the catalyst was filtered and washed with acetone. The solvent was evaporated and finally the product was isolated from the reaction mixture using ethanol and water. The solid product obtained was dried in vacuum and weighed to obtain isolated yield.



Scheme 6.2 Knoevenagel condensation of cinnamaldehyde with ethylcyanoacetate

6.5.1 Effect of the different catalysts

The catalytic activity of SBA/CA was investigated for Knoevenagel condensation of cinnamaldehyde with ethylcyanoacetate in liquid phase (Scheme 6.2). The catalytic activity results showed 98% conversion with 96% selectivity of desired product (A). The catalytic activity and selectivity was also compared with chloroacetic acid (homogeneous conditions) under similar reaction conditions. No difference in the activity was observed however very low selectivity (75%) of the desired product (A) was obtained under homogeneous conditions corroborating our endeavor to heterogenize the chloroacetic acid in SBA-15. The increased product selectivity over SBA/CA is attributed to the high surface area and better dispersion of active sites on heterogenization of chloroacetic acid (Table 6.1). It is important to mention here that 18% activity was observed without catalysts (blank) and 20% conversion was obtained with SBA-15 catalyst indicating that more acidic centers are required for the higher conversion of reaction. The blank or with SBA-15 activity (18-20%) may be due to the high electrophilic nature of the reactant cinnamaldehyde which was not observed for other substituted aldehydes.

Table 6.2 Variation of conversion of products over different catalysts.

Catalyst	Surface area (m ² /g)	^a Conversion (%)	Product Selectivity (%)		^b Yield (%)
			A	B	
Blank	-	18	91	8	15
SBA-15	656	20	90	10	14
CA	-	95	75	20	65
SBA/CA	129	98	96	4	93

Conditions: 1mmol- cinnamaldehyde, 1.2 mmol- ethylcyanoacetate, Temp- 100⁰C, SBA/CA catalyst-100mg.

^a %Conversion is based on total products formed.

^b isolated yield of desired product (A)

CA –stands for chloroacetic acid

6.5.2 Effect of the solvent

The variation of different solvents (Figure 6.7) infers that the highest activity and selectivity can be obtained under solvent free conditions.

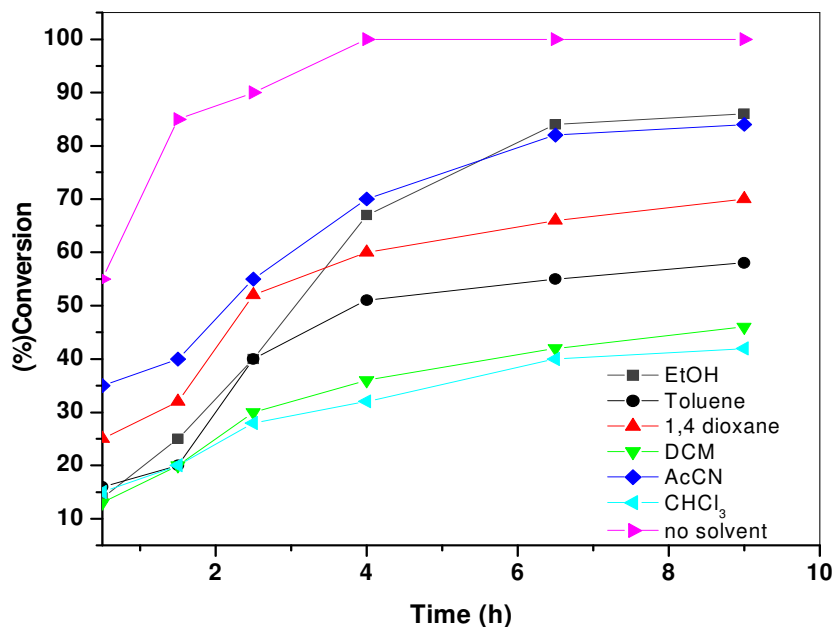


Figure 6.7 Effect of different solvents on the conversion of product (A).

Careful examination of the solvent concludes that the conversion of the product increased with increasing polarity of the solvent. However lower activity was observed using non polar solvents. This may be due to better stabilization of transition state in polar solvents than in non-polar solvents. We believe that ethylcyanoacetate, because of its high polarity itself, may act as a solvent and stabilize the transition state in a better way to generate the desired product.

6.5.3 Effect of the catalyst weight

Table 6.3 showed the effect of catalyst weight on the conversion of product (A).

Table 6.3 Effect of catalyst weight on the conversion of product (A) over SBA/CA catalyst.

Catalyst Weight	Conversion (%)	Product Selectivity (%)		Yield (%)
		A	B	
200	100	98	2	95
100	98	96	4	93
75	90	92	6	85
50	85	91	6	78
25	82	91	5	74
10	57	90	7	50

Conditions as in Table 6.2

The results concluded that the conversion and the selectivity of the product (A) increased with increase in the weight of the catalyst and maximum conversion can be achieved with 200mg of the catalyst within 2h. However, 100mg of the catalyst was selected for carrying out further studies.

6.5.4 Effect of reaction temperature

Figure 6.8 showed the effect of temperature on the conversion and selectivity of ethyl (4*E*)-2-cyano-3-hydroxy-5-phenylpent-4-enoate (A). The results concluded that the conversion of the product (A) and the selectivity of the product increased with increase in the temperature up to 100°C and maximum conversion is achieved within 3h. Remarkable effect on product selectivity was observed at lower temperature wherein selectivity of product (A) is reduced. This may be due to the high electrophilic nature of transition state (C) at higher temperature compared to transition state (D) at lower temperature (Scheme 6.3) indicating the influence of thermodynamic vs kinetically controlled product.

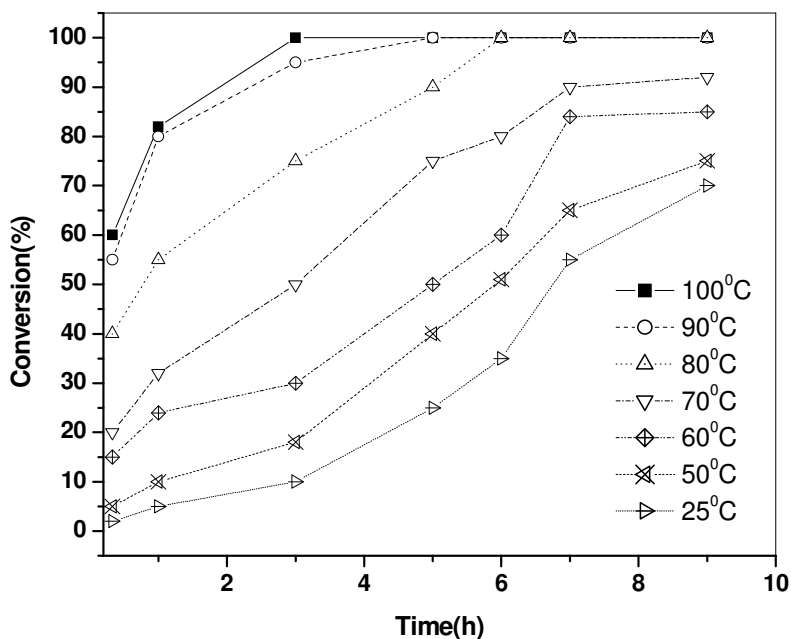
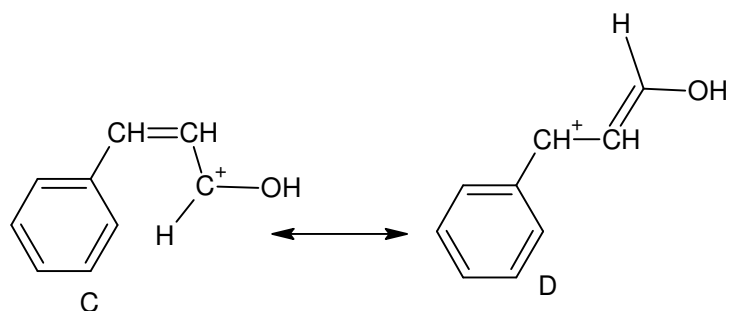


Figure 6.8 Variation of reaction temperature on the conversion of product (A) over SBA/CA catalyst.



Scheme 6.3 Transition States

6.5.5 Time on stream studies (TOS)

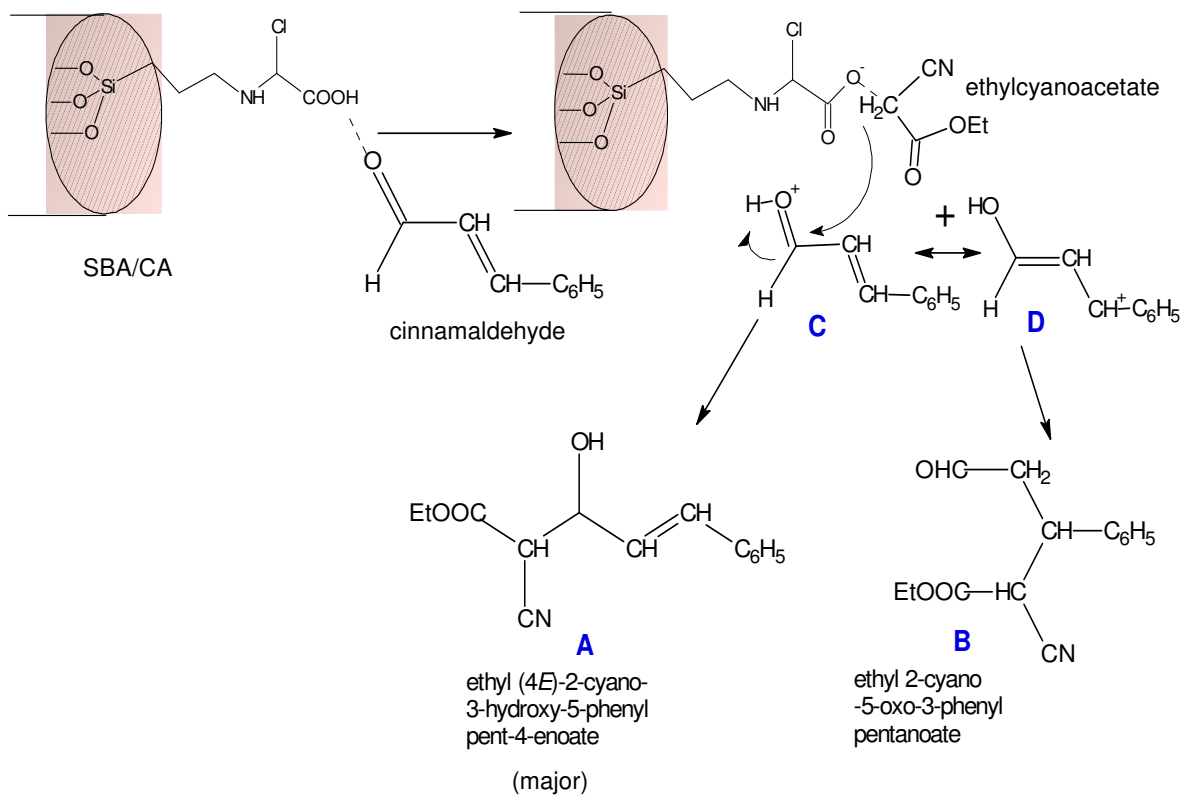
Time on stream studies (Figure 6.8) also indicates that the total conversion increased with increase in the reaction time at all temperatures. Although maximum conversion is achieved within 3h at 100°C yet the reaction was allowed to proceed for 24h to check the formation of secondary products (either through product decomposition or inter conversions of the products). However no difference in the activity and selectivity was observed after 24h indicating the promising use of the catalyst. .

6.5.6 Plausible Mechanism

The probable mechanism (Scheme 6.4) for the synthesis of ethyl (4*E*)-2-cyano-3-hydroxy-5-phenylpent-4-enoate (A) selectively over SBA/CA is due to the kinetically controlled formation of intermediate C. The reaction proceeds via S_N2 mechanism in concerted manner wherein intermediate C subsequently reacts with deprotonated ethylcyanoacetate which further leads to the formation of product (A).

6.5.7 Reusability

In order to check the heterogeneity of the catalyst, a hot filtration test was carried out. The catalyst SBA/CA, after the completion of the reaction, was filtered and washed thoroughly with acetone and water. The catalyst was dried and again subjected to fresh reaction. No significant (5-8%) difference in the activity and selectivity of the product was noted after 24h indicating the stability of the functional group in SBA/CA catalyst.



Scheme 6.4 Plausible Mechanism

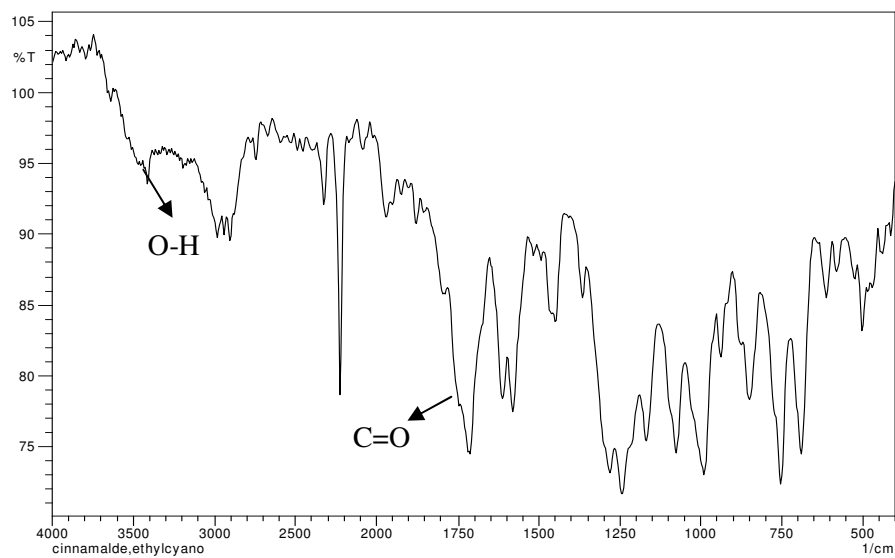


Figure 6.9 FT-IR of product (A) (4*E*)-2-cyano-3-hydroxy-5-phenylpent-4-enoate

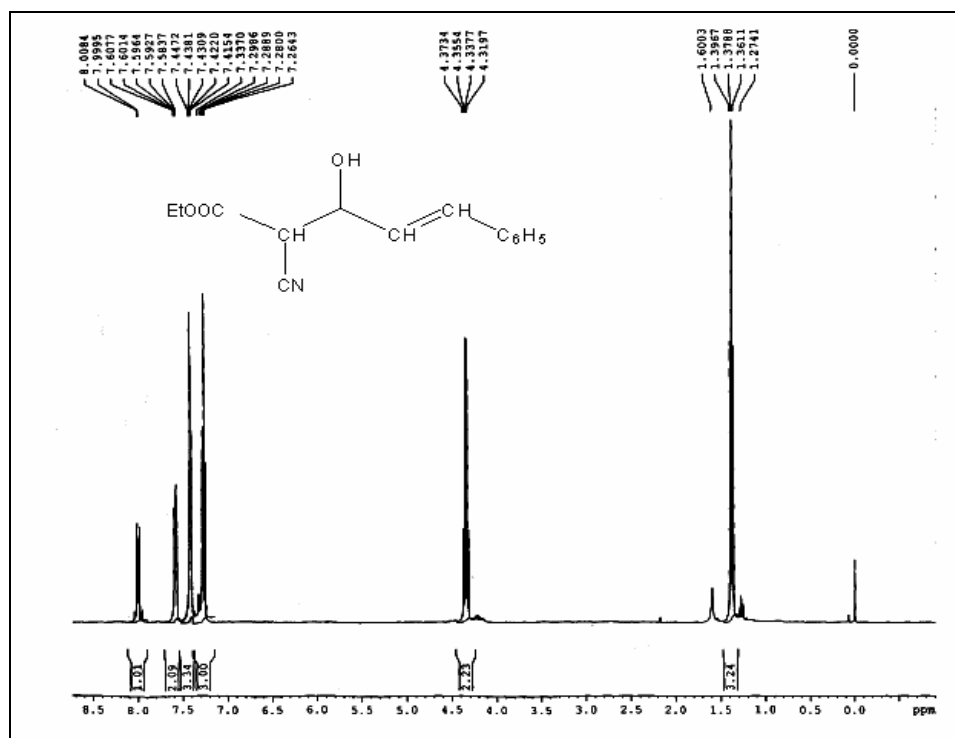


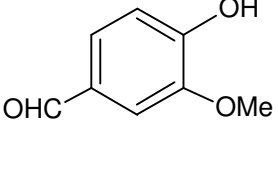
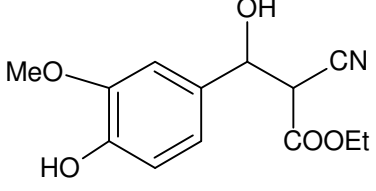
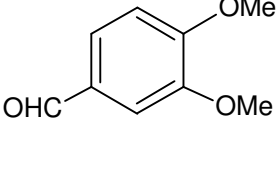
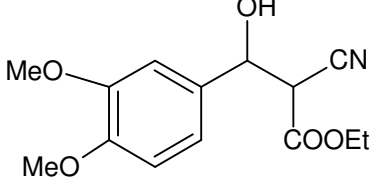
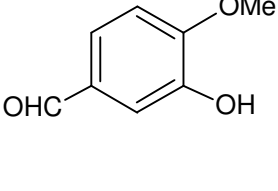
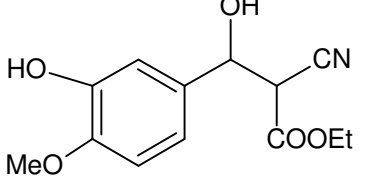
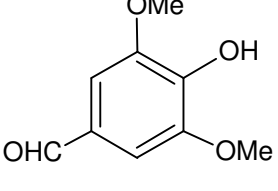
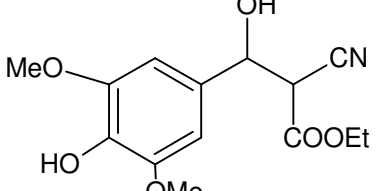
Figure 6.10 ¹H-NMR of product (4E)-2-cyano-3-hydroxy-5-phenylpent-4-enoate

6.5.8 Effect of the different aldehydes

The interesting results obtained on this model reaction were extended to different substituted aldehydes (Table 6.4) having the universal utility of their products in photosensitive or ultraviolet absorbing compounds.

Table 6.4 Knoevenagel condensation of aromatic aldehydes with ethyl cyanoacetate using SBA/CA catalyst. (Conditions as in Table 6.2)

Reactants	Products	Conversion (%)	Yield (%)	Time (h)
		100	93	3

		96	91	4.5
		90	88	6
		95	90	5
		88	84	7

Overall 88-96% conversion was noted with different aldehydes, however, the effect of the electronic environment could not be generalized.

6.6 Conclusions

1. Chloroacetic acid was post-synthetically grafted to SBA-15 to generate mild acid catalyst. The SBA/CA catalyst was characterized by standard characterization techniques PXRD, FT-IR, EDXRF, adsorption isorption and SS-NMR.
2. The efficient protocol for the preparation of phenylcinnamate's in liquid phase was reported with SBA/CA catalyst with very high activity, selectivity and product yield.
3. The catalyst was optimized and further evaluated for the synthesis of other substituted aldehydes.

6.7 References

1. A. Wight, M. Davis, *Chem.Rev.* 102 (2002) 3589-3614.
2. M. Davis, *Nature* 417 (2002) 813-821.
3. F. Hoffmann, M. Cornelius, J. Morell, M. Fröba, *Angew. Chem. Int. Ed.* 45 (2006) 3216-3251.
4. L. Rong, X. Li, H. Wang, D. Shi, S. Tu, Q. Zhuang, *Synth. Commun.* 36 (2006) 2407-2412.
5. K. Priya, G. Buvaneswari, *Mater. Res. Bull.* 44 (2009) 1209-1213.
6. N. Shaath, *Evolution of modern sunscreen chemicals*, New York
7. K. Tanaka, F. Toda, *Chem. Rev* 100 (2000) 1025-1074.
8. H. Teichmann, W. Thierfelder, *Ger. Patent (East)* 129 (1978) 959.
9. T. Jin, X. Wang, L. Liu, T. Li, *J.Chem.Res.* 2006 (2006) 346-347.
10. A. Corma, S. Iborra, *Adv.Catal.* 49 (2006) 239-302.
11. T. Reddy, R. Varma, *Tetrahedron Lett.* 38 (1997) 1721-1724.
12. F. Texier-Boullet, A. Foucaud, *Tetrahedron Lett.* 23 (1982) 4927-4928.
13. F. Khan, J. Dash, R. Satapathy, S. Upadhyay, *Tetrahedron Lett.* 45 (2004) 3055-3058.
14. S. Muthusamy, S. Babu, C. Gunanathan, *Synth. Commun.* 32 (2002) 3247-3254.
15. P. Shanthan Rao, R. Venkataratnam, *Tetrahedron Lett.* 32 (1991) 5821-5822.
16. D. Prajapati, J. Sandhu, *J. Chem. Soc., Perkin Trans. I* 1993 (1993) 739-740.
17. D. Shi, X. Wang, C. Yao, L. Mu, *J.Chem.Res.* 2002 (2002) 344-345.
18. S. Lai, R. Martin-Aranda, K. Yeung, *Chem. Commun.* 2003 (2003) 218-219.
19. M. Kruk, M. Jaroniec, C. Ko, R. Ryoo, *Chem. Mater* 12 (2000) 1961-1968.
20. A. Dubey, B. Mishra, D. Sachdev, M. Sowmiya, *React. Kinet. Catal. Lett.* 93 (2008) 149-155.
21. F. Rouquerol, J. Rouquerol, K. Sing, *Adsorption by Powders and Porous Solids: Principles (1999)*.

Chapter 7
Synthesis, Characterization and Catalytic
Applications of Silica-Polymer
Nanocomposites Functionalized with
Piperazine

7.1 Introduction

In the previous chapters, emphases were devoted to functionalize mesoporous SBA-15 material with different moieties as a mild acid catalyst. In the same manner interest emerged to develop solid base catalyst by incorporating basic moiety piperazine in SBA-15 by direct functionalization and functionalization after surface modification. Having known that functionalization after surface modification can significantly alter the selectivity of the desired product, the surface properties of SBA-15 can be modified by in-situ growth of vinyl monomers into the mesopores of SBA-15¹. Therefore, the present chapter aims at the systematic synthesis and characterization of SBA-15/piperazine nanocomposites via different routes for the activity and selectivity of nitroaldol condensation. Furthermore, the structure-activity relationships of these modified catalysts were studied and explained with mechanism

7.2 Synthesis of β -nitro alcohols over Silica-Polymer nanocomposites functionalized with piperazine

During the past few decades, many heterogeneous systems have been developed for acid catalyzed conversions compared to solid bases despite of having a decisive role in the synthesis of fine chemicals². In fact 10-20% of the industrial processes such as isomerizations, additions, condensation, alkylations and cyclizations proceed selectively with higher rates by solid bases³⁻⁶. Hence, the development of new one step, green and recyclable solid base catalytic systems is strongly encouraged⁷. Considering the solid base applications, amino-functionalized mesoporous silica materials⁸ were effectively designed either by grafting (post-synthetic) or co-condensation (direct during synthesis) methods to obtain organic-inorganic hybrid materials for many catalytic conversions⁸⁻¹¹. Particularly, the introduction of primary and secondary aliphatic amino groups on mesoporous silica materials has also been widely reported for nitroaldol condensation or michael addition reactions^{10, 12-14}. Various methods were attempted to modify the surface properties of the silica framework and to achieve maximum selectivity of the products, but in almost all the methods, the resulting materials obtained were either non porous or disordered in nature^{15, 16}. The surface modified amino functionalized ordered mesoporous silica were also reported for Knoevenagel condensation¹⁷.

Nitroaldol condensation is also a key reaction in the synthesis of β -nitroalkanol that are used as an extensively important intermediates in various organic transformations^{18, 19}.

β -nitroalkanols can further be converted to obtain 2-aminoalcohols for intermediates in chloroamphenicol,²⁰ ephedrine, norephedrine^{21, 22}, drugs like S-propranolol^{23, 24} and to achieve amino sugars and ketones²⁵. However, selective synthesis of β -nitroalcohols from nitroaldol condensation is quite challengeable because of its predominant dehydration to nitro alkenes that are susceptible for further polymerization. Moreover the aldehydes in presence of strong base results in self condensation to give aldol product²⁶. Therefore in order to overcome these difficulties, various primary and secondary amino groups were directly incorporated into MCM-41 materials^{12, 13} but, piperazine as a secondary cyclic amines has not been functionalized on to the surface modified SBA-15 materials via radical polymerization of monomers into the silica framework. The method of surface modification provides a powerful approach by ion-pair mechanism in controlling β -nitroalcohol selectivity almost exclusively.

7.3 Synthesis of SBA-15

The synthesis of SBA-15 is carried out using Pluronic (P123) (EO₂₀PO₇₀EO₂₀, MW = 5800, Aldrich) and TEOS as the surfactant and silica source respectively²⁷. In a typical synthesis batch with TEOS, 3 g of P123 was dissolved in 100 g of distilled water and 5.9 g of conc. HCl (35%). After stirring for 1h, 7.3 g of TEOS (ACROS, 98%) was added at 35°C maintaining the molar ratio of P123: H₂O: HCl: TEOS as 1: 5562.9:86.29: 42.51 and stirring for 24h. Subsequently the mixture was heated for 24 h at 100°C under static conditions in a closed polypropylene bottle. The solid product obtained after the hydrothermal treatment was filtered and dried at 80°C. The template was removed by calcinations at 550°C for 6h.

7.4 Synthesis of direct functionalized SBA-Piperazine catalyst (SBA/PP)

Piperazine was incorporated via post synthetic grafting technique. Typically, to 1g of SBA-15, 10ml of 3-chloropropyltriethoxysilane (CPTS) was stirred in dry toluene (20ml) under inert atmosphere (Figure 7.1). The product SBA/CPTS was filtered and exhaustively washed with ethanol in Soxhlet extractor for 24h. SBA-15 functionalized with CPTS was dried under vacuum and used further for functionalization with piperazine. Typically, 1g of SBA/CPTS was mixed with 1g of piperazine in 15 ml of triethylamine (acts as a solvent for neutralizing HCl generated during the functionalization) and refluxed for 24h under stirring conditions. Finally piperazine functionalized SBA-15 was filtered and washed thoroughly with dil HCl

and water. The functionalization of SBA-15 with piperazine was further confirmed by ninhydrin test that changed the color of solid from white to pink. The sample was named as SBA/PP.

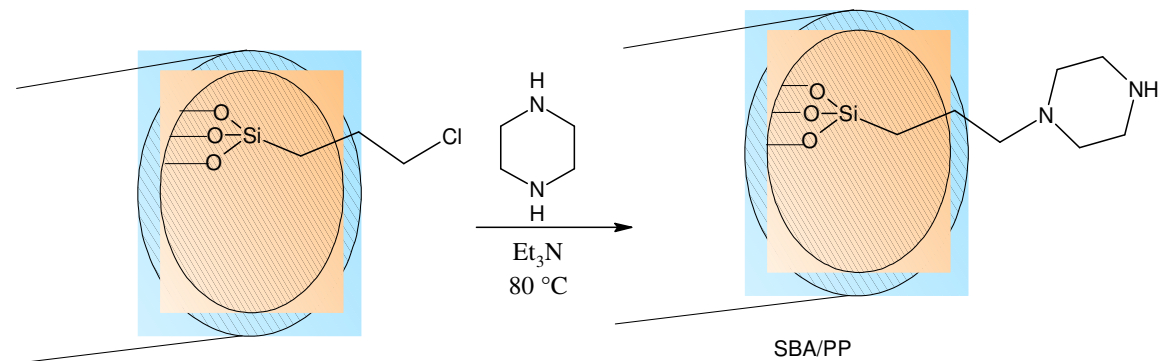


Figure 7.1 Direct functionalization of SBA-15 with piperazine (SBA/PP)

7.5 Synthesis of SBA-Polymer nanocomposites (SBA-PS) functionalized with piperazine (SBA/PS/PP).

The synthesis methodology of SBA/PS (Figure 7.2) involves the incorporation of vinyl monomers (4-chloromethylstyrene and divinyl benzene), cross linkers and radical initiators into the SBA-15 mesopore walls via the wet-impregnation method and equilibrated under reduced pressure to achieve a uniform distribution ¹. The monomers adsorbed on the mesopore walls were subsequently polymerized with temperature programmed heating. Typically, for 10 wt% polymer loading, 0.0827 g of 4-chloromethylstyrene (CS) (80 mol %), 0.0175 g divinylbenzene (20 mol %), 0.0065 g of AIBN, a, a-9-azoisobutyronitrile (3% relative to the total vinyl group) were dissolved into 2 ml of solvent (dichloromethane). The role of

4-chloromethylstyrene is to make the nature of the surface more hydrophobic and functionalize piperazine by replacing chloro groups in polymer. After impregnating the solution, the sample was heated to 40°C to remove the dichlorobenzene and subjected to freeze–vacuum–thaw to remove the residual solvent and air.

The sample was sealed in a pyrex tube and subjected to control temperature programming for polymerization. The temperature scheme follows 45°C for 24 h, 60°C for 4 h, 100°C, 120°C and 150°C for 1 h.

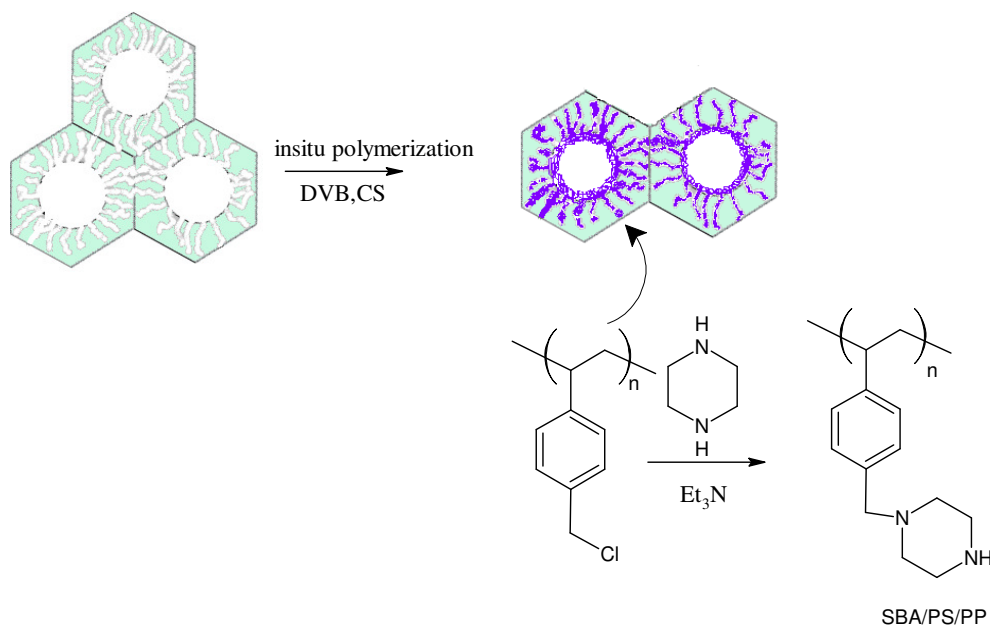


Figure 7.2 SBA-15 Polymer nanocomposites (SBA-PS) functionalized with piperazine.

Finally the polymer was washed with ethanol to remove the adsorbed monomers. Similarly 30 wt% and 20wt% polymer loading over SBA-15 was carried out. The polymer loaded samples were further subjected to functionalization with piperazine. The sample was named as SBA-xPS where x stands for wt% polymer loading. In a typical synthesis of SBA/PS/piperazine 1g of SBA-xPS was refluxed with 420mg of piperazine in presence of 10ml of triethylamine for 24h. The solid was filtered and washed well initially with dil HCl and then thoroughly with water to remove unreacted piperazine. Finally the samples were named as SBA-xPS/PP where PS stands for polymer and PP stands for piperazine.

7.6 Physicochemical Characterizations

7.6.1 PXRD

PXRD pattern of the samples at low angles (Figure 7.3) showed the diffraction pattern similar to SBA-15 sample. The diffraction at (100), (110), and (200) planes can be indexed to reflections comprising of hexagonal $p6mm$ space group indicating that the materials possess the ordered mesoporous structure and piperazine has been uniformly incorporated into the framework²⁷. A careful examination of the spectrum showed the increase in the intensity of the base peak in SBA-(10)PS/PP catalyst compared to the SBA/PP catalyst due to

the polymer formation inside the mesopores of silica materials resulting in an increase in the apparent density of the mesopore walls²⁸.

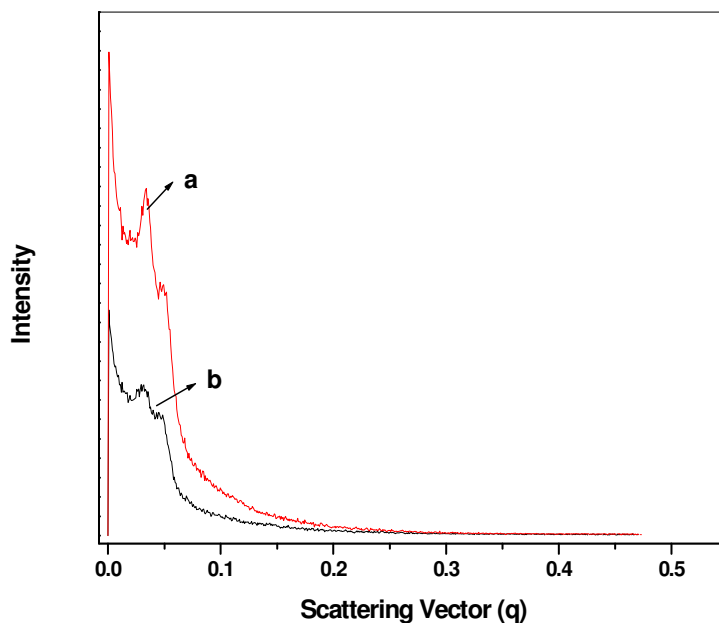


Figure 7.3 PXRD pattern of (a) SBA-(10)PS/PP and (b) SBA/PP catalysts

7.6.2 N₂ Adsorption-Desorption studies

The nitrogen adsorption-desorption isotherm (Figure 7.4) of the catalysts showed a type IV adsorption isotherm according to the IUPAC classification with H1 hysteresis loop²⁹ indicative of mesoporous nature of the samples³⁰

Table 7.1 Structural parameters of the SBA/PP catalysts.

Entry	Materials	Surface area (m ² /g)	Pore Volume (cm ³ /g)	Pore Size BJH _{Ads} (nm)
1.	SBA-15	678	1.2	8.2
2.	SBA/PP	76	0.16	7.7
3.	SBA/(10)PS/PP	294	0.32	5.1

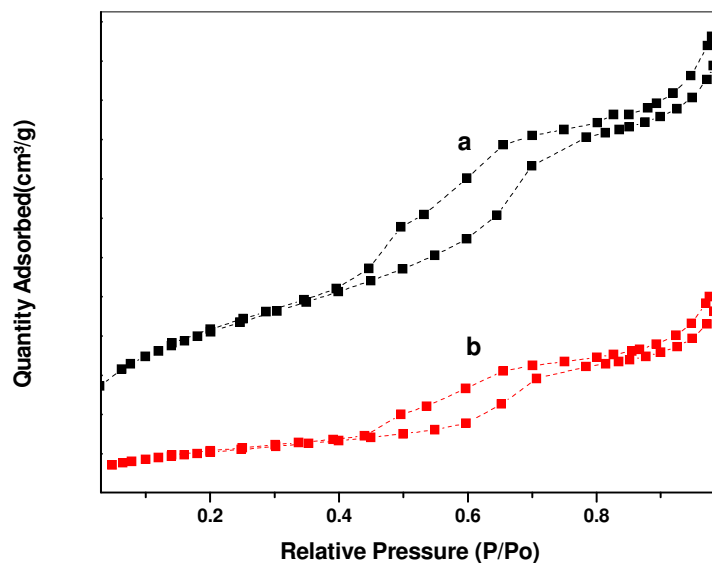


Figure 7.4 N₂-adsorption –desorption isotherm of (a) SBA-(10)PS/PP and (b) SBA/PP catalysts

The shapes of the isotherms are slightly deviated from the parallel shape due to the strain generated in the mesopores of SBA-15 during the incorporation of piperazine moiety. The surface area, pore volume and pore diameter decreased with the incorporation of piperazine, indicating that the piperazine has been incorporated inside the SBA-framework. All the structural parameters of the catalysts are included in Table 7.1.

7.6.3 SS -NMR

The incorporation of piperazine into the silica framework was further confirmed by ¹³C CPMAS SS NMR. The spectrum of SBA/PS (Figure 7.5) showed peaks at 128, 139 and 120 ppm indicating the presence of aromatic carbons of the polymer resulted from the monomers 4-chloromethyl styrene and divinyl benzene³¹. The peak at 25ppm shows the presence of the carbon directly linked to mesoporous silica (-CH₂-Si)³². Furthermore piperazine linkage to polymeric chain was indicated by sharp peak at 48.3 ppm (CH₂ piperazine)³³.

The intensities of peaks were not recognized fully because of the different concentration of piperazine in SBA/PP and SBA-(10)PS/PP catalysts. However, the peaks obtained were

sharper in direct functionalized piperazine^{33, 34} compared to the polymeric derived SBA-PS/PP catalysts.

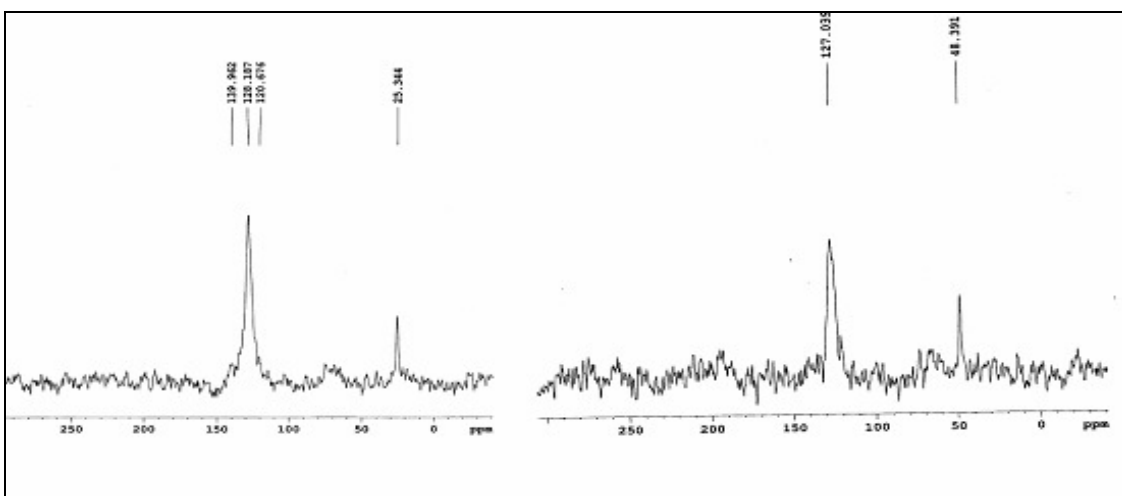


Figure 7.5 ¹³C CPMAS NMR spectra of (a) SBA/PS and (b) SBA-(10)PS/PP catalysts.

The post-synthetic grafting of chloropropyltriethoxysilane was confirmed by ¹³C magic angle spinning (MAS) NMR. NMR spectrum of the CPTMS/SBA-15 samples showed the presence of three main peaks at 9.3, 25.8 and 46.3 ppm respectively corresponding to three carbon atoms of chloropropyl SBA-15 sample.

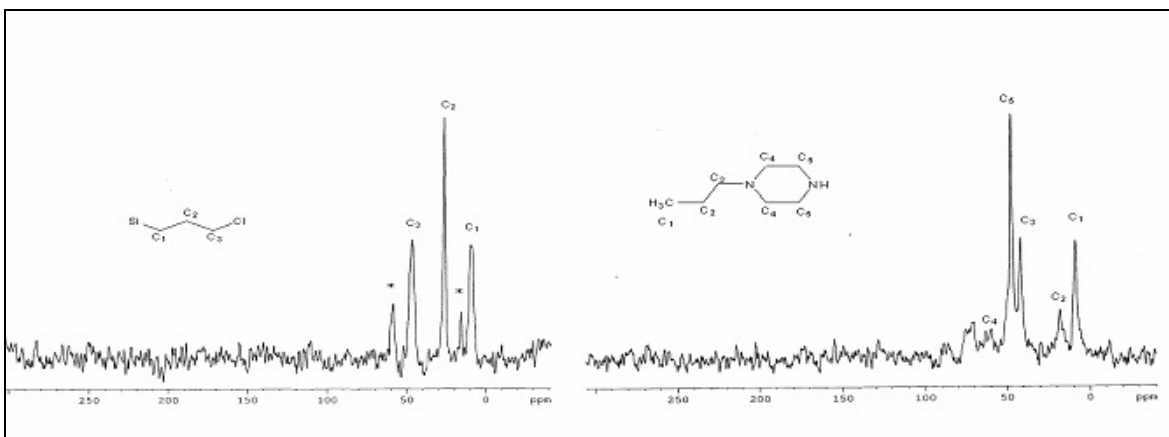


Figure 7.6 ¹³C CPMAS NMR spectra of A) SBA/CPTS and B) SBA/PP catalysts.

The presence of peak at 15 and 58ppm indicates the presence of residual ethoxy groups of TEOS³⁴. Furthermore the functionalized chloropropyl on SBA-15 was further linked with piperazine (SBA/PP) which was confirmed by SS-NMR (Figure 7.6). ¹³C CPMAS NMR of

SBA/PP catalyst showed five peaks at 8.7, 17, 41, 47 and 59 ppm. The two signals assigned at 47ppm and 59 ppm for piperazine carbon is attributed to different chemical environment of carbon in piperazine moiety attached to SBA-15³³. The peak at 59ppm is not intense which may be due to the quadrupolar coupling of carbon with nitrogen.

7.6.4 Scanning Electron Microscopy (SEM)

The SEM images (Figure 7.7) of SBA/PS/PP (10%) and after piperazine incorporation in SBA-(10%) PS/PP showed the rod shape particles with relatively 1 μ m uniform size. These rod shaped structures are uniformly dispersed on ordered mesoporous silica material resulting in better activity and selectivity of the β -nitroalcohols.

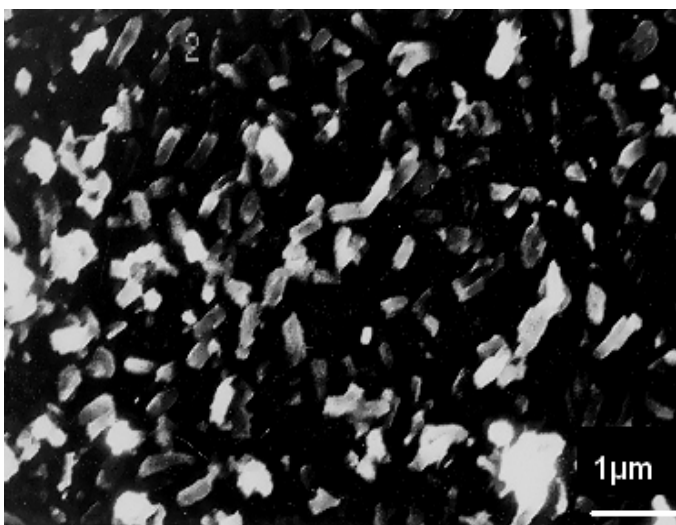


Figure 7.7 SEM image of SBA-(10)PS/PP.

7.6.5 FT-IR

The FT-IR spectrum (Figure 7.8) showed a broad peak around 3500 cm^{-1} in all the samples confirming the presence of N-H stretching of secondary amine (piperazine) incorporated into the mesoporous SBA-15 framework.

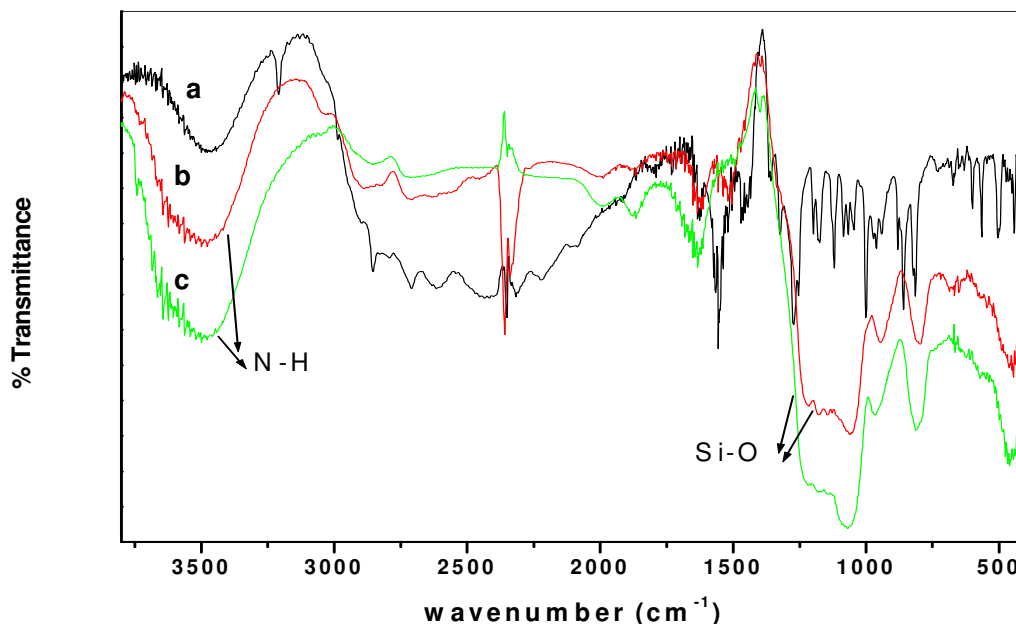


Figure 7.8 FT-IR spectra of piperazine a) PPA (neat), b) SBA/PP and c) SBA-(10)PS/PP catalysts.

7.6.6 Basicity Measurements

The number of basic sites on the catalyst surface was determined by Hammett indicators including bromthymol blue ($H= 7.1$), phenol red ($H= 7.4$), cresol purple ($H= 8.3$), thymol blue ($H= 8.9$), phenolphthalein ($H= 9.7$), and alizarine yellow ($H= 11.0$). Soluble basicity was also determined by stirring 500mg of SBA/PP and SBA/PS/PP with 0.02M HCl solution for 12h and finally unadsorbed H^+ ions were titrated with Na_2CO_3 .

Basicity of the catalyst was calculated by Hammett indicator method and found in range of $8.3 < H_0 < 11$. The number of basic sites was also determined by the titration method; 200mg of the varied catalyst prepared were stirred with 10ml of 0.02mol/l of HCl for 12h and the solution was filtered from the catalyst. The residual H^+ ions were titrated with 0.02mol/L of Na_2CO_3 to obtain the amount of HCl adsorbed on the piperazine functionalized SBA-15. The basicity of SBA-PP catalyst was found to be lower compared to the SBA-PS/PP catalysts (Figure 7.9). This may be due to the better dispersion of the piperazine moiety after the surface modification in polymeric derived catalysts.

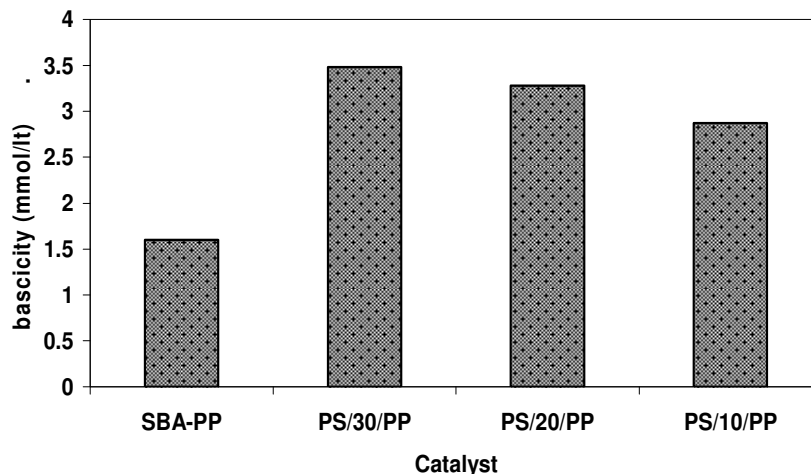
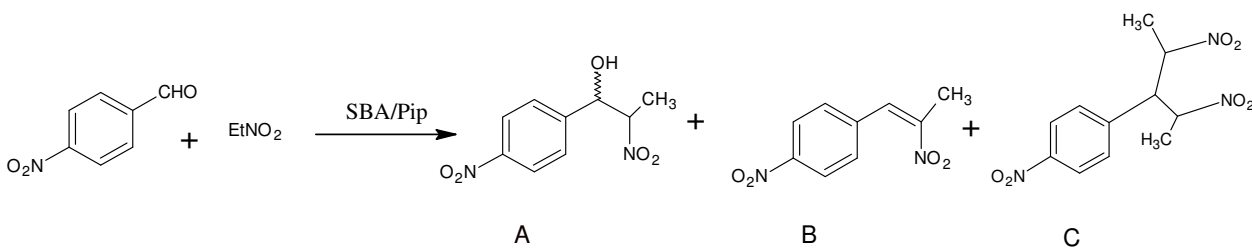


Figure 7.9 Basicity of SBA-Piperazine catalysts

7.7 Catalytic Studies

Nitroaldol reaction (Scheme7.1) was chosen as model reaction in liquid phase and investigated over piperazine functionalized catalysts prepared by different methodologies. To evaluate the catalytic efficiency of the synthesized catalyst SBA/Pip and SBA/PS/Pip the reaction of p-nitrobenzaldehyde with nitroethane was examined.



Scheme 7.1 Nitroaldol Condensation

Synthesis of β -nitroalcohols

The catalytic activity studies were carried out in the liquid phase. 3mmol of p-nitrobenzaldehyde and 5ml of nitroethane were mixed at 65°C (Scheme7.1). The desired amount of the catalyst (10-500mg) was added to the reaction mixture under inert atmosphere and the reaction was monitored for 24h. The products of the reaction were identified by gas chromatography after considering the response factors of the authentic samples using n-decane as internal standard. After the completion of reaction, catalyst was filtered and washed with solvent. Product was isolated using column chromatography using ethyl acetate: Hexane (2%). The melting point of the sample was also in agreement with the literature.

7.7.1 Effect of the different catalysts

Table 7.2 showed the total conversion and the selectivity of the desired product (A) for nitroaldol condensation (Scheme 7.1). Careful analysis of the results revealed very high conversion of the products (92%) with 95% selectivity of the product (A) on SBA-(10) PS/PP catalyst. The catalytic activity decreased with increase in the percentage loading of the monomers up to 30%. Comparatively lower activity (70%) and selectivity (85%) of the desired product (A) was obtained over direct functionalized SBA/PP catalysts. This may be due to the higher surface area and better dispersion of the active centers inside the surface modified catalyst compared to the direct grafted catalyst (Figure 7.2).

Table 7.2 Effect of different catalyst on the conversion of nitroalcohol

Catalyst	^a Conversion (%)	Product Selectivity (%)		
		A	B	C
Piperazine	63	72	17	11
SBA-15	0	0	0	0
SBA-NH ₂	75	7	90	1
SBA/Pip	70	85	12	3
SBA-(30)PS/PP	80	96	4	0
SBA-(20)PS/PP	85	98	2	0
SBA-(10)PS/PP	92	98	2	0

Conditions: 3mmol (p-nitrobenzaldehyde), 5ml (nitroethane), temp-65°C, time (24h) and catalyst wt (200mg).

^a % conversion is based on total products.

It is to be mentioned here that only 63% conversion of the products and 70% selectivity of the desired product was obtained on pure piperazine (homogeneous) indicating the effect of the surface modification or heterogenization of the silica framework in controlling the overall selectivity of the product(s). The higher product selectivity of the nitroalcohol is in agreement with earlier reports wherein the secondary amine preferentially gives nitroalcohol over nitroalkene^{12, 13}. The best catalyst SBA-(10) PS/PP was selected for further studies. The variation of the catalyst weight on the conversion of the products showed increasing trend on both the catalyst. Hence catalyst weight of 200mg is selected for further catalytic studies.

7.7.2 Effect of the solvent

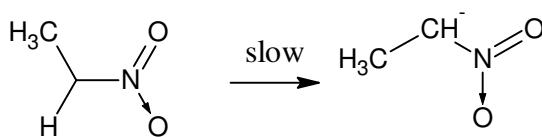
To further optimize the nitroaldol condensation of p-nitrobenzaldehyde with nitroethane, different solvents were chosen to see the influence on total conversion of the products. A careful examination of solvents under study (Table 7.3) indicates that solvent free conditions are the best conditions to carry out reaction selectively with high conversions.

Table 7.3 Effect of different solvents on the conversion and selectivity of the nitroalcohol

Solvents	SBA/PP	SBA/PP		SBA-(10)PS/PP	SBA-(10)PS/PP	
	Conv. (%)	Product Sele. (%)		Conversion	Product Sele (%)	
		A	B	(%)	A	B
Nitroethane	70	85	12	93	98	2
Ethanol	60	80	14	68	96	3
Chloroform	46	90	5	60	97	3
Tetrahydrofuran	35	82	10	38	96	3
Acetonitrile	25	84	7	26	98	2
Methanol	20	80	15	25	98	2

Conditions as in Table 7.2

Higher conversion in nitroethane is attributed to its high dielectric constant 28.06 which helps to stabilize the transition state as well enhance the solubility of p-nitrobenzaldehyde (dielectric constant-20). The conversion and selectivity in other solvents depends on how reluctantly nitronoate ion is generated and stabilized by these solvents (Scheme 7.2).



Scheme 7.2 Stability of Nitronoate ion.

7.7.3 Effect of the catalyst weight

Figure 7.10 showed variation in yield of β-nitroalcohols with change in weight SBA/PP and SBA-(10)PS/PP catalyst. It was observed that the product yield increases with increase in

amount of both catalyst and maximum conversion was obtained with SBA-(10)PS/PP catalyst. This may be due to the hydrophobic nature of SBA/PS/PP catalyst due to the polymer coating on OMS. A careful examination of variation of weights showed that 10mg of the SBA/PS/PP also gave promising yields.

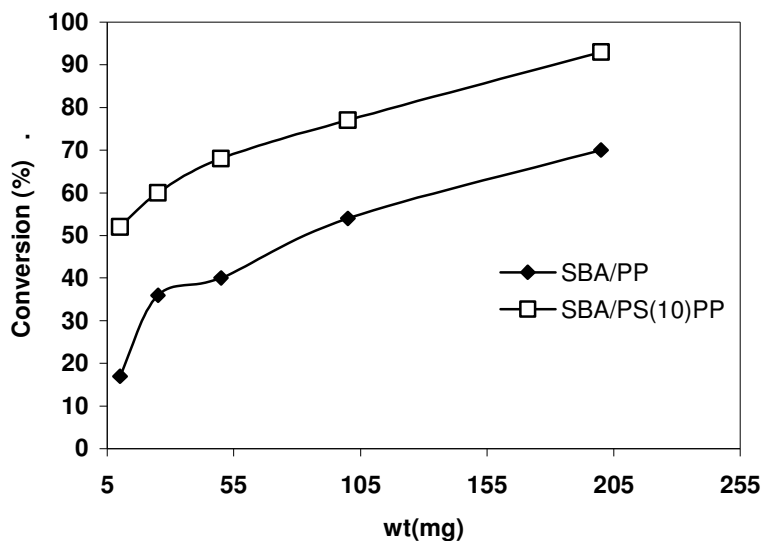


Figure 7.10 Effect of the catalyst weight on the conversion of β -nitroalcohols

7.7.4 Effect of the reaction temperature

Figure 7.11 showed the effect of temperature on the conversion and selectivity of nitro alcohol.

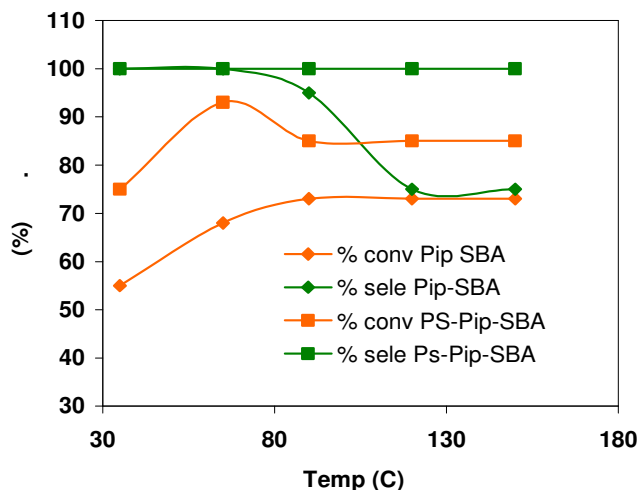


Figure 7.11 Variation of conversion and selectivity of β - nitroalcohol with temperature

The results concluded that the conversion of the products and the selectivity of nitro alcohol product increased with increase in the temperature up to 65°C and then decreased with

further increase in temperature. This decrease in the selectivity of nitro alcohol product (A) may be due to the formation of nitroalkene by dehydration of nitro alcohol at higher temperature. Hence the best temperature 65⁰C was chosen for further catalytic activity studies.

7.7.5 Time-on-stream studies

Very interesting observations were observed on the conversion of the products with time. The initial kinetics of the reaction was faster in SBA-(10) PS/PP catalyst compared to SBA/PP catalysts indicating the influence of the surface modification (Figure7.12).

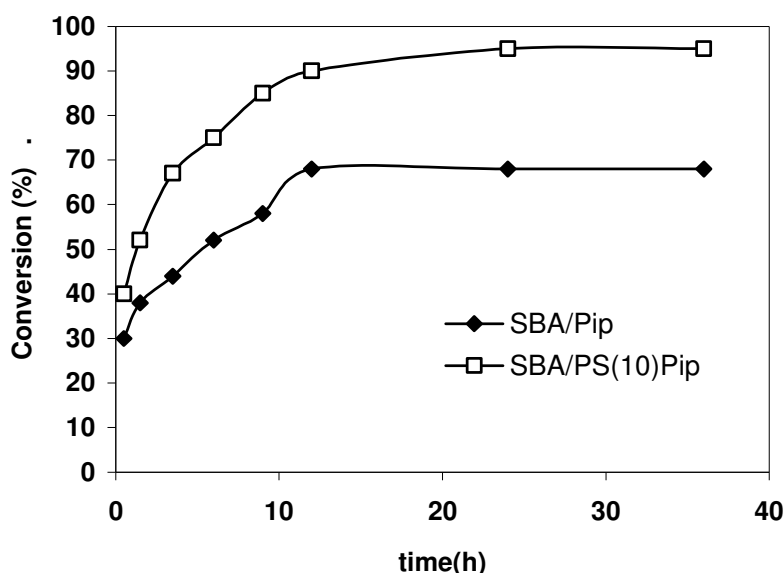


Figure 7.12 Variation of conversion and selectivity of β - nitroalcohol with time

Secondly, the slight color change (colorless to brown) was observed in SBA/PP catalysts during the progress of the reaction indicating that the reactant molecules might be adsorbing on to the surface of silica and may be blocking the active sites of the catalyst, resulting in lowering the conversion of the products. However, no such color change was noted in the polymer grafted catalyst with the progress of the reaction indicating that the surface modification helps to avoid the adsorptions of the reactant molecules and hence enhancing the conversion of products¹³. The catalyst after the completion of the reaction was washed thoroughly with nitroethane, solvents and with water. The catalyst was dried and still the color change of the catalyst was observed in SBA/PP catalysts.

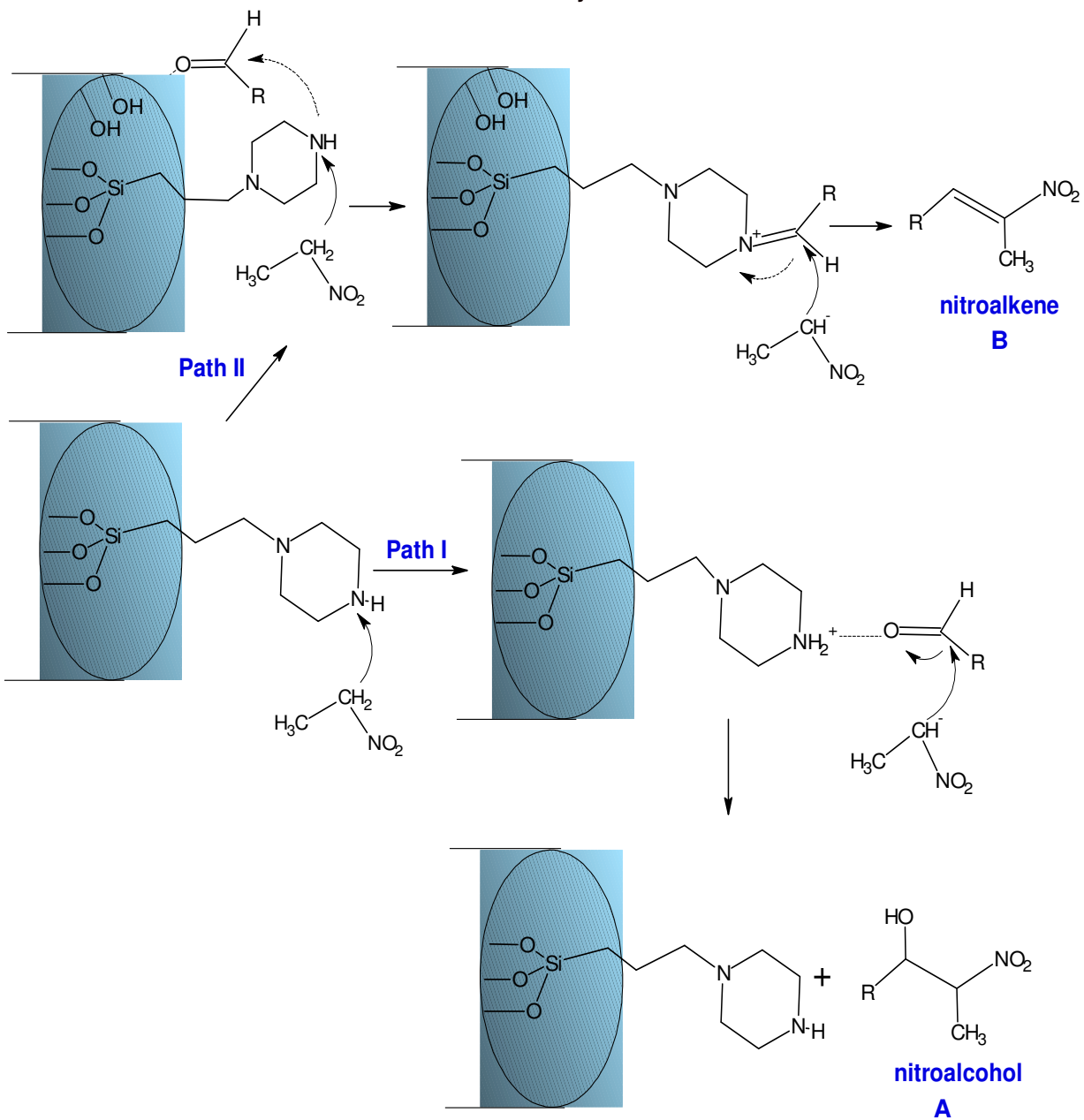
7.7.6 Plausible Mechanism

Mechanistically, we believe that piperazine functionalized SBA-15 both through direct and after surface modification selectively gives nitroalcohol via ion-pair mechanism^{14, 19}. However, in direct functionalized piperazine, the formation of minor product nitroalkene (B, Scheme 7.3) was also observed. This selectivity difference resulting in the formation of nitroalkene may be due to the presence of residual silanol groups that remained after the silylation with chloropropyltriethoxysilane and hence follows the reaction pathway II³⁵. Comparatively, the surface modified piperazine, totally caps the silanol group and preferentially favors the reaction by pathway I in generating selectively nitro alcohol product (A). The reaction product was identified and characterized by FT-IR (Figure 7.13).

7.7.7 Reusability

In order to see the reusability of the catalysts SBA-(10) PS/PP, the catalyst after first cycle was filtered, washed thoroughly with chloroform, acetone and finally with water, dried at 150°C in the air oven and subjected to fresh reaction under identical reaction conditions. Not much difference in the activity and selectivity was observed up to two cycles (not tested further) indicating the promise use of these catalysts.

Plausible Mechanism for the synthesis of nitroalcohols



Scheme 7.3 Plausible Mechanism

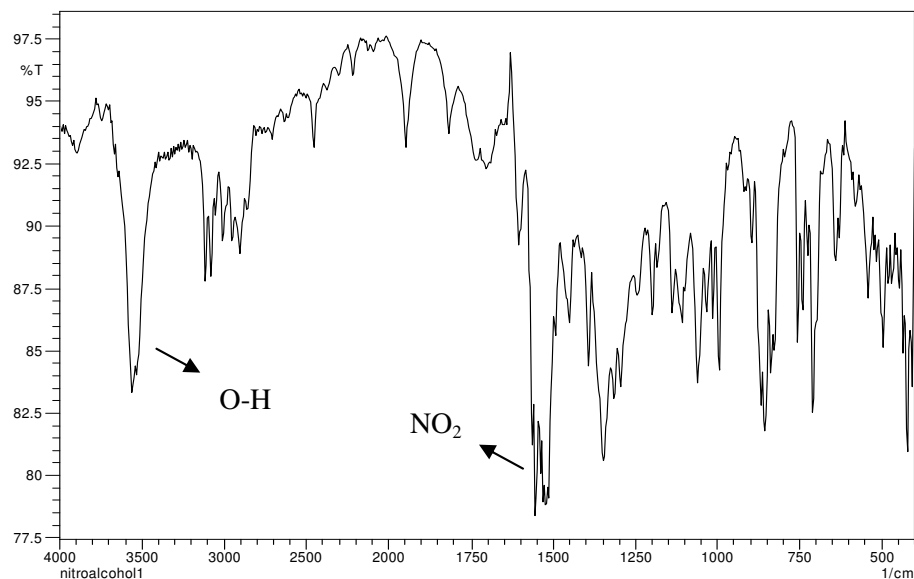


Figure 7.13 FT-IR of β -nitroalcohol

7.8 Conclusions

1. SBA-15/PP nanocomposites were synthesized by functionalizing direct and after surface modification methods. The nanocomposites were characterized by PXRD, N_2 adsorption-desorption, FT-IR, SEM and SS-NMR.
2. PXRD pattern and SS-NMR confirms the uniform incorporation (retained mesoporous structural order) and covalent linkage of piperazine respectively to SBA-15 framework
3. The catalytic activity results for nitroaldol condensation over SBA/PS/PP catalysts showed very high activity and selectivity of β -nitroalcohols. The selectivity of the product could be fairly controlled by the degree of polymerization in the surface modification method.
4. The degree of surface modification by different methods may pave the role for different organic transformations.

7.9 References

1. A. Dubey, M. Choi, R. Ryoo, *Green Chem* 8 (2006) 144-146.
2. F. Figueras, L. Kantam, M. Choudary, *Curr Org Chem* 10 (2006) 1627-1637.
3. H. Hattori, *Chem Rev* 95 (1995) 537-558.
4. H. Hattori, *Appl Catal A* 222 (2001) 247-259.
5. Y. Ono, T. Baba, *Catal. Today* 38 (1997) 321-337.
6. J. Weitkamp, M. Hunger, U. Rymasa, *Microporous Mesoporous Mater* 48 (2001) 255-270.
7. C. Hong, X. Wenlei, L. Hui, *Application of Solid Base Catalysts in Organic Synthesis*, Sichuan Chemical Industry, 2008.
8. N. Al-Haq, R. Ramnauth, S. Kleinebiekel, D. Ou, A. Sullivan, J. Wilson, *Green Chem* 4 (2002) 239-244.
9. S. Cheng, X. Wang, S. Chen, *Top Catal* 52 (2009) 681-687.
10. B. Choudary, M. Kantam, P. Sreekanth, T. Bandopadhyay, F. Figueras, A. Tuel, *J Mol Catal A Chem* 142 (1999) 361-365.
11. S. Saravanamurugan, D. Han, J. Koo, S. Park, *Catal Commun* 9 (2008) 158-163.
12. A. Anan, R. Vathyam, K. Sharma, T. Asefa, *Catal Lett* 126 (2008) 142-148.
13. Q. Wang, D. Shantz, *J Catal* (in press).
14. S. Huh, H. Chen, J. Wiench, M. Pruski, S. Victor, *J Am Chem Soc* 126 (2004) 1010-1011.
15. C. Wu, T. Bein, *Science* 264 (1994) 1757-1759.
16. C. Wu, T. Bein, *Science* 266 (1994) 1013.
17. R. Guillet-Nicolas, L. Marcoux, F. Kleitz, *New J Chem* 34 (2009) 355-366.
18. K. Akutu, H. Kabashima, T. Seki, H. Hattori, *Appl Catal A* 247 (2003) 65-74.
19. A. Cwik, A. Fuchs, Z. Hell, J. Clacens, *Tetrahedron* 61 (2005) 4015-4021.
20. K. Yang, H. Fang, J. Gong, L. Su, W. Xu, *Mini-Rev Med Chem* 9 (2009) 1329-1341.
21. K. Yamaguchi, K. Ebitani, T. Yoshida, H. Yoshida, K. Kaneda, *J Am Chem Soc* 121 (1999) 4526-4527.
22. D. Buchanan, D. Dixon, F. Hernandez-Juan, *Org. Biomol. Chem.* 2 (2004) 2932-2934.
23. F. Palacios, M. Jesús, D. Aparicio, *ARKIVOC* 9 (2005) 405-414.
24. N. Ono, *The nitro group in organic synthesis*, Vch Verlagsgesellschaft Mbh, 2001.

25. F. Luzzio, *Tetrahedron* 57 (2001) 915-945.
26. C. Palomo, M. Oiarbide, A. Laso, *Eur J Org Chem* (2007) 2561-2574.
27. M. Kruk, M. Jaroniec, C. Ko, R. Ryoo, *Chem. Mater* 12 (2000) 1961-1968.
28. M. Liu, H. Ahn, R. Ryoo, *J Am Chem Soc* 127 (2005) 1924-1932.
29. F. Rouquerol, J. Rouquerol, K. Sing, *Adsorption by Powders and Porous Solids: Principles (1999)*.
30. F. Hoffmann, M. Cornelius, J. Morell, M. Fröba, *Angew Chem Int Ed* 45 (2006) 3216.
31. L. Errede, R. Newmark, J. Hill, *Macromolecules* 19 (1986) 651-654.
32. S. Itsuno, G. Darling, H. Stover, J. Frechet, *J Org Chem* 52 (1987) 4644-4645.
33. I. Wawer, M. Pisklak, Z. Chilmonczyk, *J Pharm Biomed Anal* 38 (2005) 865-870.
34. E. Prasetyanto, S. Lee, S. Park, *Microporous Mesoporous Mater* 118 (2009) 134-142.
35. J. Bass, A. Solovyov, A. Pascall, A. Katz, *J Am Chem Soc* 128 (2006) 3737-3747.

Chapter 8
Summary and Conclusions

8.1 Summary and Conclusions

One of the key challenges in the field of heterogeneous catalysis is high yield and selectivity and to meet this goal nanoporous materials especially mesoporous material with pore size (>2nm) were found to be of profound interest. Traditional amorphous nanoporous materials such as silica gels, alumina, and activated carbons showed limited shape selectivity because of their textural porosity with broad pore size distribution. Hence mesoporous materials with high surface area, tunable pore sizes, flexibility of incorporation of organic moieties and better dispersion of active sites are immensely important and exhibit greater control over activity and selectivity. Selectivity of the reaction by these materials can further be enhanced by increasing the homogeneity of surface or through uniform distribution of active species over these materials. Therefore in order to achieve the above cited goals the present research work aimed at synthesis, characterization of hydrotalcite like materials and ordered mesoporous silica materials and to compare the different catalyst systems to gain insight on how the different mesoporosity's generated affect the catalytic activity.

In the first part of the thesis emphasis were laid on the catalytic applications of Hydrotalcite like materials wherein the basic character of M(II)Al binary hydrotalcites were exploited for the synthesis of an important drug phenytoin. The heterogeneous synthesis of phenytoin over calcined MgAl-HTlc was employed for the first time. The catalytic activity results showed very high conversions (80-95%) with high selectivity (90-95%) of the product phenytoin.

So far, various redox-mediated transformations have been investigated over the transition metal containing hydrotalcites. However, copper in the sheets of HTlc were of particular interest owing to their selective oxidation behaviour. Therefore the potential use of CuMgAl-ternary HTlc was chosen for the first time for the oxidation of vanillin and benzoin. The catalyst yielded high conversions and selectivity of the desired product vanillic acid and benzil. No leaching of copper metal ions was observed during the course of the reaction which confirmed the reusability of the catalyst without any loss of activity.

In the second part of the thesis efforts were devoted to non-ionic surfactant templating approach for the fabrication of highly ordered mesoporous silica materials which results in exceptional properties i.e. large surface area, uniform pore size and flexibility to incorporate organic moiety or isomorphous substitution of metal ions in silica framework.

In the initial part of the work with OMS material, SBA-15 was impregnated with different amounts of Al. This mild heterogeneous catalyst SBA/Al was characterized by standard characterization techniques. The catalytic activity was investigated for the synthesis of 3,4-dihydropyrimidine-2(1H)-ones in the liquid phase and resulted in very high conversion and yields of the products.

In continuation to the previous studies polyphosphoric acid (PPA) was incorporated via different methodologies (insitu or direct) in SBA-15. Different strategies of catalyst synthesis were investigated for acylation of naphthalene. However low conversions (20-25%) of the product 2-acylnaphthalene with high selectivity (94%) over these mild SBA/PPA catalysts was detected.

Having known such remarkable properties of OMS materials, the enlarged pore size (2-15nm) of OMS was post-synthetically grafted with organic moiety dichloroacetic acid to obtain the organo-silica hybrid materials with mild acidity. The grafting approach for the synthesis of catalyst gave more stability and flexibility to the catalyst which resulted in high accessibility of the catalyst surface to the reactant molecules and overall resulted in high yields for Knoevenagel condensation of cinnamaldehyde with ethylcyanoacetate.

An alternate route for surface modification was employed through radical polymerization of the vinyl monomers into the silica framework. Cyclic secondary amine as a mild base was functionalized via post synthetic grafting and polymeric methods. The synthetic strategy of silica-polymer nanocomposite using vinyl monomers provided remarkable advantages of incorporating piperazine within the mesoporous silicas via the formation of a C-C bond rather than hydrolysis-susceptible siloxane bonds through direct functionalization (without polymer). Structure activity relationships of synthesized catalysts via different methodologies were investigated for nitroaldol condensation. The new protocol for nitroaldol condensation over polymer nanocomposites resulted in very high conversions of β -nitroalcohol with very high selectivity.

8.2 Future Scope of the research work

Mesoporous materials have shown credibility in the field of catalysis especially hydrotalcites like materials represents a more efficient and greener catalyst. As an alternative to the use of homogeneous alkali hydroxides or alkoxides, HTs offer precious advantages such as decreased corrosion of the reactor, ease of separation from the reaction medium, recycling possibilities. Forthcoming research especially tuning and optimising the basicity of the material: changing the nature and proportion of the cations, introduction of other charge compensating anions by exchange or via the “memory effect”, changing the degree of hydration, application of thermal treatment, introduction of alkaline dopes on these materials and will further broaden their range of application as heterogeneous catalysts.

The development of ordered mesoporous silica via non-ionic surfactant templating approach has gained lot of attention. Non-ionic surfactants because of the low cost and absence of toxicity, hydrogen-bonding interactions with precursors and rich mesophase behaviors are effective templates in design and synthesis of mesoporous solids. Further explorations in the this field can be conducted to increase the pore size to 50 nm, and suitable block copolymers can be used to form hierarchical pores, and chiral pore channels in mesoporous silica.

Further explorations will be conducted over the incorporation of multiple functional groups wherein synergistic catalytic effect of two different entities will be involved. The groups when act together will increase the rate of a reaction beyond the sum of the rates achieved from the individual entities alone. This strategy will encourage the site specificities and enantioselectivities. Moreover this co-operative catalysis will help us to understand and synthesize materials that are closer to enzymes.

Appendices

List of Publications

[A-1]

-
1. D.Sachdev, A.Dubey, B.G.Mishra and S.Kannan, "Environmentally benign liquid phase oxidation of vanillin over copper containing ternary hydrotalcites," *Catalysis Communications*, 9 (2008), 391-94.
 2. A.Dubey, B.G.Mishra, D.Sachdev and M. Sowmiya, "Heterogeneous liquid phase synthesis of 3, 4-dihydropyrimidine-2 (1H)-ones using aluminated mesoporous silica," *Reaction Kinetics and Catalysis Letters*, 93 (2008), 149-55.
 3. D.Sachdev, M.Naik, A.Dubey and B.G.Mishra, "Environmentally benign aerial oxidation of benzoin over copper containing hydrotalcite," *Catalysis Communications*, 11 (2010), 684-88.
 4. D.Sachdev and A.Dubey, "One step liquid phase heterogeneous synthesis of Phenytoin over MgAl Calcined Hydrotalcites," *Catalysis Communications*, (2010) (doi:10.1016/j.catcom.2010.05.004).
 5. M.A. Naik, D. Sachdev and A. Dubey, "Sulfonic acid functionalized mesoporous SBA-15 for one-pot synthesis of substituted aryl-14H-dibenzo [a, j] xanthenes and bisindolyl methanes," *Catalysis Communications* (in press, 2010)
 6. D.Sachdev and A.Dubey. "Synthesis and Characterization of Silica-Polymer nanocomposites functionalized with piperazine for the synthesis of β -nitro alcohols". *Catalysis Letters* (under revision).
 7. D.Sachdev and A.Dubey, "Knoveneganel Condensation of Cinnamaldehyde with Ethylcyanoacetate over Chloroacetic acid Functionalized SBA-15," (communicated).

8. D.Sachdev and A.Dubey, "Synthesis and Characterization of mesoporous Silica/polyphosphoric acid (SBA-15/PPA) nanocomposites for acylation of naphthalene," *(communicated)*.

List of papers presented in conferences [A-2]

1. Oral presentation in National Conference on Green & Sustainable Chemistry Organised (2010) held at BITS, Pilani “*Copper Containing Hydrotalcites as an Efficient, Environmentally Benign Catalyst for Benzoin Oxidation Under Aerobic Conditions*”.
2. Oral presentation in 19th National Symposium on Catalysis for sustainable energy and chemicals (CATSYMP-19) (2009) held at NCL-Pune “*Synthesis, Characterization and Catalytic Applications of Silica -Polymer nanocomposites functionalized with Piperazine*” (**Received first prize for best oral presentation**)
3. Poster presentation in 13th National Conference on Surfactants, Emulsion & Biocolloids with Special Focus on Biomimetic Systems (NATCOSEB-BIMS), 2007 held at BITS, Pilani. “*Liquid phase oxidation of Veraterldehyde over copper containing hydrotalcites*”
4. Attended International Conference on the interface of chemistry-Biology in Biomedical Research held at BITS-Pilani 2008, held at BITS, Pilani.

BRIEF BIOGRAPHY OF THE CANDIDATE

[A-3]

Divya Sachdev completed her M.Sc (Chemistry) from Delhi University in 2001 and specialized in the field of organic chemistry. She worked as a guest lecturer of Chemistry at Shaheed Rajguru College of Applied Science for Women in (2003-2004). After her marriage she joined BITS-Pilani in 2006 for her doctoral studies under the supervision of Dr. Amit Dubey and received Senior Research Fellowship (SRF) from Council of Scientific and Industrial Research (CSIR) for her research work. She has published research articles in well renowned international journals and presented papers in conferences/symposium.

BRIEF BIOGRAPHY OF THE SUPERVISOR

[A-4]

Dr. Amit Dubey is an Assistant Professor in Chemistry Group, Birla Institute of Technology and Science, Pilani. He started his initial career of research as a scientist fellow at Physical Research Laboratory-Ahmedabad (A Unit of Dept. of Space, Govt of India) from (1997-1999). He received his Ph. D degree from Central Salt and Marine Chemicals Research Institute-Bhavnagar (CSIR) 2003. For his doctoral degree, he worked with Dr. Srinivasan Kannan, Senior Scientist in the research area of Nanomaterials and heterogeneous Catalysis. After his doctorate, he worked as a post-doctoral fellow (2003-2005) with Prof. Ryong Ryoo, Director, Centre for Functional Nanomaterials, Daejeon at Korea Advanced Institute of Science and Technology-Daejeon, South Korea. After his post-doctoral studies he worked as a research associate under the pool scientist scheme at National Chemical Laboratory, Pune during (Aug –Dec) 2005. He joined BITS, Pilani as a lecturer in 2006 and became Assistant Professor in 2007. At present, besides teaching and research he is actively contributing in administrative duties of BITS, Pilani. He has been involved in research for the last 14 years and in teaching for 5 years. As a result of his research accomplishment, he has international publications in peer reviewed journals. Currently Dr. Amit Dubey is guiding two Ph. D. students. Additionally, to his credit he is also handling a project from DST.